

STUDIES OF A GAS-TO-GAS HEAT EXCHANGER

USING FLUIDIZED SOLIDS

by

HISASHI HATTORI

A thesis

submitted for the

Degree of

Doctor of Philosophy

Department of Mechanical Engineering

The University of Aston in Birmingham

OCTOBER 1983

The University of Aston in Birmingham

Studies of a gas-to-gas heat exchanger  
using fluidized solids

by

HISASHI HATTORI

A THESIS SUBMITTED FOR THE DEGREE OF DOCTOR OF PHILOSOPHY

1983

SUMMARY

The work reported in this thesis concerns the heat transfer rates and fluidization phenomena encountered when solids are heated by a high temperature gas stream, then transported away and brought into contact with a cold gas stream.

Transport of solids through the "particle heater" fluidized bed is achieved by inclining the distributor at various angles up to 20° to the horizontal and returning the cooled solids to the top of the slope by mechanical means so as to maintain continuous circulation of solids. A review of the literature established that no similar system had been reported upon and that data on previously reported fluidization phenomena were not directly applicable to design of the type of system investigated here.

A small experimental heat exchanger was built at the University to test the feasibility of the concept. Experiments with this heat exchanger showed that its performance was sufficiently good to justify further development work. Parameters explored included, inclination of the distributor, mean particle size, fluidizing velocity and solids flow rate.

A theoretical model was also developed during the course of the studies to assist design of laboratory apparatus and to predict the performance of larger scale equipment. The model predicted that, for two given gas streams, the rate of heat transferred between the gases is dependent on the circulation rate of the solids and the gas-to-particle heat transfer coefficient. The analysis led to the conclusion that more than one the bed is required to achieve a sufficiently large rate of heat transfer between two gas streams to satisfy industrial criteria, yet the power required to fluidize and to transport the solids is relatively small.

The effect of the solids flow rate and the gas-to-particle heat transfer coefficient upon gas-to-gas heat exchanger design and performance have been evaluated.

The project detailed in this thesis has been sponsored by Komatsu Ltd. The author wishes to acknowledge the advice given to him by Dr. J.R. Howard and the assistance given in construction of apparatus and laboratory work by the staff of Department of Mechanical Engineering.

## CONTENTS

	Page No.
List of tables	vi
List of figures	vii
Nomenclature	xi
Chapter 1 Introduction	
1.1 Fluidized beds	1
1.2 Waste heat recovery	2
1.3 Fluidized bed heat exchangers	3
Chapter 2 Review of literature	
2.1 Introduction	5
2.2 Fluidized beds	5
2.2.1 Minimum fluidizing velocity and pressure drop	7
2.2.2 Particle motion in fluidized bed	10
2.2.3 Entrainment velocity	14
2.2.4 Design of distributor	15
2.2.5 Heat transfer between fluidized bed and wall of the containing vessel	17
2.2.6 Heat transfer between gas and particle	18
2.2.7 Flow of fluidized solids	22
2.2.8 Vertical transport of solid-gas mixture	27
2.2.9 Electrostatic inter-particle effects	34
2.3 Waste heat recovery techniques	35
2.3.1 Rotating regenerators	37
2.3.2 Heat pipe heat exchanger	38
2.3.3 Run-around coil	40
2.3.4 Recuperator	40
2.3.5 Fluidized bed heat exchanger	41
2.3.6 Dilute phase streaming bed	43
2.3.7 Heat storage	44

	Page No.
2.4 Summary of existing work	44
Chapter 3 Theoretical considerations of the heat exchanger design	
3.1 Introduction	69
3.2 Heat transfer model of single stage fluidized bed	70
3.3 Heat transfer model of multi-stage fluidized bed	74
3.4 Theoretical considerations of the design of heat exchanger	77
3.4.1 Overall efficiency of the heat exchanger	77
3.4.2 Basic design of the heat exchanger	79
3.4.3 Prediction of the time to reach steady-state	81
Chapter 4 Experimental heat exchanger	
4.1 Introduction	100
4.2 Aim to the experiments	100
4.3 Design of the experimental unit	101
4.4 Experimental unit	102
4.4.1 Fluidized bed "particle heater"	102
4.4.2 Fluidized bed "particle cooler"	106
4.4.3 Hoppers and vibratory feeder	107
4.5 Instrumentation	108
4.5.1 Air flow measurement	108
4.5.2 Solids flow measurement	108
4.5.3 Temperature measurement	108
4.5.4 Pressure measurement	109
4.5.5 Bubbling observation	110
4.6 Experimental procedure	110
Chapter 5 Operational characteristics of the experimental heat exchanger	

	Page No.	
5.1	Introduction	125
5.2	Distributor plate pressure drop characteristics	125
5.3	Minimum fluidizing velocity of the particle	126
5.4	Fluidization in the bed on inclined distributor	127
	5.4.1 Observation of fluidization	127
	5.4.2 Pressure drop characteristics	128
	5.4.3 Heat transfer between solids and air	129
5.5	Solids flow rate through the "heater"	130
5.6	Heat recovery performance	132
	5.6.1 General review of the data	132
	5.6.2 Effect of the heat capacity flow ratio	133
	5.6.3 Effect of the distributor and the inclined angle	133
	5.6.4 Effects of the flow rates of solids and air	134
5.7	Summary of overall performance of the "particle heater"	134
Chapter 6 Assessment of the fluidized bed gas-to-gas heat exchanger		
6.1	Introduction	157
6.2	Design criteria for large units	157
6.3	Further work	159
	6.3.1 Larger size heat exchanger operating at higher temperature	159
	6.3.2 Advancing basic understanding	160
Chapter 7 Conclusions		
7.1	Conclusions	163
Appendix 1		166
Appendix 2		168
Appendix 3		170
List of references		175

LIST OF TABLE

	Page No.
2.1 ( $C_D$ of irregular shape particle)/( $C_D$ of spherical particle) at various $Re_p$	46
4.1 Specifications of distributor plates used	112
4.2 Basic properties of the bed material	112
5.1 Experimental results of the "particle heater"	136
6.1 Recommended design values for large gas-to-gas heat exchanger	161

## LIST OF FIGURES

	Page No.
2.1 Schematic diagram of a fluidized bed	46
2.2 Pressure drop characteristic of a fluidized bed	47
2.3 Particle motion around a rising bubble	48
2.4 Schematic diagram of a spouted bed	49
2.5 Pressure drop characteristic of a spouted bed	50
2.6 Particle classification for fluidization	51
2.7 Particle motion in a fluidized bed	52
2.8 Diagram of single-section equipment with gas admission through a slot	53
2.9 Schematic diagram of a whirling bed	54
2.10 Correlation for heat transfer at container wall	55
2.11 Continuously fed flowing fluidized bed	56
2.12 Inclined channel flow	56
2.13 Open horizontal channel flow	56
2.14 Idealised section of distributor plate	57
2.15 Pneumatic escalator	57
2.16 Possible upflow patterns in vertical pneumatic conveying showing two types of systems	58
2.17 Rotating regenerator	59
2.18 A heat pipe	60
2.19 A heat-pipe heat exchanger	61
2.20 A liquid coupled indirect heat exchanger, or 'run-around' coil	62
2.21 A unit combining the functions of radiant tube heater and recuperator	63
2.22 Shallow fluidized bed waste heat exchanger	64
2.23 Shallow fluidized bed gas-to-gas heat exchanger	65
2.24 A multi-stage fluidized bed with perforated plates	66

	Page No.
2.25 A falling cloud heat exchanger	67
2.26 A zig-zag contactor	68
3.1 Gas-to-gas heat exchanger	83
3.2 Types of contacting of gas and solids	84
3.3 A heat balance over the differential element of bed length	85
3.4 Efficiency of perfect backmixing solids flow and horizontal plug solids flow for "particle heater"	86
3.5 Efficiency of perfect backmixing solids flow and horizontal plug solids flow for "particle heater" as a function of air velocity	87
3.6 Efficiency of perfect backmixing solids flow and horizontal plug solids flow for "particle heater" as a function of $R_s/R_g$	88
3.7 Efficiency of cross-current contacting for single stage "heater" as a function of $R_s/R_g$	89
3.8 Efficiency of counter-current contacting for the "particle heater" as a function of $R_s/R_g$	90
3.9 Efficiency of the "particle heater" with two-stage beds as a function of $R_s/R_g$	91
3.10 Efficiency of "heater" with three-stage beds as a function of $R_s/R_g$	92
3.11 Efficiency of the gas-to-gas heat exchanger which consists of equal designed single-stage contacting	93
3.12 and 3.13 Efficiency of the gas-to-gas heat exchanger which consists of equal designed multi-stage contacting	94-95
3.14 Three kinds of contacting of gas and solids	96
3.15 Depth of bed with an inclined distributor, $L_f$	97

	Page No.
3.16 Schematic diagrams of gas flow pattern	97
3.17 Model for heat transfer between the gas and the bed	98
3.18 Time to reach steady-state	99
4.1 "Particle heater" configuration	113
4.2 "Particle cooler" configuration	114
4.3 Performance curve of Secomak fan 492/2	115
4.4 Photograph of the complete installation	116
4.5 Schematic diagram of experimental system	117
4.6 Photograph of the equipment on the inclined table	118
4.7 Dimensions of gas distributor for "particle heater"	119
4.8 Dimensions of partitions	120
4.9 Photograph of the vibratory feeder	121
4.10 Particle feed rate of vibratory feeder versus controller scale setting	122
4.11 The standard curve for a 65A Rotameter	123
4.12 Dimensions of transparent bed containment	124
5.1 Pressure drop across distributor plate	137
5.2 Pressure drop across bed	138
5.3 Photograph of fluidization in the bed with horizontal distributor	139
5.4 to 5.9 Photograph of fluidization in the bed with inclined distributor	139-142
5.10 Photograph of fluidization in the "particle heater"	143
5.11 Pressure drop across the bed on inclined distributor	144
5.12 Pressure distribution in bed	145
5.13 Logic diagram for computer simulation of unsteady-state experiments	146

	Page No.
5.14 to 5.16 Dimensionless exit air temperature change	147-149
5.17 and 5.18 Maximum solids flow rate versus inclined angle	150-151
5.19 An example of operating condition of "heater"	152
5.20 Range of the experimental variables	153
5.21 Performance characteristics of the "particle heater"	154
5.22 Effect of the air flow rate	155
5.23 Effect of the solids flow rate	156
6.1 Flow chart for scaling-up the heat exchanger design	162
A1. Model for heat transfer across solids to gas interface during time $\delta t$	173
A2. Model for heat transfer between adjacent cells	174

## NOMENCLATURE

### Variables

A	cross sectional area of bed or tube
$A_W$	area of heat exchange surface
Ar	Archimedes number $Ar = gd_p^3(\rho_s - \rho_g)\rho_g / \mu_g^2$
a	bed length
B	dimensionless quantity given by equation 2.7
C	specific heat at constant pressure
$C_D$	drag coefficient
$C_{DV}$	valve coefficient
D	diameter of tube
$D_h$	distributor plate hole diameter
$d_p$	diameter of particle
$d_t$	diameter of bed
$F_W$	pressure gradient caused by friction
Fr	Froude number $Fr = U^2/(gD)$
f	friction factor
g	accelation due to gravity
h	heat transfer coefficient
L	bed depth
$L_T$	solids height in downcomers
$L_h$	length of heat exchange surface
M	number of cells
m	mass flow
N	number of stages
Nu	Nusselt number $Nu = h_p d_p / \lambda$
P	pressure
$P_h$	distributor hole pitch
Pr	Prandtl number $Pr = \mu_g C_g / \lambda$
Q	heat transfer rate
R	feed rate of heat capacity or solid loading ratio in equation 2.14

Re	Reynolds number $Re = \rho_g U d_p / \mu_g$
S	surface area of particles
T	temperature
T <sub>av</sub>	average air temperature
T <sub>s,f</sub>	solids temperature at feed point
t	time
U	velocity
U <sup>+</sup>	dimensionless velocity
U <sub>o</sub>	gas velocity
W	height of weir
W <sub>b</sub>	weight of bed
W <sub>s</sub>	solids mass flow
z	tube length
ε	voidage
η	efficiency
λ	thermal conductivity of gas
μ	viscosity
ρ	density
σ <sub>n</sub>	standard deviation
φ	particle sphericity

Subscripts

a	air
b, b1, b2	bed
c	"particle cooler"
d	distributor
f	fluidizing
g	gas
h	"particle heater"
in	inlet
mf	minimally fluidized
m	mean

max	maximum
O	orifice
o	initial
out	outlet
p	particle
s	solids
T	terminal
t	tube
tr	transition
W	wall

CHAPTER ONE  
INTRODUCTION

1.1 FLUIDIZED BEDS

Fluidization is the process by which a quantity of solid particles can be made to behave in a fluid-like manner by passing a gas or a liquid through the spaces between the particles. It is not a new technique. An American patent of 1879 (1) describes a process for roasting of minerals whereby mineral ore particles are fluidized under high temperature conditions, (although the word "fluidized" is not used). Attention was drawn to outstandingly uniform temperature in this patent. The next important use of fluidized beds was by Fritz Winkler for the gasification of powdered coal in 1926 (2). In the early 1940's a major successful application of gas-fluidized bed techniques was to the engineering of the catalytic cracking process (3). The techniques of fluidization provided the means whereby the cracking and regeneration reactions could be carried out. The problem of transferring the used catalyst from the reactor to the regenerator and back seemed to have been solved from 1942 onwards (3). Subsequently, the chemical and oil industries concentrated for many years largely on the applications of gas-fluidized systems which exploit the advantages of good gas-to-solid contact and good mixing for chemical reactions and ease of transporting solids. Although the heat transfer properties of the fluidized systems have often been essential to successful operation of a process, this inherent quality was usually taken for granted and not separated out as a primary reason for the particular process application. Nevertheless

the advantageous heat transfer properties find application in fields as diverse as the heat treatment of metals (4), coal combustion furnaces and boilers (5), dryers (6) and heat exchangers (7).

The main purpose of the work described in this thesis was to study heat transfer processes in fluidized beds with a view to establishing whether fluidized beds could be used for industrial gas-to-gas heat exchange operations.

## 1.2 WASTE HEAT RECOVERY

A crisis over supplies of energy was brought to a head in 1973/4 by the formation of OPEC and its collective action at that time which resulted in quadrupling of oil price. Since then accelerated research and development has been in progress worldwide (a) to explore for new source of oil, (b) to provide alternative energy technology to augment the dwindling supply of petroleum and natural gas, and (c) to use energy more efficiently with less waste.

This thesis is concerned with <sup>the</sup> development of a method of recovering heat from hot gases which would otherwise be discharged directly to the atmosphere. One large source of waste energy is hot exhaust gas from combustion systems and heating systems of all types. The degree of commercial viability of such a heat recovery scheme depends strongly on the use to made of the recovered heat (8) and the reliability of the heat recovery equipment. It is important therefore that sight is not lost of these commercial considerations when investigating the technology.

In the particular application in mind here, recovered heat from a furnace exhaust gases would be transferred to the air to be heated.

Necessary characteristics for such a system would be,

1. The system should present a low pressure to the exhaust so as to minimise the pumping power needed.
2. The capital cost and the maintenance cost of the system should be minimal and be small in comparison with the annual cost of providing the same amount of energy by alternative means (e.g. by burning fuel).
3. The size and the complexity of the system should be sufficiently small to make the construction easy and functioning reliable.
4. The system can be operated over a sufficiently wide range of the conditions of hot exhaust gas and the particular fluid to be heated up.

### 1.3 FLUIDIZED BED HEAT EXCHANGERS

Waste heat recovery units based on shallow beds are now commercially available for transferring heat to steam or hot water and they have the all characteristic mentioned above (9). On the other hand, a novel fluidized bed gas-to-gas heat exchanger was proposed and patented by Elliott and Virr in 1978 (10), and the feasibility of this patent was exploited by Newey (11, 12). His results showed that there is a limitation for the pressure difference between two gas streams if a large amount of leakage between them is to be avoided. It seems more difficult to maintain the leakage at a low level for a multi-stage unit

heat exchanger than a single-stage unit heat exchanger. However a multi-stage unit is very necessary if a higher effectiveness than 60% is to be achieved. This effectiveness is normally achievable by some other types heat exchanger such as <sup>the</sup> rotating regenerator and heat pipe heat exchangers.

CHAPTER TWO  
REVIEW OF LITERATURE

2.1 INTRODUCTION

This review studies the ~~existing~~ present state regarding work relevant to the design and ~~the~~ development of ~~the~~ gas-to-gas fluidized bed heat exchanger. Firstly there is a section dealing with some properties of fluidized beds. The second section describes the several types of heat recovery systems

2.2 FLUIDIZED BEDS

A fluidized bed can be considered as a mass of particles supported by a fluid stream as shown in Figure 2.1. The bed of solid particles is contained in a vessel with a porous base through which a fluid flows upward into the bed. This fluid permeates the voids between the particles at low flow rates as shown in Figure 2.1 (i). The bed in this condition is a fixed bed. As the fluid velocity increases, so does the drag force on the particles. At some velocity the drag force on the smallest particles becomes equal to their weight and they become supported on the flow. As the velocity increases progressively, more of the particles become supported and the bed expands gradually with increasing<sup>e in</sup> the number of the particles supported. Eventually a sufficient number of the particles are fully supported<sup>v</sup> by the fluid and the particles then have just sufficient freedom for random movement as shown in Figure 2.1 (ii).

The fixed bed becomes incipiently fluidized at this point. With further small increase in velocity the bed is fully fluidized and exhibits fluid-like properties. The pressure drop across the bed will be equal to the weight of the bed although it is likely that this pressure drop will be exceeded just prior to the achievement of fluidization with gas-fluidized systems because the residual packing and interlocking of particles within the bed must first be broken down. This is indicated by the hump in the stylized curve OAB in Figure 2.2 for bed pressure drop as a function of the fluid flow rate.

With further increase in fluid velocity it makes little difference whether the fluid is a liquid or a gas. If the fluid is a liquid, the bed continues to expand uniformly with increase in the velocity as shown in Figure 2.1 (iii). If the fluid is a gas, the system becomes unstable and cavities containing few solids are formed as shown in Figure 2.1 (iv). These look like bubbles of vapour in a boiling liquid. The upward movement of the bubbles is responsible for the mixing of the particles in the bed. As shown in Figure 2.3 (13), a rising bubble has a wake which tends to lift particles and so induces vertical mixing. The bubbles increase in size by coalescence as they rise.

When the bubbles become comparable in size with the containment at high fluid velocities, the bed is in the slugging regime as shown in Figure 2.1 (v) (14). Slugging is strongly affected by the vessel geometry, especially in tall beds of small diameter. It is usually considered undesirable since it increases the problems of entrainment and lowers the performance potential of the bed.

Further increase in gas velocity will eventually lead to the stage when the terminal velocity of the particles is exceeded locally or generally and the particles become entrained in the gas stream. This is exploited in pneumatic transport systems and is often termed ~~the~~ dilute phase fluidization (15).

For large particles ordinary fluidization may not be practical and so a modified contacting scheme, the spouted bed, may be used. The spouted bed is a combination of a jetlike upward moving dilute fluidized phase surrounded by a slow downflow moving bed through which gas percolates upwards, ~~As~~ shown in Figure 2.4, To date the application of the spouted bed has been limited to a few physical operations such as the drying of grains and peas (16).

All the work reported here concerns gas fluidized beds only, and liquid fluidized system will not be mentioned further. Therefore the results and conclusions of this thesis should not be regarded as indicative of the likely properties of liquid fluidized system similar to that described here.

#### 2.2.1 Minimum fluidizing velocity and pressure drop

Minimum fluidizing velocity,  $U_{mf}$ , is the superficial gas velocity at which the fluidized state is considered to begin. The onset of fluidization occurs when the drag force on the particles becomes equal to the weight of particles. Then the pressure drop developed across the bed by the passage of the gas is equal to the weight of the bed per unit area of the distributor plate:

$$\delta P_b = \frac{W_b}{A} = L_{mf}(1 - \epsilon_{mf}) \left\{ (\rho_s - \rho_g) g \right\} \quad (2.1)$$

The pressure drop through <sup>a</sup>fixed bed of uniformly sized solids has been correlated by Ergun (17) using the equation,

$$\frac{\delta P_b}{L} = \frac{150(1 - \epsilon)^2 \mu_g U}{\epsilon^3 \phi^2 d_p^2} + \frac{1.75(1 - \epsilon) \rho_g U^2}{\epsilon^3 \phi d_p} \quad (2.2)$$

The particle shape factor,  $\phi$  (required for non-spherical particles),  $\epsilon_{mf}$ , are not normally known. To avoid this difficulty, Wen and Yu (2) suggested the empirical correlation equation 2.3 might be of greater practical use:

$$\frac{d_p U_{mf} \rho_g}{\mu_g} = \left\{ 33.7^2 + \frac{0.0408 d_p^3 \rho_g (\rho_s - \rho_g) g}{\mu_g^2} \right\}^{\frac{1}{2}} - 33.7 \quad (2.3)$$

Equation 2.3 was obtained by using the following experimental results obtained from studies of packed beds,

$$\frac{1}{\epsilon_{mf}^5 \phi} \approx 14 \quad \text{and} \quad \frac{1 - \epsilon_{mf}}{\phi^2 \epsilon_{mf}^3} \approx 11$$

and inserting them in equation 2.1 and 2.2, and solving the resulting quadratic equation when 2.1 and 2.2 are combined. For 284 data points <sup>over the</sup> Reynolds number range of 0.001 to 4000 these expressions have been found to give predictions of  $U_{mf}$  with a standard deviation of  $\pm 34\%$ . Using equation 2.1 and 2.2, Todes, Goroshko and Rosenbaum (18) obtained equation 2.4 for

approximate calculations (with an accuracy of the order of  $\pm 20\%$ ), assuming that the particles, so that

$$\phi \simeq 1 \quad \text{and} \quad \epsilon_{mf} \simeq 0.4$$

$$\frac{d_p U_{mf} \rho_g}{\mu_g} = \frac{Ar}{1,400 + 5.22\sqrt{Ar}} \quad (2.4)$$

where

$$Ar = \frac{gd_p^3(\rho_s - \rho_g)\rho_g}{\mu_g^2}$$

Both equation 2.3 and equation 2.4 assume that no interaction occurs between the particles as the equations are based on the packed bed condition rather than a fluidized bed. This approach is equivalent to regarding the limit of stability as the limiting state of a still stationary bed.

If a bed of granular material is fluidized for the first time, it has to be expanded before reaching the minimum fluidization velocity. With a further increase in gas velocity, the packed bed suddenly "unlocks", resulting in a decrease in pressure drop to the static pressure of the bed, as given by equation 2.1. However real systems do not have a clearly definable transition to the fluidized state as shown OCB in Figure 2.2.

The transition is gradual for a number of reasons, the most important of which is that all the particles will normally be of different sizes and shapes and so the drag force on each of them is different for a given  $U_f$ . Hence, not all the particles

become fully supported simultaneously and there is a range of  $U_f$  before the entire bed is in <sup>the</sup> fluidized state.  
^

A pressure drop versus velocity diagram is useful as a rough indication of the quality of fluidization, especially when visual observation is not possible. For example <sup>an</sup> ~~the~~ abnormally low pressure drop suggests incomplete contacting with particles only partly fluidized, called "channelling" (2).

<sup>a</sup>  
In the case of <sup>^</sup>spouted bed, the pressure drop versus velocity diagram depends on not only the bed height and the particle nature, but also the geometry of the equipment. More of the gas flows through the peripheral annulus as the diameters of the apparatus and gas inlet are made larger, or as the air velocity and angle of the conical inlet section are reduced (19). Figure 2.5 shows typical curves for the relationship between the pressure drop and gas velocity both before and after the beginning of spouting. Leva (20) explains the nature of these curves as follows. Initially, the fluid permeates through the bed, (section OA) after which a short channel forms in the lower portion; as a result of this the bed resistance begins to fall (section ABC) when the velocity is further increased, since the channel then grows higher. When the channel finally extends through the whole bed, there is another sharp fall in  $\Delta P$  (section CD) and a stabilization of the bed resistance as spouting sets in. If the air flow rate were now reduced, spouting does not cease at point D in Figure 2.5 but at point  $D_{m,s}$ , corresponding to the so-called minimum spouting velocity.

### 2.2.2 Particle motion in fluidized bed

The motion of the particles in the bed is largely induced by

bubbles rising through the bed, and it causes intensive mixing of the particles and fluid, which has very important effects on heat and mass transfer and on chemical reaction. Bubble formation and particle motion induced by bubbling is of considerable practical importance and has occupied the attention of many researchers, but because of the complexity of the phenomenon the subject is still not fully understood.

One approach has been ~~done~~<sup>made</sup> by Geldart (21), who classified granular materials according to the way they behave when they are fluidized. Four categories emerge from this attempt at classification and Figure 2.6 illustrates this. Particles belonging to Group C are either very small or cohesive and are generally very difficult to fluidize. Group C particles are characterised by being so small that the inter-particle forces are large in comparison to the gravitational force on the particle. Group A particles with size in the range 20 to 100  $\mu\text{m}$  are used extensively in the petrochemical industry, but these are too light to be of use in heat recovery units because of their low entrainment velocity. This group is marked by high bed expansions and limited bubble growth. Group B particles with size in the range 40 to 500  $\mu\text{m}$  show a bubble growth proportional to the bed height, and Group D particles with size over 600  $\mu\text{m}$  fluidize unstably with a lot of cross-coalesced bubbles and are capable of forming a spouted bed. Group B particles might be suitable for the heat recovery units, however it is possible to reduce the size of the unit by using Group D particles because of the enlarged gas velocity through the beds.

In describing the usual particle circulation in small-diameter fluidized bed, Leva (20) noted that the particles could be seen through the transparent walls of a tube to move downward and then

suddenly away from the walls into the bed as shown in Figure 2.7. However in shallow beds the descending particle motion around the walls is feebly developed, and particle motion appears to be more uniform, bubble size small, and less bubble, the particle motion is caused by the passage of bubbles. Various authors (22, 23, 24) have observed that particles are carried upwards by the bubble wake and move downwards elsewhere.

In a few cases the description of the solid mixing is based on a circulation rate of the solid (25), because some experimental findings suggest (2) that it can be estimated from the number and size of bubbles passing through the bed. Heertjes et al (26) proposed a model for shallow beds with cross flow of solids. A number of units was used, equal to the average number of gas bubbles breaking through the surface. The authors distinguish between a top layer with a relatively fast horizontal solid transport and an underlying layer with perfect mixing. Although their result calculated from the model had a reasonable agreement with the experimental results using silica gel particles of a particle size between 150  $\mu\text{m}$  and 250  $\mu\text{m}$ , it seems difficult to apply their equations in situations where <sup>the</sup> particle size or distributor is different from their experimental condition. They simply identified the number of units from the number of bubbling at the top of bed, and it may depend on the particle size or the design of distributor.

Diffusion models have been used to account for and describe the solid mixing in beds. A number of investigators (27, 28, 29, 30) have used the diffusion model approach but with different experimental methods for vertical and lateral mixing. Comparison of ~~the~~ both mixing results suggests that vertical mixing is some five to ten times faster than lateral mixing. This result is of

importance when we consider the residence time distribution of particles in flowing fluidized beds.

On the other hand, the movement of particles within a spouted bed follows a regular and easily studied pattern. Several investigations on particle flow in the spout and the annulus, solid circulation rates and mixing characteristics have been reported (31, 32). Particles entering the spout near the orifice from the annular region accelerate rapidly from rest to a peak velocity, and then begin to slow down until they reach zero velocity at the spout top. The main accelerating force is due to the frictional drag on the particles by the jet, while deceleration is caused by gravity and by collisions between the particles and the spout wall. The particles which have reached the bed surface from the spout top travel down the annulus along an approximately parabolic path towards the spout (19). If the slot inlet is so arranged that the spouting gas enters the bed tangentially, as shown in Figure 2.8, the bed solids are transported upward as a dilute phase along one wall of the column and slide downward as a dense phase along the opposite wall. The vortex movement thus established is reported by Mitev (6) to be more stable than with vertical introduction of the spouting gas, and could be achieved for a wide variety of solids.

The whirling bed as proposed by Baxerres and Gibert (33) is essentially a solid circulation system in which a high intensity mixing movement is obtained using a special distributor. Basically, the idea is to prevent uniform gas distribution at the bottom of the column by fixing a wedge on the grid plate. One example working with cylindrical columns is illustrated on Figure 2.9. It also shows the cyclic solids movement in the column; the solids travel upwards by pneumatic transport above the free

zone of the distributor, and downwards in the space above the wedge. Rios et al (34) show the whirling (or circulating) bed improves the contact efficiency between gas and particles, which is poor in "ordinary fluidized beds" of Group D particles because of a very strong tendency to slugging and channelling.

### 2.2.3 Entrainment velocity

The terminal velocity of a free particle falling in the gas,  $U_T$ , is often assumed to be the same as the entrainment velocity of the particles. An expression for  $U_T$  for a spherical body can be derived from fluid mechanics (35),

$$U_T = \left\{ \frac{4gd_p(\rho_s - \rho_g)}{3\rho_g C_D} \right\}^{\frac{1}{2}} \quad (2.5)$$

where  $C_D$  is an experimentally determined drag coefficient. Empirical approximate  $C_D$  and  $U_T$  in the Reynolds number range is as follows.

$$(a) \quad C_D = \frac{24}{Re_p}, \quad U_T = \frac{gd_p^2(\rho_s - \rho_g)}{18\mu_g} \quad \text{for } Re_p < 1$$

$$(b) \quad C_D = \frac{10}{Re_p^{\frac{1}{2}}}, \quad U_T = \left\{ \frac{4(\rho_s - \rho_g)g}{225\rho_g\mu_g} \right\}^{\frac{1}{3}} d_p \quad \text{for } 1 < Re_p < 500$$

$$(c) \quad C_D = 0.44, \quad U_T = \left\{ \frac{3g(\rho_s - \rho_g)d_p}{\rho_g} \right\}^{\frac{1}{2}}$$

for  $500 < Re_p < 200000$

However, real particles are not spherical. Shirai et al (36) report that  $C_D$  <sup>for</sup> irregular shape particles is larger than <sup>for</sup> spherical ~~shape~~ <sup>particles</sup> specially in <sup>the</sup> high  $Re_p$  ranges shown as Table 2.1.

#### 2.2.4 Design of distributor

The purpose of the distributor is to provide even fluidization and to support the bed weight. In the shallow beds at low temperature the latter is easy to achieve, but for the high temperature bed the materials of the distributor must be chosen carefully according to the physical properties at the operating temperature and the corrosion resistance if the distributor works in corrosive environments. To obtain uniform fluidization the distributor should provide equal gas flows to all areas of the bed and should do this with as low a pressure drop as possible to minimise the pumping power needed. The quality of bubbling fluidization is strongly influenced by the type of gas distributor (37, 38). If it has only a few openings the bed may channel or slug and the bed density fluctuates widely. This is particularly severe in shallow beds. Use of shallow beds for heat transfer system distributors are normally restricted to either porous media or pierced plates with closely pitched holes or slots. Other distributor types, like bubble caps, tuyeres or simple orifices, such as are used in deep bed, are hardly used because

sufficient lateral gas diffusion to give uniform fluidization cannot occur until some distance above the distributors. The latter condition would lead to spouting or channelling in shallow beds.

Many investigators have paid special attention to the criterion of distributor for uniform fluidization. For instance Whitehead (6) has suggested that the distributor pressure drop should be at least 40% that of the deep bed. Agarwal et al (39) recommend that pressure drop across the distributor plate be roughly 10% of the shallow bed, with minimum pressure drop in all cases of about 35 cm H<sub>2</sub>O. However the value chosen depends upon many other factors (2), and it is generally desirable to keep pressure drops as low as possible to limit the pumping power required. Fluidization can easily become unstable with severe channelling and local defluidization when such low pressure drop distributor are used, so care must be taken.

When commercial development is anticipated, the material will be finally chosen according to the structure of bed and the environmental condition. Especially at temperatures higher than 700°C the design of the distributor and the support parts should be carefully decided, because the thermal stress may cause large distortion or cracks on the distributor plate and it will make the fluidization uneven. ~~The~~ Corrosive material or the dust carried in <sup>the</sup> gas might block or damage the distributor. It should also be noted that quality control is normally difficult in the manufacture of distributors, and supposedly identical plates may differ substantially in actual performance.

2.2.5 Heat transfer between fluidized bed and wall of the containing vessel

A number of experimental investigation have been reported on heat transfer between fluidized bed and the wall of the containing vessel (40, 41, 42, 43). However there are considerable differences among the results of different works. This may be caused by various factors affecting the heat transfer coefficient such as the physical properties of the gas and the particles and the size of the bed. Wen and Leva (44) correlated the data of four groups of investigators (42, 43, 45, 46, 47), and obtained the following expression

$$\frac{h_w d_p}{\lambda} = 0.16 \left( \frac{C_g \mu}{\lambda} \right)^{0.4} \left( \frac{d_p \rho_g U_o}{\mu} \right)^{0.76} \left( \frac{\rho_s C_s}{\rho_g C_g} \right)^{0.4} \left( \frac{U_o^2}{g d_p} \right)^{-0.2} \cdot \left( \frac{L_{mf}}{L_f} \right)^{0.36} \quad (2.6)$$

where  $\eta_f$  is the fluidization efficiency defined as

$$\eta_f = \frac{U_o - (\text{superficial velocity for uniform expansion of bed})}{U_o}$$

This correlation covers a broad range of test materials, and about 95% of the data used fell within  $\pm 50\%$  of the values predicted.

Another generalized correlation was presented by Wender and Cooper (48). This is based on five studies (40, 42, 45, 46, 47, 49).

Figure 2.9 shows the diagram of

$$B = \frac{(h_w d_p / \lambda) / [(1 - \epsilon_f) C_s \rho_s / C_g \rho_g]}{1 + 7.5 \exp[-0.44(L_h / d_t)(C_g / C_s)]} \quad (2.7)$$

against  $Re_p (= U_o d_p / \mu)$ . However Botterill (50) recommended the simple approximate correlation which has been given by Zabrodsky (51) for the maximum bed to surface heat transfer coefficient with

particles of Geldart's class "B". This has the form:

$$h_{W,max} = 35.8 \rho_s^{0.2} \lambda^{0.6} d_p^{-0.36} \quad (2.8)$$

One might expect to obtain values of 70% of this maximum under reasonable operating conditions.

The mechanism of heat transfer between the wall and fluidized bed was pursued and some proposals were made (43, 52, 53). Though the detail descriptions of the mechanism is omitted, it should be emphasized that the gas boundary film formed along the wall surface, the motion of particles in this region are regarded to be very important factor controlling the heat transfer to the emulsion phase adjacent to the wall.

#### 2.2.6 Heat transfer between gas and particle

In the process of the design or the evaluation of the heat exchanger performance, it is very necessary to know the gas-to-particle heat transfer coefficient under <sup>the</sup> proposed bed operating conditions. Gas-to-particle heat transfer in fluidized bed systems in general, has been extensively studied and many correlations for the heat transfer coefficient have been developed over a wide range of operating conditions. However, great difficulty in interpretation of gas-to-particle heat transfer is caused by the wide variation in the published data. Kunii and Levenspiel (2) state that this variation is over one thousandfold between different observers. They observed that there is wide variation the experimental conditions used and in data interpretation among them. In particular, these must be examined to see how to determine gas-to-particle heat transfer coefficient, namely, through measurement of gas temperature, measurement of particle temperature and flow pattern assumption for the gas.

Essentially two types of experiments have been used to find  $h_p$  in fluidized bed: the steady-state and the unsteady-state experiment. In the steady-state, hot gas enters a bed which is kept cool. Most investigators probed the changing gas temperature close to the bed entrance. However it is difficult to evaluate the gas temperature by measurement because the gas temperatures of bubble and emulsion are different and most measurement read their some average. In the unsteady-state setup the temperatures of entering and exit gas are measured with time, and a heat balance gives the temperature of solids at any time, from which  $h_p$  is found. ~~The~~ All investigators made one of two assumptions for <sup>the flow</sup> gas, either backmix or plug flow. The majority, noting that large disturbances of gas exist in the bed, assumed complete mixing of gas throughout the bed, hence backmix flow of gas.

The results are usually presented with the dependent variable being a Nusselt number,  $Nu = h_p d_p / \lambda$ , which includes  $h_p$ , the gas-to-particle heat transfer coefficient. The simplest case of gas-to-particle heat transfer is that of a single sphere in an infinite medium. In this instance  $Nu$  is given by Ranz and Marshall (54) as

$$Nu = 2 + 0.6 Pr^{1/3} Re^{1/2} \quad (2.8a)$$

which demonstrates that the minimum value of  $Nu$  is 2, which represents heat transfer in an infinite stagnant medium, a condition which depends only on the thermal conductivity of the medium.

On the other hand, Frantz (55) discussed the variation of the experimental results of different investigators on the gas-to-

particle heat transfer in fluidized beds. He calculated  $Nu \cdot Pr^{-1/3}$  from the results of Walton (56) and Heertjes (57), who measured the gas and the solids temperatures in a steady-state fluidized bed, and plotted it against  $Re$ . Walton measured the solids temperature,  $T_s$ , by a bare thermocouple within the main portion of the bed, and Heertjes showed that the same value of  $T_s$  was given substantially by the different methods such as measuring <sup>with</sup> a bare thermocouple in a collapsed bed or measuring the exit gas temperature. They both measured the gas temperature by a suction thermocouple which only sampled the gas. The resultant expression from their experiments is

$$Nu = 0.015 Re^{1.6} Pr^{1/3} \quad (2.9)$$

Frantz nominated  $h_p$  thus obtained as the true heat transfer coefficient and separated it from the apparent heat transfer coefficient obtained by measuring the gas temperature with bare thermocouples. Kunii and Levenspiel (2) considered that data calculated assuming that the gas flow pattern was plug flow were more reliable because the data appears to be more consistent. Nevertheless this assertion of reliability may be challenged, because experimental findings show that gas flow in fluidized bed is nearly the extremes of backmix flow. (34) However all available data reported on this basis are correlated by

$$Nu = \overset{0.03}{0.3} Re^{\overset{1.3}{1.3}} \cdot 0.02 \quad (2.10)$$

The comparison between the two gas-to-particle heat transfer coefficients for a single sphere in a infinite medium and for particles in fluidized beds, obtained from equations 2.8 and 2.10, shows that  $h_p$  for fluidized beds is considerably smaller than the theoretical value of a single sphere in ordinary gas convective

operating conditions at lower Re than 25; Nu of fluidized bed falls below 2 for <sup>the</sup> single sphere condition of conduction alone. This discrepancy was explained by Kato and Wen (58) who considered that the effective heat transfer area is much less than the total particle area because the regions near the points of contact between the particles cannot be contacted by the gas. The thermal boundary layers which surround the particles overlap and the gas cannot easily penetrate these to reach the particles' surfaces. Chang and Wen (59) suggested the important relation between the gas film of particles and the bed depth. Based on the bubble assemblage model, Kato and Wen (58) re-examined the results of selected investigators and attempted to introduce the bed depth,  $L_f$ , as a variable when comparing the results of these investigators. Kato et al (60) obtain <sup>ed the</sup> following empirical equation in the range of  $3 < Re < 50$ , assuming no lateral mixing of gas in the bed.

$$Nu = 0.59 Re^{1.1} \left( \frac{d_p}{L_f} \right)^{0.9} \quad (2.11)$$

Equation 2.11 suggests that as the bed depth increases, the thickness of the thermal boundary layers decreases so Nu rises towards the predictions of the single sphere equation.

Furthermore, McGaw (61) pointed out that the geometry of the containment and the distributor is important to estimate  $h_p$ . He developed the following correlation for shallow beds of particles a few mm in size, up to 33 mm in depth and with a distributor having holes on a triangular array, assuming no lateral mixing of gas in the bed and perfect mixing of particles in <sup>the</sup> vertical plane:

$$\text{Nu} = 0.353 \text{Re}^{0.9} \left( \frac{d_p}{L_f} \right)^{0.47} \left( \frac{D_h}{P_h} \right)^{0.19} \quad (2.12)$$

where  $D_h$  is distributor plate hole diameter and  $P_h$  is distributor hole pitch. The range of Reynolds numbers investigated was  $100 < \text{Re} < 850$ , which is larger than the range of  $\text{Re}$  of equation 2.11.

The determination of a gas-to-particle heat transfer coefficient in a spouted bed is complicated by the difficulty of selecting the appropriate temperature driving force and the corresponding heat transfer area. Although the particle temperature can reasonably be taken as uniform throughout the bed since the solids are well-agitated, the gas temperature is far from being uniform. Uemaki and Kugo (6) measured the temperature profiles in the spouted bed, and obtained the heat transfer coefficient which were estimated to be 1/5 - 1/10 of values expected for a fluidized bed under similar conditions. The reason for the low values was considered to be that in a spouted bed, only a small fraction of the total bed solids reside in the heat transfer zone. In addition, it is the same reason for the poor heat transfer between gas and particles in a partly fluidized or channelling bed.

#### 2.2.7 Flow of fluidized solids

It is apparent that the many attractive features of a fluidized bed originate in its fluidity. To study this property a number of investigators (62, 63, 64, 65) measured the viscosities of beds by different methods. Their results suggest the following conclusions.

1. Gas velocity plays but minor roles in influencing viscosities except close to  $U_{mf}$  where the viscosity ~~rises~~ <sup>falls</sup> sharply. *as velocity increases from just less than  $U_{mf}$  and then rises gradually again.*
2. The viscosity is strongly affected by the particle size and the size distribution; — the larger the solids, the higher the viscosity. The increase is normally more marked in deeper beds due to the reduced homogeneity therein when fluidizing large particles. However adding a relatively small amount of fine particles to a bed of large material sharply reduces the viscosity to that of a bed of fines. The fines may act as a lubricant to reduce the friction between coarse material.
3. The viscosity of a shallow fluidized bed increases with the bed depth, due to the disturbing influence of the larger bubbles present in deeper beds.

On the other hand, there are five distinct methods by which fluidized beds have been made to flow; *see Figs 2.11 to 2.15*

- (i) a fluidized bed may be fed continuously from a hopper at one end and the depth kept constant by a weir at the other. (26, 61, 66, 67, 68, 69)
- (ii) the distributor may form the base of an inclined channel. (65, 70, 71)
- (iii) the distributor can be formed into continuous loop shaped like a running track, the bed being fluidized in the usual manner but paddle wheels push the material around the circuit. (71)
- (iv) the gas flow from a distributor having jets discharging at an acute angle to the plane of the distributor may supply the transverse momentum to particles to enable them to flow. (11, 12)
- (v) the fluidized bed may be sectionalized to a number of cells

and the distributor inclined, the dividing plates being arranged so that the solids can flow from one cell to the next, as shown in Figure 2.15. (72, 73)

The study of vertical flow in continuously fed beds has been carried out for a number of years to investigate various models of solid mixing (66). Although the reported work on a rectangular section fluidized bed with a weir at the other end of the solid inlet (Figure 2.11) is very limited in extent, its use has been reported for process heating of granular coke and for cooling granular fertilizers, sulphur and powdered milk (67). Thermal analysis on such a system <sup>has</sup> ~~have~~ been carried out by McGaw (61, 68). He measured the particle residence time distribution in a continuously fed bed (69). He used 1.25 mm diameter glass beads in a fluidized bed 29.4 cm long, 5.1 cm wide and from 16 to 63 mm deep. The actual distributions were always between plug flow and perfect mixing. As the bed depth decreased the distribution approached plug flow, though the fluidizing air velocity did not appear to affect the mixing greatly. He stated that heat transfer was faster with plug flow and so shallower beds should be better. In contrast to McGaw's work, Heertjes et al (26) reported that fluidizing gas velocity affected the particle residence time distributions using smaller particles between 150  $\mu\text{m}$  and 250  $\mu\text{m}$ . They stated that shallower bed and lower gas velocities lead to an increased minimum residence time and approached plug flow. The lack of agreement of two works' results seems to be caused by the difference of the contribution of excess gas to the bubbling in the beds with different size particles.

Studies of the flow of fluidized beds down inclined channels (Figure 2.12) have been carried out mainly to understand flow

phenomena such as slip and viscosity. McGuigan (65) intended to elucidate the flow behaviour of the bed and its associated viscosity and shear properties for industrial application. He found that at low fluidizing velocities, the flow was adversely affected by settlement of stagnant layer of particles on the distributor, which gave rise to increased flow resistance, especially in shallow beds. Conversely at higher fluidizing velocities, the resistance at the distributor appeared to be less than at the walls. Ishida et al (70) measured the flow velocity of solid particles in a open channel using an optical probe and classified the flow patterns into five types depending on the fluid velocity and the inclination angle. Only when the air velocity increased beyond  $U_{mf}$  and with very low angle of inclination, less than  $5^\circ$ , was bubbling observed. As the inclination angle was increased, the rapid stream of particles extinguished the bubbles as remarked by McGuigan (65) and Botterill and Abdul-Halim (71). The particle shows laminar movement and the velocity near the surface of bed is higher at than the bottom.

The fluidizing particles in a horizontal continuous loop channel bed can be moved by a paddle-wheel arrangement as shown in Figure 2.13. Botterill and Abdul-Halim (71) reported experiments on the forced flows of two kinds of solids, a catalyst of mean diameter  $77 \mu\text{m}$  and a sand of  $200 \mu\text{m}$ , in a open channel. Their results showed that the catalyst expanded stably and flowed as on an air slide; on the other hand, the flow properties of the sand were strongly influenced by bubble development. The trends in the horizontal and inclined channels are qualitatively similar, but quantitative agreement was not apparent, possibly due to the difficulties of calibrating the viscometers accurately. Especially for bubbling rising flow, it will possess different

flow characteristics between the vertical and horizontal directions.

*and (12)*

Newey (11)<sub>f</sub> reported on the development of a fluidized bed gas-to-gas heat exchanger, where fluidizing particles are moved by fluidizing gas emerging with a significant transverse component of velocity. Figure 2.14 shows a suitable design for a distributor which has directional air flow properties. The fluidizing gas emerges as a jet in a direction inclined to the plane of the distributor and under certain conditions there is a sufficiently large transverse component of momentum to make the solid flow. He measured the solids' velocity by timing the *distance travelled* ~~passage~~<sup>by</sup> of a float, although its use has been criticised by McGuigan (65) as being unrepresentative of the flow velocity of the solids. However the use of a float remained the only simple method of assessing solids velocity. Newey reported that the onset of solids' flow is quite sudden when  $U_f$  is about  $2 U_{mf}$  and that the shallower bed flows more easily.

A pneumatic escalator can be devised for transporting particles; the particles are blown up along inclined plate and conveyed to the next cell with air (Figure 2.15). It was developed initially to convey particles through a duct with air or gas by Shinohara and Tanaka (72). They investigated the average residence time, the pressure drop of air or gas, and the power required to convey solids. Shinohara and Yasuda (73) reported on its heat transfer characteristics with particles. They found that  $Nu$  increases with  $Re$ , particle concentration and average temperature of air and with decreasing particle size as

$$\text{Nu} = 1.52 \times 10^{-4} \text{Re}^{1.72} (1 - \epsilon)^{-0.51} \left( \frac{T_{\text{av}}}{T_{\text{s,f}}} \right)^{0.25} \exp \left( -46.7 \frac{d_p}{D} \right) \quad (2.13)$$

They stated the pneumatic escalator could be utilized satisfactorily for simultaneous heat transfer and particle conveying in a continuous dry system.

A few common properties may be found among these five distinct methods of solids transport. Firstly the shallow beds flow more easily due to the absence of large bubbles. The heat transfer between gas and particles is faster with plug solid cross flow and so shallow beds flow is suitable for heat exchanger. Secondly there is no accurate method to measure the total amount of solid flow in the bed. Only an external catch pot system seems an unquestionable method for accurate measurement of steady state solids flows. Lastly it seems very difficult to estimate the solid mixing in the flowing bed because the solid flow is not homogeneous in vertical cross section of a bed.

#### 2.2.8 Vertical transport of solid-gas mixture

The scope of the review in this section is confined to (i) upflow of particulate solids in a tube as occurs in vertical pneumatic conveying and riser-reactors; and (ii) downflow of particulate solids in a vertical standpipe. The aim is to present some view on the status of knowledge of the subjects so as to design the solids circulation system of a fluidized bed gas-to-gas heat

exchanger and to develop the system.

The different flow regimes in vertical upflows of granular materials may be described in terms of a flowchart as shown in Figure 2.16 (74). At a very high gas velocity, solids are conveyed in an apparently uniform suspension in so-called "lean" or "dilute phase" flow at a voidage close to one. As the gas velocity is reduced at a fixed solid flow rate, solid concentration in the tube increased. In ~~the~~ systems of coarse particles in small tubes, which are commonly used for the pneumatic transport of fluidized bed solids, a sharp transition point will eventually be reached at which the uniform suspension collapses and the solids are then conveyed upward in dense phase slugging flow with solids carried upwards mainly in the wakes of rising slugs. A number of empirical correlations (75) are available for the prediction of this sharp transition point which is known as the "choking point". Leung (74) recommended Yang's correlation which is rewritten in the following dimensionless form

$$R = \left[ 1 - \left\{ 0.05 \text{Fr} \left( U_g^+ - 1 \right)^2 + 1 \right\}^{-0.213} \right] \left( 1 - \frac{1}{U_g^+} \right) \left( \frac{\rho_s}{\rho_g} \right) \quad (2.14)$$

where  $U_g^+ = U_g / U_{tr}$  and  $\text{Fr} = U_{tr}^2 / (gD)$

The transition gas velocity,  $U_{tr}$ , is defined as the choking velocity for the particular solid loading ratio,  $R$ . In dense phase slugging conveying, if the gas velocity is further reduced at the same solid flow rate, a point will eventually be reached when slip velocity is no longer sufficient to support the particles in suspension and transition from dense-phase slugging conveying to

packed bed or moving bed flow occurs. This type of gas-solid-tube system is represented by the right hand branch of the flow chart in Figure 2.16. On the other hand, fine particles in large tubes tend to exhibit the non-choking phenomenon as represented by the left hand branch in Figure 2.16. For the prediction of demarcation between choking and non-choking systems, Leung (74) recommended Yang's equation which criterion becomes

$$0.35 \sqrt{gD} > U_{tr} \quad \text{for no choking}$$

$$\text{or} \quad U_{tr} / (gD)^{0.5} > 0.35 \quad \text{for choking to occur} \quad (2.15)$$

A large number of correlations for predicting pressure gradient in lean phase vertical pneumatic conveying is available in the literature. The vertical pneumatic conveying can be described by means of one-dimensional, isothermal steady-state mass and momentum balances. The common differential equations are as follows (76).

fluid continuity

$$\frac{d}{dz} (\epsilon \rho_g U_g) = 0 \quad (2.16)$$

solid continuity

$$\frac{d}{dz} [(1 - \epsilon) \rho_s U_s] = 0 \quad (2.17)$$

mixture momentum

$$\begin{aligned} -\frac{dp}{dz} &= (1 - \epsilon) \rho_s U_s \frac{dU_g}{dz} + \epsilon \rho_g U_g \frac{dU_s}{dz} \\ &+ [\rho_s (1 - \epsilon) + \rho_g \epsilon] g + F_w \end{aligned} \quad (2.18)$$

$F_w$  in equation 2.18 represents the pressure gradient caused by friction between the gas-solid mixture and the wall. It is usual to consider wall friction to be made up of two additive components, one for gas and one for the solid, i.e.

$$F_w = \frac{2f_g \rho_g U_g^2}{D} + \frac{2f_s (1 - \epsilon) \rho_s U_s^2}{D} \quad (2.19)$$

where  $f_s$ ,  $f_g$  are solid and gas friction factors respectively and  $f_g$  is often assumed to be the same as the Fanning friction factor. For a given  $\rho_s$ ,  $U_s$ ,  $\rho_g$ ,  $U_g$  and  $D$ , there are two unknowns before pressure gradient can be estimated, viz.  $U_s$  (or  $\epsilon$ ) and  $f_s$ . Konno and Saito (77) proposed the following correlation.

$$U_g - U_s = U_{tr} \quad (2.20)$$

and

$$f_s = 0.0285 / (U_s / \sqrt{gD}) \quad (2.21)$$

Modi et al (78) suggested that this correlation gave reasonable agreement with published results on pneumatic conveying of coal. However it does not take into account the parameter of the coefficient of friction between particle and wall. Leung (74) suggested that this omission throws doubt on whether their correlations may be extrapolated with confidence. A number of workers considered the contribution of the particle-wall coefficient of friction (79), but the validity of their equations is as yet unknown because information on the coefficient of friction between particle and wall is often not available for evaluation of the equations.

Downflow of particulate solids in a standpipe occurs in flow out

of a fluidized bed, down a hopper outlet and down a cyclone dipleg. Smooth operation in the standpipe of a system is often critical and problems such as flow interruption, flow fluctuations and general flow instability can often be traced to mal-operation in the standpipe. Leung and Jones (80) stated that these problems are caused by the possibility of four different flow patterns and the coexistence of more than one flow pattern in the standpipe. They distinguished the four flow modes as following.

1. Dense phase fluidized solids flow (DENFLO) in which particles are in suspension often at a voidage close to  $\epsilon_0$ . It is also known as "bubbly dense phase flow" to indicate the occasional presence of bubbles. The bubbles usually flow downwards in industrial standpipes.
2. Lean phase fluidized solid flow (LEANFLO) in which particles flow down at high voidage sometimes in the form of "streamers".
3. Packed bed flow (PACFLO) in which solids flow en bloc with little relative motion between gas and solids. The slip velocity here will be less than that at minimum fluidization.
4. Slip-stick flow (STIKFLO) in which solids flow is jerky, oscillating between flow and non-flow.

In both LEANFLO and DENFLO, particles are in suspension. Thus the two flow regimes can generally be classified as fluidized solid flow. In both PACFLO and STIKFLO, slip velocity is less than minimum fluidization velocity and they can be classified as non-fluidized solid flow.

Leung and Jones (80) combined the previously published equations to indicate the conditions for a standpipe with fixed terminal pressures and a slide valve near its lower end where different flow modes would occur. In particular it was shown that there is a critical aeration rate above which either PACFLO throughout

the pipe or DENFLO throughout the pipe would occur. However there was some uncertainty about whether operation would occur, which depends on the characteristics of solid.

Eleftheriades and Judd (81) experimentally investigated the solid flow in downcomers, using sand of mean diameter 0.5 mm. The dynamic behaviour of this system has been studied and a simple force-momentum balance equation

$$-\delta P - \frac{W_s^2}{\rho_s(1 - \epsilon_{mf})} - 2f_s \frac{L_T W_s^2}{D \cdot \rho_s(1 - \epsilon_{mf})} + \rho_s(1 - \epsilon_{mf})g L_T = 0 \quad (2.22)$$

and a modified Ergun equation (from equation 2.22)

$$-\frac{\delta P}{L_T} = 150 \left( \frac{1 - \epsilon_{mf}}{\epsilon_{mf}} \right)^2 \frac{\mu_g \delta U}{\phi^2 d_p^2} + 1.75 \left( \frac{1 - \epsilon_{mf}}{\epsilon_{mf}} \right) \frac{\rho_g \delta U}{\phi d_p} |\delta U| \quad (2.23)$$

where

$$\delta U = (\text{slip velocity}) = U_g - U_s = \frac{U_g}{\epsilon_{mf}} - \frac{W_s}{\rho_s(1 - \epsilon_{mf})}$$

can be used to describe moving bed flow in a downcomer. They suggested an iterative scheme for sizing downcomers.

In many industrial standpipes, a slide valve or some other restriction is often present at the lower end for control of solid flow and pressure balance. Often such a restriction is

necessary to give adequate pressure build-up in the standpipe. For design of an orifice for flow of fluidized particles, Leung (74) recommended ~~to~~ use <sup>of</sup> the following equation which can predict solid mass flow rate.

$$|W_s| = C_{DV} (A_0 / A) \sqrt{\rho_s (1 - \epsilon_{mf}) \delta P_0} \quad (2.24)$$

Predictions from this equation with  $C_{DV}$  in the range of 0.5 to 0.65 were shown to agree with extensive results. For flow of a fluidized mixture through an orifice, the solid and gas flow rate may be related by adapting the Ergun equation as following.

$$\delta P_0 = K_1 D_0 \left( \frac{A}{A_0} \right) \frac{\delta U}{4} + K_2 D_0 \left( \frac{A}{A_0} \right) \frac{\delta U |\delta U|}{4} \quad (2.25)$$

where

$$K_1 = [150 \mu_g (1 - \epsilon)^2] / (\phi d_p \epsilon)^2$$

$$K_2 = 1.75 \rho_g (1 - \epsilon) / (\phi d_p \epsilon)$$

Leung (74) stated that equation 2.25 permits the calculation of gas flow through an orifice if  $\delta P_0$  is known. For solid flow rate through non-mechanical valves such as an L-valve, a J-valve or reverse seal. Knowlton and Aquino (82) reported that the most aeration-efficient non-mechanical valve was the L-valve, which was just slightly more efficient than the J-valve. They also stated that the non-mechanical valves generally used less gas to feed solids into the lift line than the lift-pot devices.

While some progress has been made in recent years in understanding ~~of~~ <sup>the</sup> vertical transport of solid-gas mixtures, the stage seems not to have been reached when industrial transport system can be

designed with complete confidence. Only some guidelines for design are available and they are not comprehensive for different types of operating conditions. However an understanding of vertical transport may have applications to analyze the solids movement in a spouted bed or a circulating fluidized bed.

#### 2.2.9 Electrostatic inter-particle effects

The presence of electrostatic charges in fluidized beds is known to alter the character of fluidization. Generally the presence of electrostatic potential causes agglomeration, or at least restriction of movement, of particles within <sup>a</sup>bed. This leads to loss of fluidization, channelling and adherence of particles to the bed walls and immersed surfaces. Its effect is more serious in beds of small, light particles. The authors of the works on fluidized bed flow noted the significant effect charging can have on flow behaviour, hence its importance in this project. However little work appears to have been carried out on the use and effectiveness of possible precautions to prevent charging.

If the particles in transport pipeline are charged, the behaviour of the solid flow can be also affected (6). ~~The~~ Considerable static electricity can be generated while the solid particles are passed through pipes at the high velocities. It causes similar phenomena to ~~occur~~ in fluidized bed ~~and~~ solid flow rate decreases with a increase in the charge effects. It is sometimes a serious handicap to their performance.

An encouraging feature of electrostatic charging phenomena, from the point of view of heat transfer system, is that the effects appear to be less serious at high temperature. Ciborowski et al (11) reported reductions in potential over a temperature range of

20- 108<sup>0</sup> C. Indeed no difficulties attributable to charge have been reported in high temperature systems which suggests that it will not be a serious problem in the heat exchanger.

### 2.3 WASTE HEAT RECOVERY TECHNIQUES

#### Introduction

Periodic crises over supplies of energy have arisen all over the world since 1973/4 when the formation of OPEC and its collective action resulted in quadrupling of oil price. Since then accelerated research and development has been in progress world-wide for the development of techniques for saving or recovering energy and for exploitation of alternative sources of energy. For Japan, who depends on foreign supplies for the greatest part of her energy demand, the development of ~~a~~ new energy technologies to meet the long-term situation is undoubtedly necessary, but in the meantime development of energy saving systems based on existing techniques which can be brought into immediate commercial effect is required urgently.

In industrialized countries, the manufacturing industries account for the major part of the total energy consumption. For example in <sup>the</sup> United Kingdom it is some 42% (83). Industrial heat recovery systems can be also highly cost effective, even at present levels of energy costs, so that payback period ranging from a few months to a few years are achievable in a number of situations. On a national scale a really large amount of recoverable heat at high temperature is wasted. What is not generally recognised is that it is expensive simply to handle high temperature gases. The

cost of a heat recovery system may be small in relation to the inevitable cost of handling the hot effluent.

This thesis is concerned with <sup>the</sup> development of a method of recovering heat from industrial waste hot gases for the reasons mentioned above. In the particular application in mind here, recovered heat from a furnace exhaust gases would be transferred to the incoming air to be preheated, although it is important to recognize that this heat exchanger may be applicable for other systems. This section of the thesis describes the main methods of gas-to-gas heat recovery to evaluate these techniques for waste heat recovery in the manufacturing industries.

Of the techniques for waste heat recovery, it is in the area of gas-to-gas heat exchanger that the widest variety exists. However, they may be broadly grouped into two classifications: recuperators and regenerators. The recuperator functions in such a way that the heat flows steadily and continuously from one fluid to another through a separating wall. In a regenerator, however, the flow of heat is intermittent, and is typified by rotary systems such as the heat wheel, described in Section 2.3.1.

#### User considerations

From <sup>the</sup> point of view of the user, however, one of the most important distinctions in the selection of gas-to-gas heat recovery equipment is the operating temperature range. In the high range of temperature, materials degradation may occur. The liquids used in systems such as heat pipes and run-around coils may also be subject to thermal degradation at high temperatures, thus limiting their life.

Another aspect is fouling. The accumulation of matter on the

heat exchange surface affects both pressure drop and heat transfer. The waste hot gases from a industrial furnace are normally contaminated by dust or corrosive matters, so special care ~~should~~<sup>is</sup> ~~be~~ needed. The installation of the equipment must be easy and the unit should have a minimal effect on plant operation. It may be said that practicalities associated with installation, operation, maintenance and economics take precedence over thermal design.

#### Heat storage

On the other hand, the ability to store heat in a useful form for use at a later stage when demand increases has attracted an increasing amount of attention in recent years. Industry has used thermal storage devices for many years, commonly known as heat accumulators. Some accumulators are employed to store steam at high pressure for release later at a lower pressure for process use. These can cope with large fluctuations in demand. The use of hot water as a storage medium is also popular, and a major advantage of hot water storage over other heat storage media is that the water can be used both as the heat storage medium and the heat transport medium, eliminating the necessity for a heat exchanger. A recent study (8) investigated solid particle heat storage media for use at high temperature than a water storage system. The advantage of this system is the high temperature at which stored heat is available (this increases the possible applications for use of the heat) and the fact that the particles can be used as the heat transport medium. The particles may be circulated intermittently through fluidized bed heat exchangers.

#### 2.3.1 Rotating regenerators

The rotating regenerator has been used over a period of about

fifty years for heat recovery in large power plant combustion processes (84). It consists of elements, usually metallic, which are contained in a subdivided cylinder which rotates inside a casing, as shown in Figure 2.17. The elements are heated by the flue gas which flows through ~~one~~<sup>one</sup> side of the cylinder and subsequently cooled by the combustion air on the other side as the wheel rotates. Baffles subdivide the cylinder; there are also seals between the cylinder and casing to limit the amount of leakage from the air side to the flue gas side. On large units such as 660 MW boilers, this can amount to 10% of the flow, leading to inefficiencies. In other applications, where the sensitivity of the fresh air to any cross-contamination is high, purge sections may be incorporated to minimise leakage flows to as low as 0.04% by volume.

Rotational speeds are 5-20 rpm, and the effectiveness of the heat wheel is typically 65-80%, making it generally the most efficient of the gas-to-gas heat recovery systems available. Operating temperature range is up to 820° C with a stainless steel cylinder, and have been reported in excess of 1000° C using a silicon nitride matrix for the cylinder (85). Overall, rotary regenerators can be used successfully in air-conditioning and combustion processes where the leakage is not a problem. However the heat wheel is often susceptible to fouling which militates against its use in some conditions. It is important to remember that rotary regenerators work efficiently only in the condition where the supply of waste hot gas and the supply of gas required to be heated exist simultaneously.

### 2.3.2 Heat pipe heat exchanger

The heat pipe heat exchanger used for gas-to-gas heat recovery is

basically a bundle of finned tubular heat pipes assembled like a conventional air-cooled heat exchanger.

A heat pipe (Figure 2.18) is a sealed container having a wick lining the inside wall (86). The wick contains working fluid, which is the heat transport medium. If one end is heated, the liquid evaporates and the vapour is transferred by the pressure difference between the ends of the pipe. At the cooler end the vapour condenses and the liquid is returned to the heated end by the capillary action of the wick. The energy is transferred as the enthalpy of evaporation of the fluid, and the heat pipe can operate with only a small temperature difference between <sup>the</sup> ends. The gas-to-gas heat pipe heat exchanger employs these heat pipes as shown in Figure 2.19. The evaporators are located in the hot exhaust duct separated by a partition, through which each heat pipe passes, from the duct carrying the air to be heated, which passes over the condenser sections. The efficiency of heat pipe heat exchangers is typically 50-65% (87).

Heat pipe heat exchanger have technical advantages such as having no moving parts and zero leakage. They are fully reversible, can be designed with very low pressure drops and are compact because of the high thermal conductivity of heat pipes. However at present heat pipe heat exchangers can cope with exhaust gas temperatures of up to 350° C, although special models are available at high cost where temperatures in excess of this are likely to be encountered (88). Another disadvantage is that finned heat pipes are needed to utilize the heat pipe's large heat transfer capability, and the fins are liable to corrode and foul.

### 2.3.3 Run-around coil

The run-around coil system, sometimes referred to as a liquid-coupled indirect heat exchanger network, can be a highly effective and readily installed technique for waste heat recovery, particularly when it is desirable to install a heat recovery system without re-routing of ductwork. In its simplest form, used for heating, ventilating and air conditioning (HVAC) and low-temperature process heat recovery, it consists of standard extended-surface finned-tube water coils, used with a circulating pump. As illustrated in Figure 2.20, one coil is located in the exhaust gas stream, and the other is located in the duct through which the air to be heated is flowing. The liquid picks up heat from the exhaust gas as it passes through the coil in that duct, and subsequently rejects the heat to the incoming air stream before being returned to the exhaust gas coil.

Maximum efficiencies are of the order of 70%, but operation in the range 40-60% is more typical (87). <sup>The</sup> Upper temperature of operation is limited to about 300° C fluid temperature, and pumps for higher temperature organic fluids can be expensive. Another disadvantage is that freezing of the liquid filling can be a serious problem.

### 2.3.4 Recuperator

Convection or tubular recuperators come in a wide variety of forms, depending upon the operating temperature range, plant size and the nature of the fouling in the exhaust gases. One disadvantage of the tubular recuperator is that a comparatively large amount of tube has to be used in order to achieve efficiencies comparable with other types of heat exchanger<sup>s</sup>. However lack of extended surfaces does have advantages in many of

the application areas for tubular recuperators. Units fabricated with glass tubes can be used in corrosive atmospheres. If the heavily fouled gas stream is directed through the tubes, they can be cleaned easily, and it allows the equipment to be used in dusty exhausts.

Another type of recuperator is a radiation recuperator. Compared with the convection recuperator, the radiation type offers very low resistance to gas flow and in most instances never needs cleaning. As well as applications involving heat recovery from boiler and furnace exhausts, the radiation recuperator may be used in conjunction with a radiant tube heater, forming a self-contained radiant tube heater and recuperator unit, as shown as Figure 2.21. Typical savings on this gas-fired radiant tube can be in the range 25-45% of original consumption (89). It provides a means of greatly increasing the efficiency of small furnaces, particularly batch furnaces.

#### 2.3.5 Fluidized bed heat exchanger

The waste heat recovery units based on shallow beds as shown in Figure 2.22 are now commercially available for transferring heat to steam or hot water (9). These are more compact than conventional convective units because the heat transfer coefficient between bed <sup>the</sup> and immersed finned tube surface is up to ten times greater than that for air-to-surface. Major advantages of this system are that it should present as low <sup>a</sup> or pressure drop to the exhaust as possible to minimize the pumping power need, and that it can operate in heavily fouled environment because the movement of the particles in a bed prevents the immersed finned tube from fouling.

Other work on fluidized bed heat exchanger systems has been undertaken by Newey (11, 12). He studied the technical feasibility of the novel shallow fluidized bed gas-to-gas heat exchanger as shown in Figure 2.23, which was proposed and patented by Elliott and Virr (10). The novelty of the heat exchanger lies largely with the distributor plate, shown in Figure 2.13, which moves the fluidized bed across its surface because of a significant transverse component of gas velocity as described in Section 2.2.7. The solids are heated by the hot gas in one part of the bed and then the solids flow around until they are fluidized by cold gas. The particles then give up their heat to the cold gas. Thus heat is transferred from the hot to the cold gas stream. There is an inherent ~~leakage~~ <sup>crosscontamination</sup> path between the two gas streams and the amount of leakage depends greatly on a pressure difference between the freeboard zones of the two gas streams. His results show that when the pressure difference increases more than about 0.6 kPa ( $\approx 6$  cm H<sub>2</sub>O), the leakage increases significantly. It is much more difficult to maintain the leakage ~~at~~ <sup>at</sup> a low level for multi-stage unit heat exchanger described in the patent ~~than~~ <sup>the</sup> single unit heat exchanger. The maximum effectiveness of <sup>a</sup> single unit based on equal cold and hot mass flow rates is 50%, which does not seem to be very competitive, comparing <sup>ed with</sup> some other types <sup>of</sup> heat exchanger such as <sup>the</sup> rotating regenerator and heat pipe heat exchanger.<sup>3</sup>

<sup>the</sup> The efficiency of heat exchanger can be much improved by using multistage fluidized bed. Such systems have been employed for example to exchange heat between hot gas leaving a kiln and fresh cold solids. A simple analysis for design purposes has already been presented (2). Peyman and Laguérie presented experimental results using a 4 stage fluidized bed (90). They developed a model which took into account heat losses to the surroundings and

radiative exchange between consecutive stages acting as a sort of backmixing of heat. Toei and Akao (91) developed a multi-stage fluidized bed with perforated plate and without overflow pipes as shown in Figure 2.24. The particles form a fluidized bed on each plate and the gas is in contact counter-current with <sup>the</sup> particles. The advantages of this unit <sup>is that its</sup> ~~are~~ structure is very simple and even dirty gases may be used because the backflow of particles through <sup>the</sup> perforation seems to prevent dusts from fouling. They reported that the apparatus can be used effectively as a dryer, cooler or absorber of material in the range 0.5-5 mm diameter as had been confirmed by its industrial application.

#### 2.3.6 Dilute phase streaming bed

Fouling or damage to the distributor can be expected to occur if fluidized bed techniques are used for the recovery of waste heat at high temperature from very dirty or corrosive gases. A system free from this limitation is the falling cloud heat exchanger. (Figure 2.25) Such a device, described by Sanderson and Howard (92), consists of a vertical duct through which the hot dust-laden gas flows upward. Cold particles are introduced into the duct falling freely counter-current to the gas flow, picking up heat from the gas as they descend. At the bottom of the duct the hot particles are collected and transported to a fluidized bed heat exchanger or a heat storage. Once cooled in the fluidized bed unit, the particles are recirculated to the top of the duct. Alternatively, a zig-zag contactor, as shown in Figure 2.26 (93), could be used instead of the vertical duct. The characteristic common to them is that they can be operated in counter-flow, which may make it possible to gain high efficiency.

### 2.3.7 Heat storage

Heat storage for steam raising is probably the most widely applied storage application in industry. However, because of the increased awareness of energy cost, other storage media for conserving waste heat which can be collected at "off-peak" tariff rate, or accumulating heat from intermittent waste sources, are becoming of greater interest to industry and commerce.

Bergougnou et al (8) discussed about some advantages and commercial viability of the high temperature heat storage which uses solid particles as a heat storage medium. The major advantage of this system is the particles can be also used as the heat transfer medium in the situation where high temperature heat is rejected in gases heavily contaminated with dust and corrosive vapours and/or intermittently. They stated that the degree of commercial viability of such a scheme depends strongly on the end use to made of the recovered heat.

### 2.4 SUMMARY OF EXISTING WORK

The properties of fluidized beds and developments for waste heat recovery are now well-documented and commented, but not yet fully understood. The major advantages of using shallow fluidized beds for waste heat recovery are as follows.

1. The shallow beds can present a low pressure to exhaust and should have the flow and heat transfer characteristics best suited to the heat exchanger.
2. The system can be operated <sup>over a</sup> ~~in the~~ wide range of the ~~temperature of~~ hot exhaust gas. <sup>temperatures</sup>
3. The system <sup>a</sup> ~~is~~ very suitable device for input <sup>into</sup> and recovery of heat stored in hot solid particles.

4. Multi-stage units may operate to obtain higher efficiency than <sup>the</sup> 60% which can be achieved by some other types <sup>of</sup> heat exchanger.

However it is difficult to predict the total performance of the heat recovery system on the basis of other people's work.

The results from the review ~~of~~ covered by this ~~work~~ chapter suggests that a multi-stage unit with shallow fluidized beds could be used effectively for waste heat recovery equipment. Therefore in the work proposed at the University, a highly effective heat exchanger with multi-stage beds was designed, and the technical and economic feasibility of this heat exchanger was studied. The necessary criteria for the design of an industrial scale prototype were also developed.

Table 2.1 ( $C_D$  of irregular shape particle)/( $C_D$  of spherical particle) at various  $Re_p$

$Re_p$	0.3	1	10	100	1000	3000
$\frac{C_D \text{ of irregular shape particle}}{C_D \text{ of spherical particle}}$	1.003	1.03	1.3	2.03	3.4	4.0

FIGURE 2.1 SCHEMATIC DIAGRAM OF A FLUIDIZED BED

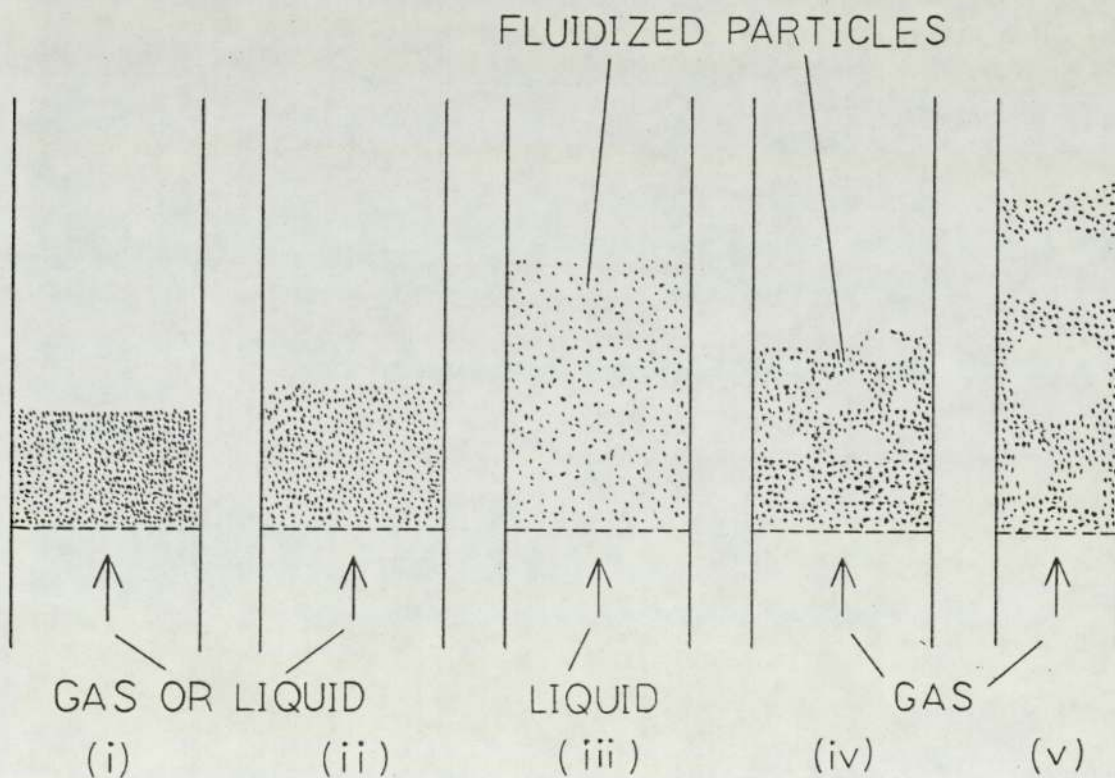


FIGURE 2.2 PRESSURE DROP  
CHARACTERISTIC OF A FLUIDIZED BED

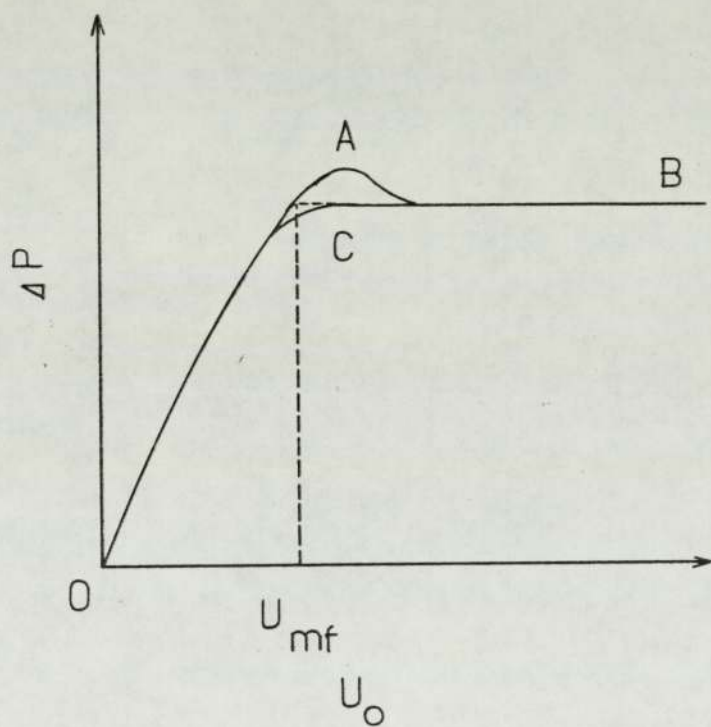


FIGURE 2.3 PARTICLE MOTION AROUND  
A RISING BUBBLE

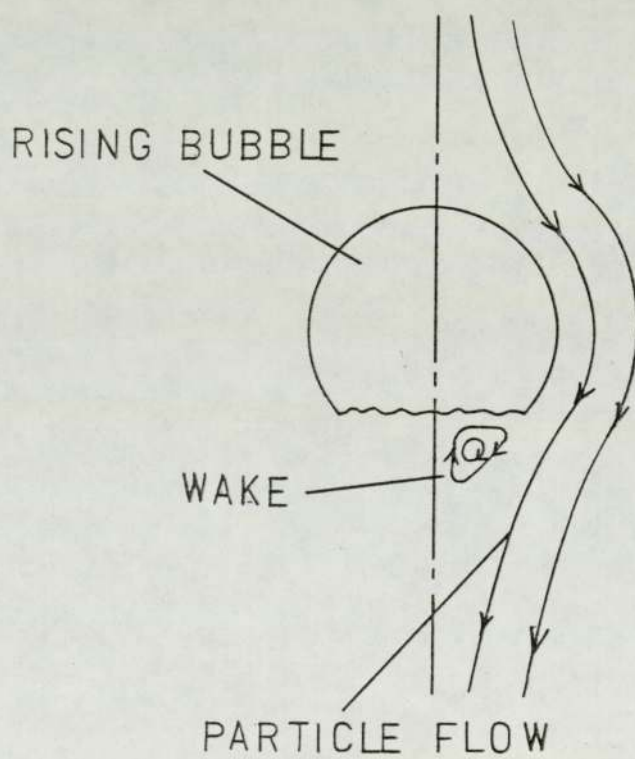


FIGURE 2.4 SCHEMATIC DIAGRAM OF A SPOUTED BED

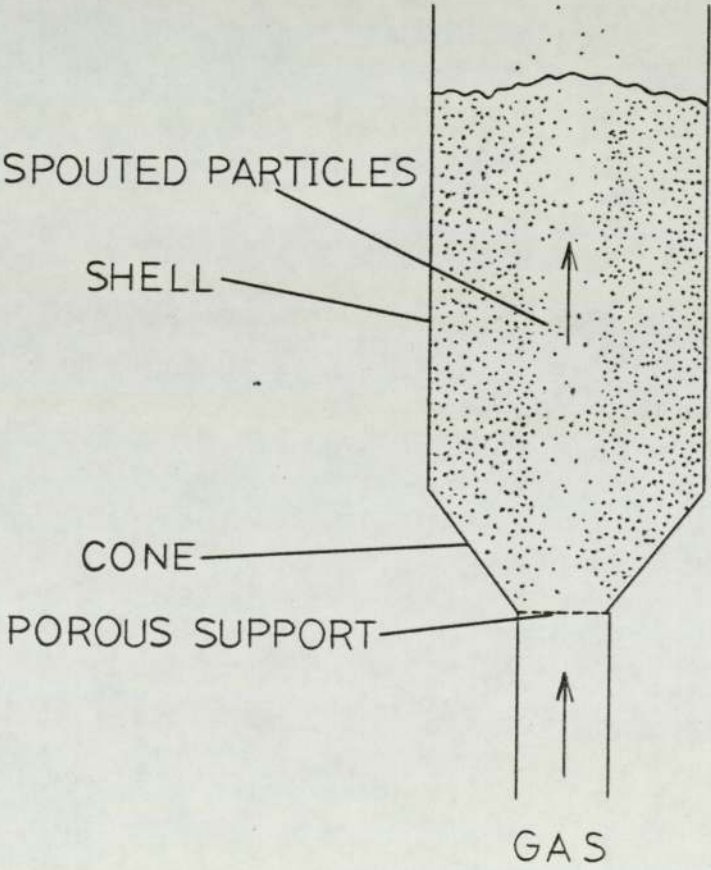


FIGURE 2.5 PRESSURE DROP  
CHARACTERISTIC OF A SPOUTED BED

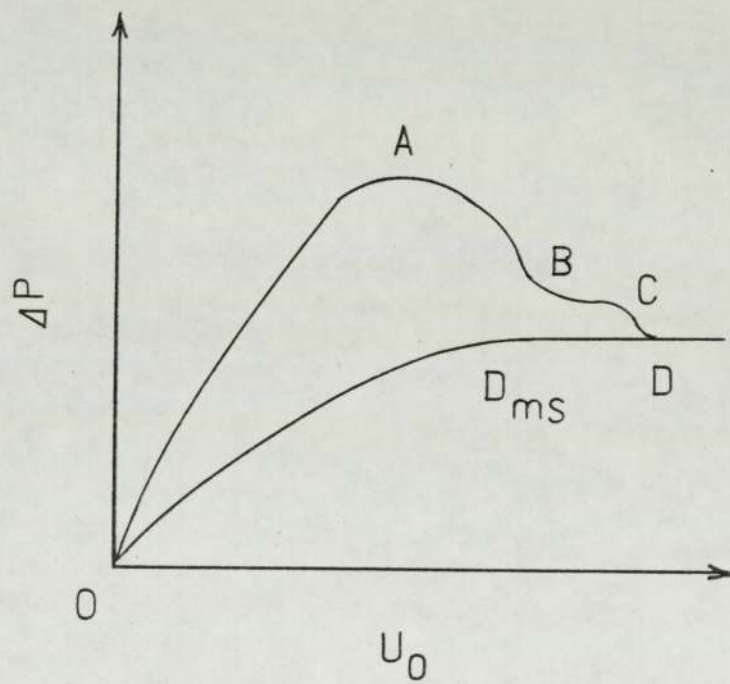


FIGURE 2.6 PARTICLE CLASSIFICATION  
FOR FLUIDIZATION from Geldart (21)

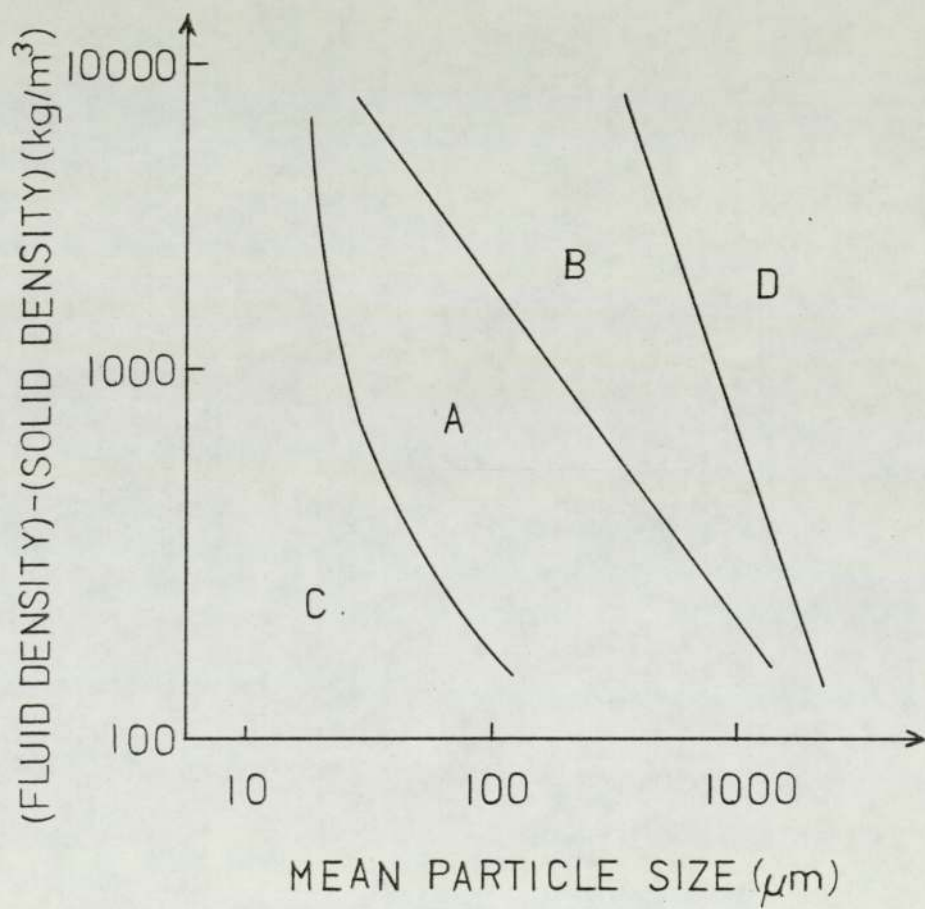


FIGURE 2.7 PARTICLE MOTION IN A  
FLUIDIZED BED from Leva (20)

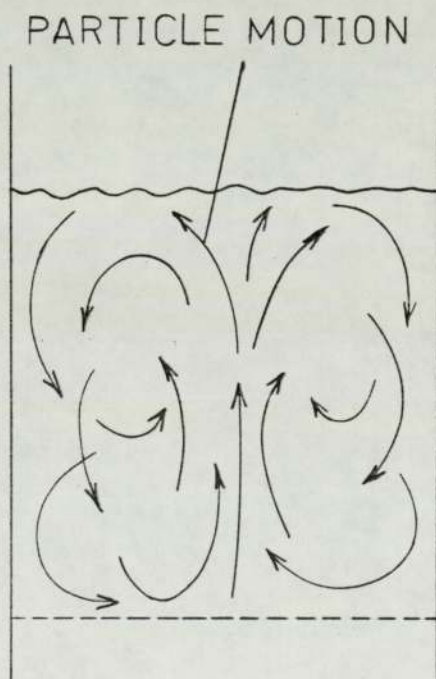


FIGURE 2.8 DIAGRAM OF SINGLE-SECTION  
EQUIPMENT WITH GAS ADMISSION THROUGH  
A SLOT from Mitev (6)

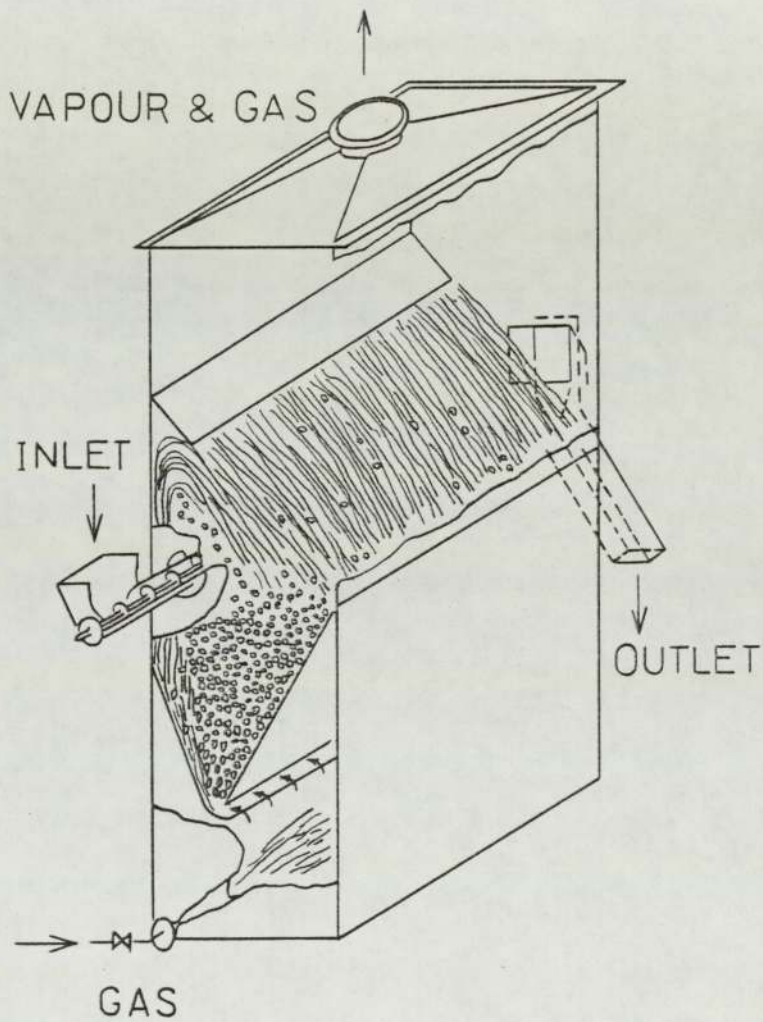


FIGURE 2.9 SCHEMATIC DIAGRAM OF A WHIRLING BED from Rios et al (34)

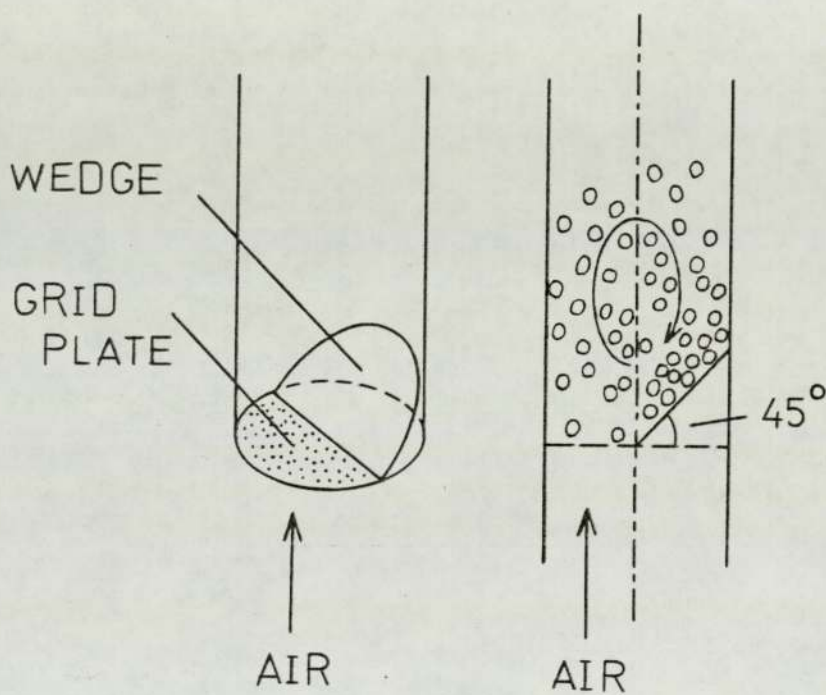


FIGURE 2.10 CORRELATION FOR HEAT  
TRANSFER AT CONTAINER WALLS  
from Wender & Cooper (48)

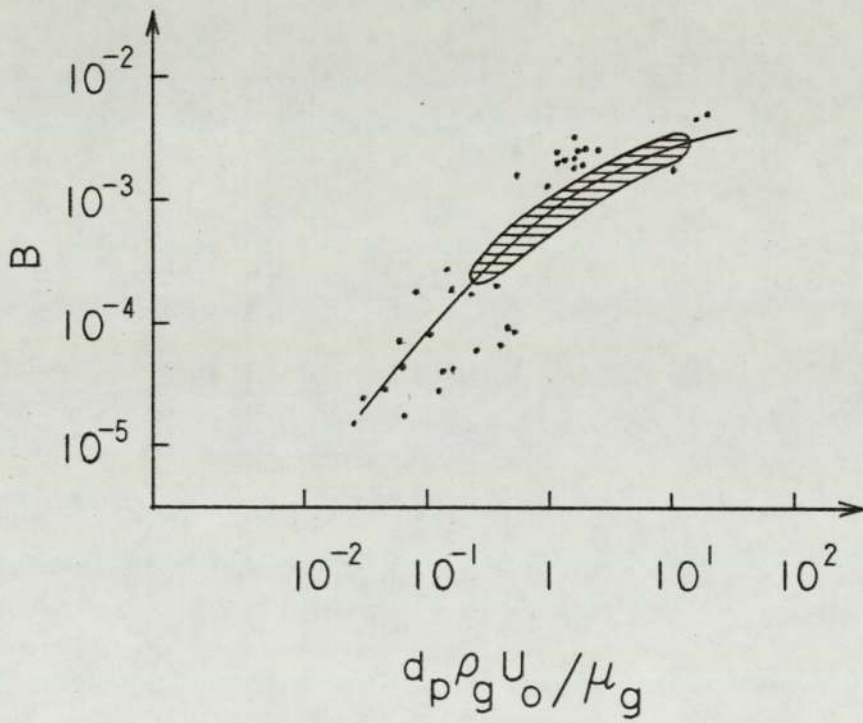


FIGURE 2.11 CONTINUOUSLY FED FLOWING FLUIDIZED BED

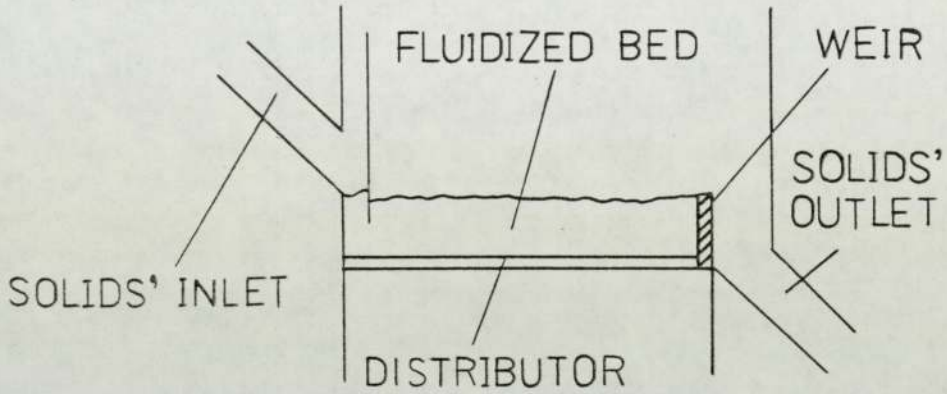


FIGURE 2.12 INCLINED CHANNEL FLOW

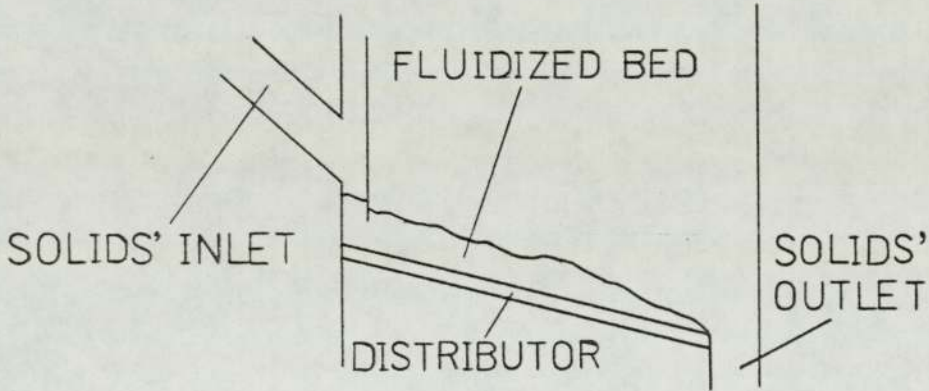


FIGURE 2.13 OPEN HORIZONTAL CHANNEL FLOW

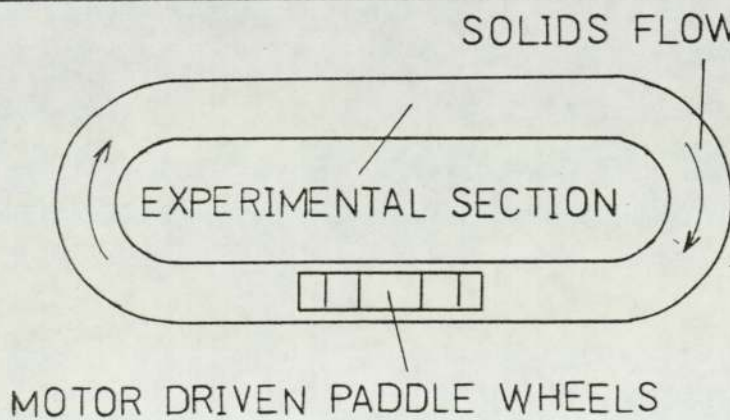


FIGURE 2.14 IDEALISED SECTION OF DISTRIBUTOR PLATE from Newey (11,12)

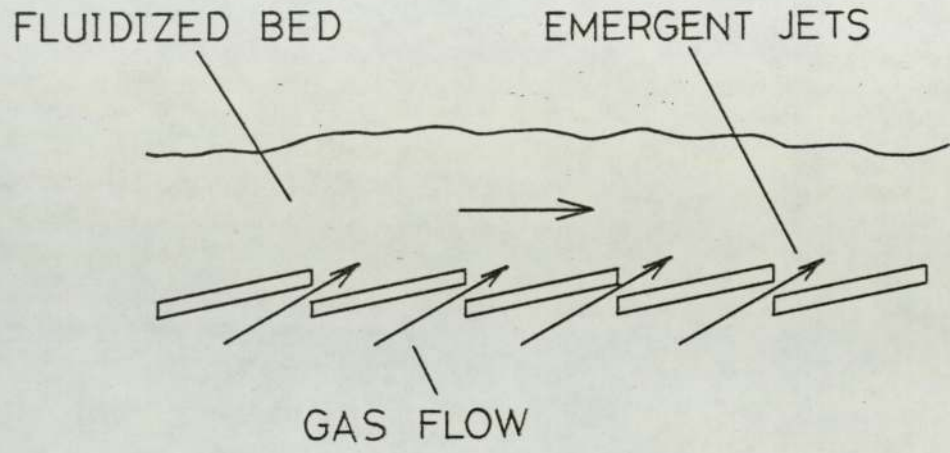


FIGURE 2.15 PNEUMATIC ESCALATER

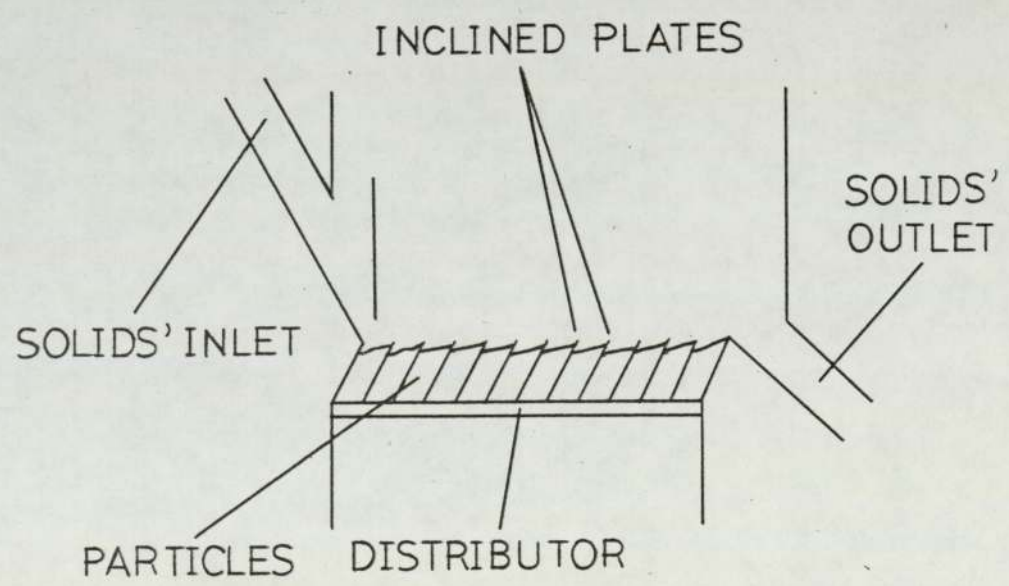


Figure 2.16 Possible upflow patterns in vertical pneumatic conveying showing two types of systems, from Leung (74)

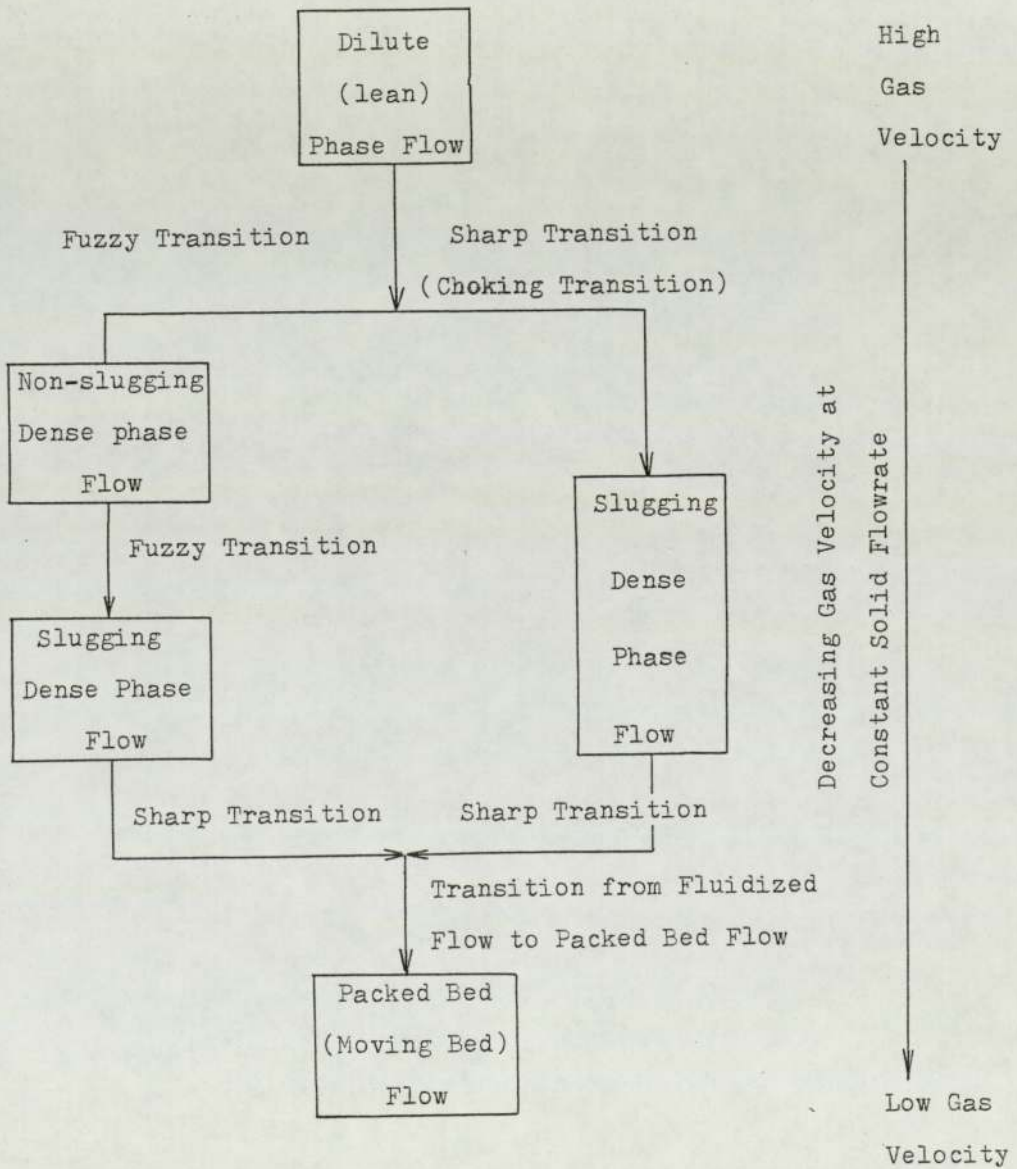


FIGURE 2.17 ROTATING REGENERATOR

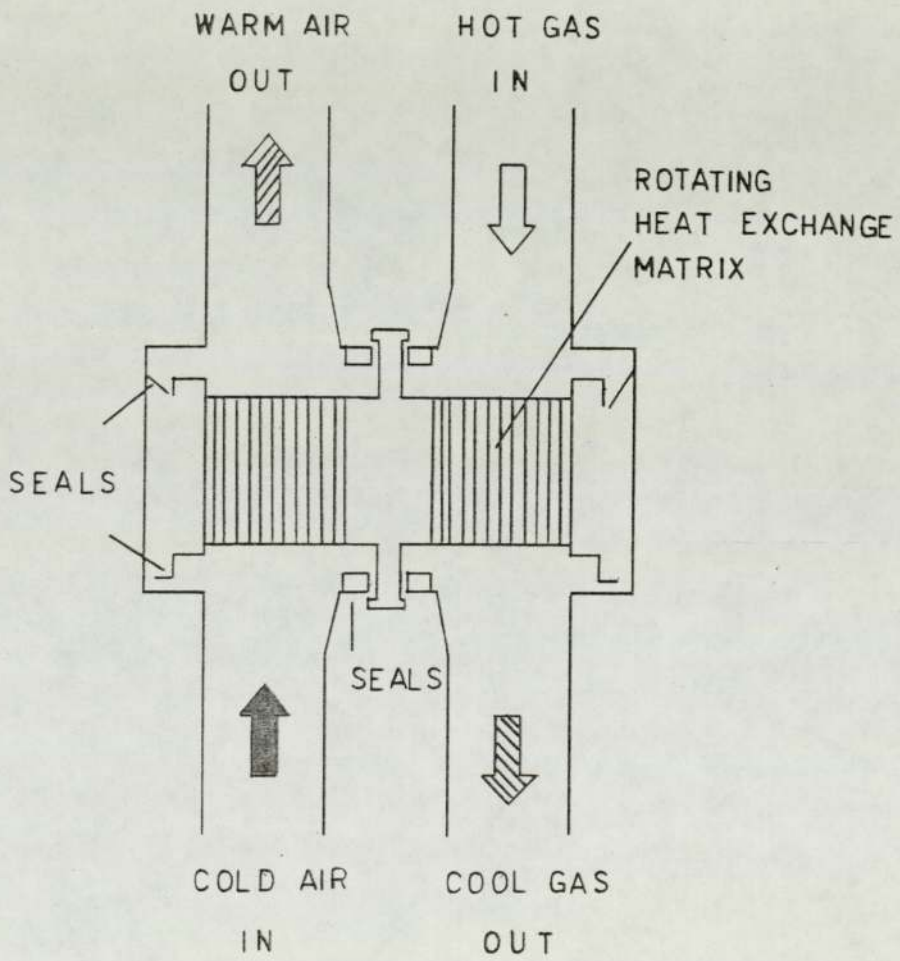


FIGURE 2.18 A HEAT PIPE

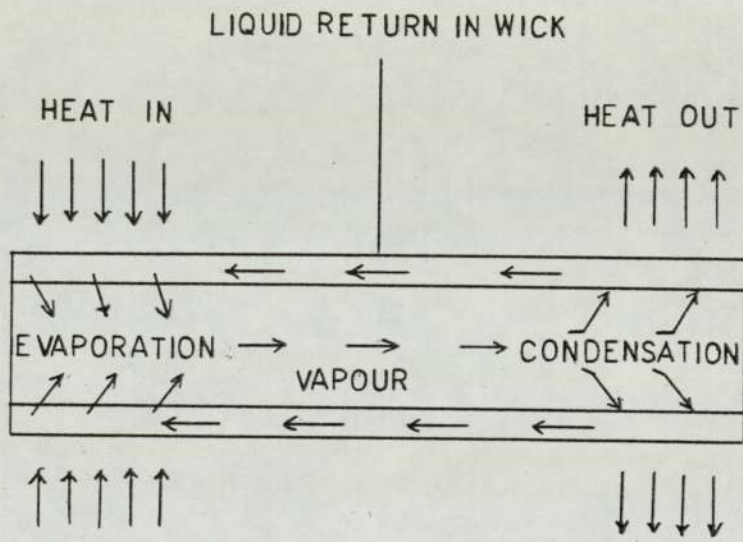


FIGURE 2.19 A HEAT-PIPE HEAT EXCHANGER

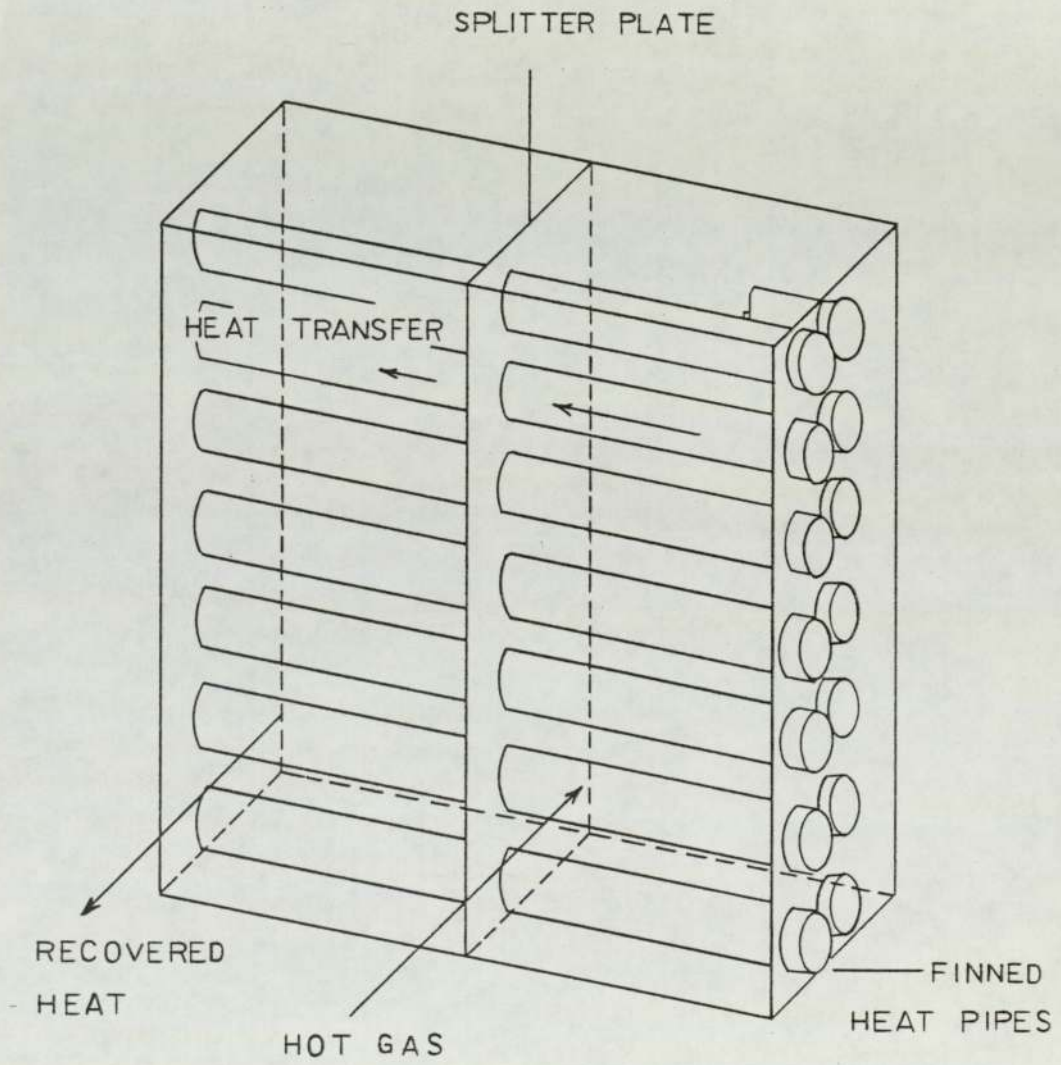


FIGURE 2.20 A LIQUID COUPLED INDIRECT  
HEAT EXCHANGER, OR 'RUN-AROUND' COIL

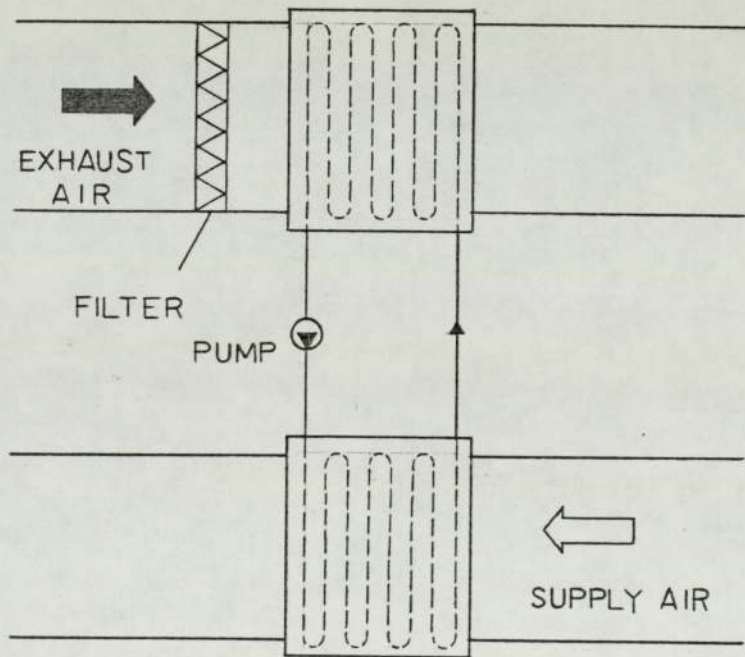


FIGURE 2.21 A UNIT COMBINING THE FUNCTIONS OF RADIANT TUBE HEATER AND RECUPERATOR

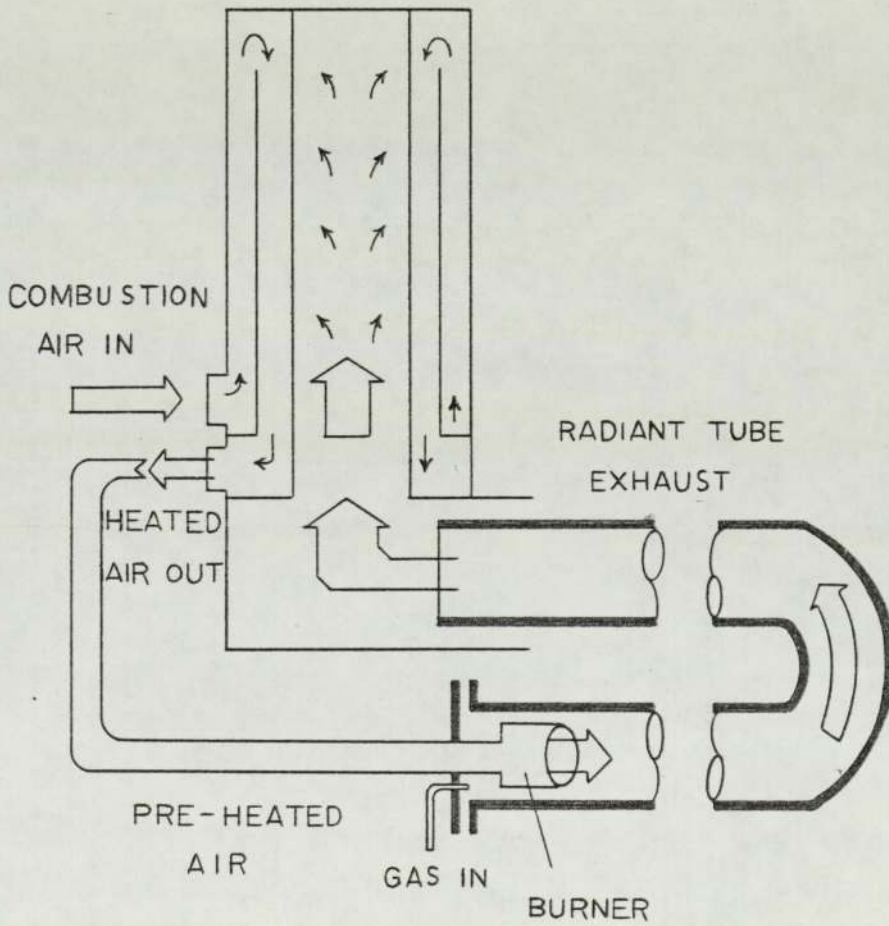


FIGURE 2.22 SHALLOW FLUIDIZED BED WASTE  
HEAT EXCHANGER

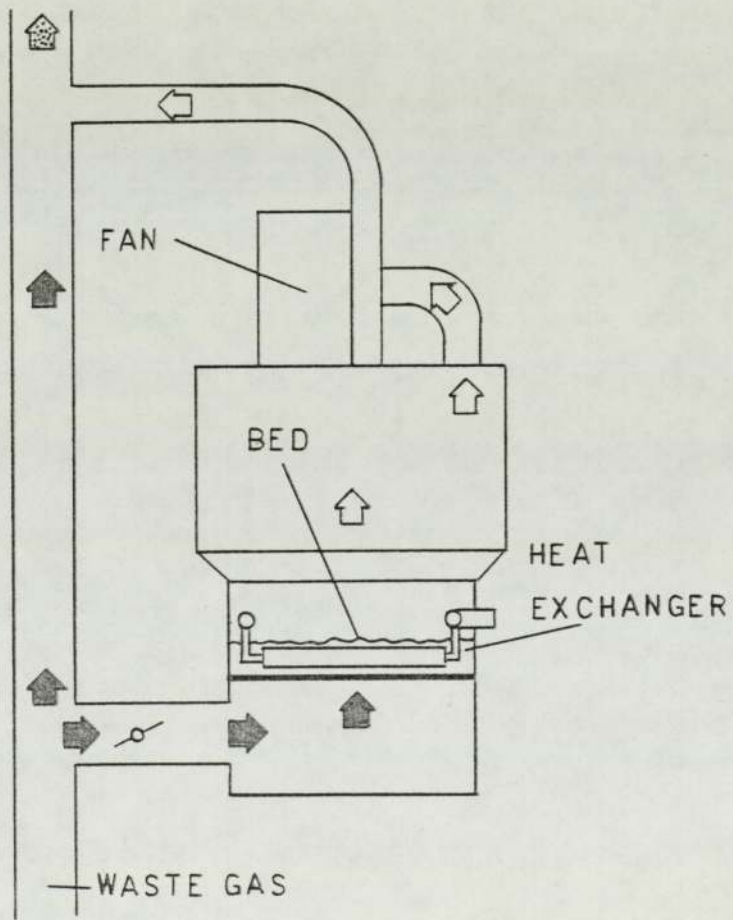


FIGURE 2.23 SHALLOW FLUIDIZED BED GAS-TO-GAS HEAT EXCHANGER

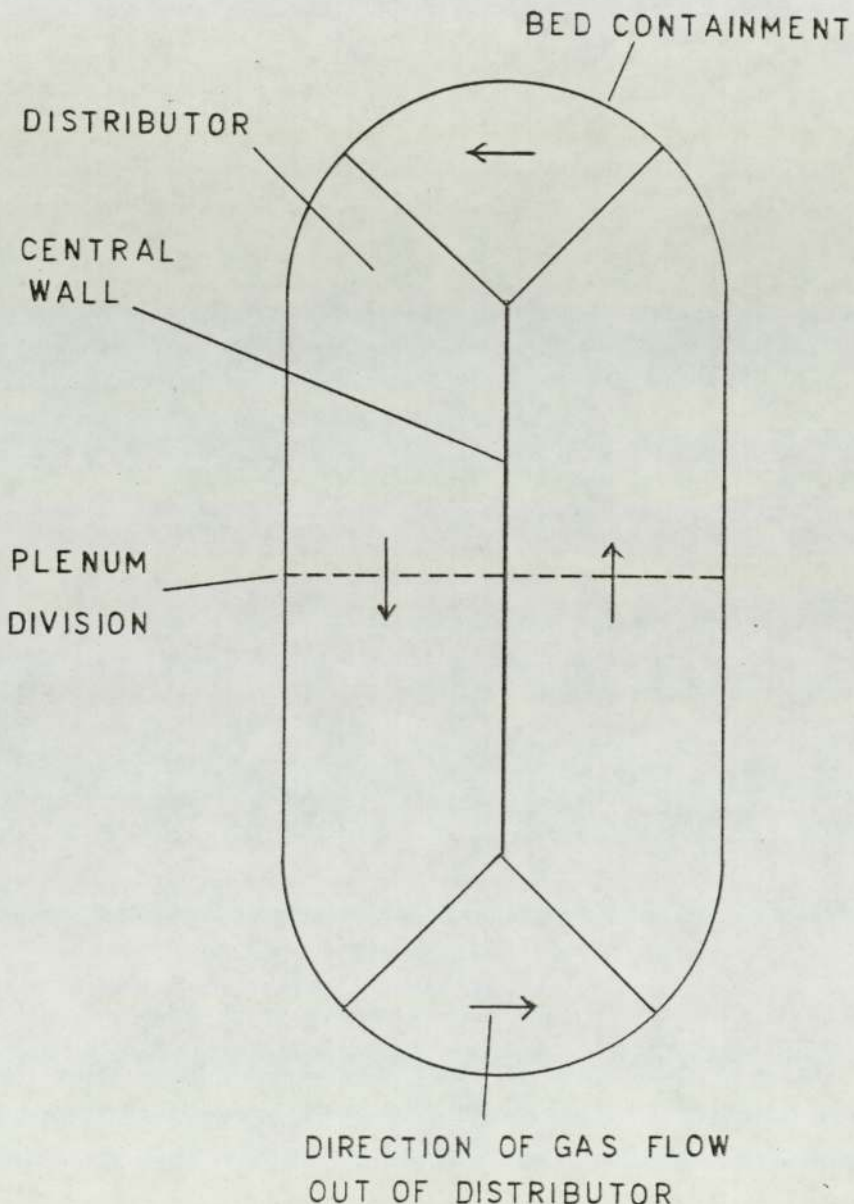


FIGURE 2.24 A MULTI-STAGE FLUIDIZED BED WITH PERFORATED PLATES from Toei and Akao (91)

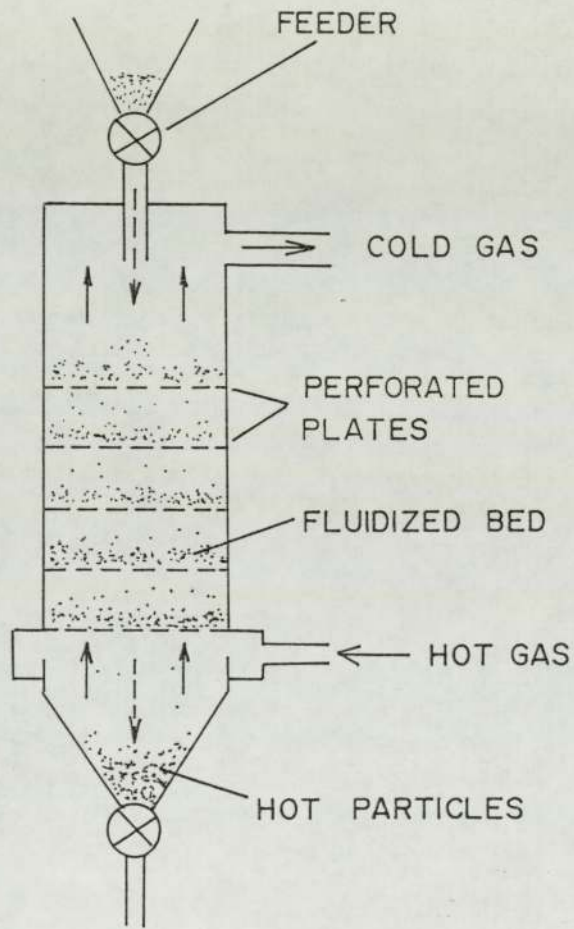


FIGURE 2.25 A FALLING CLOUD HEAT EXCHANGER  
from Sanderson and Howard (92)

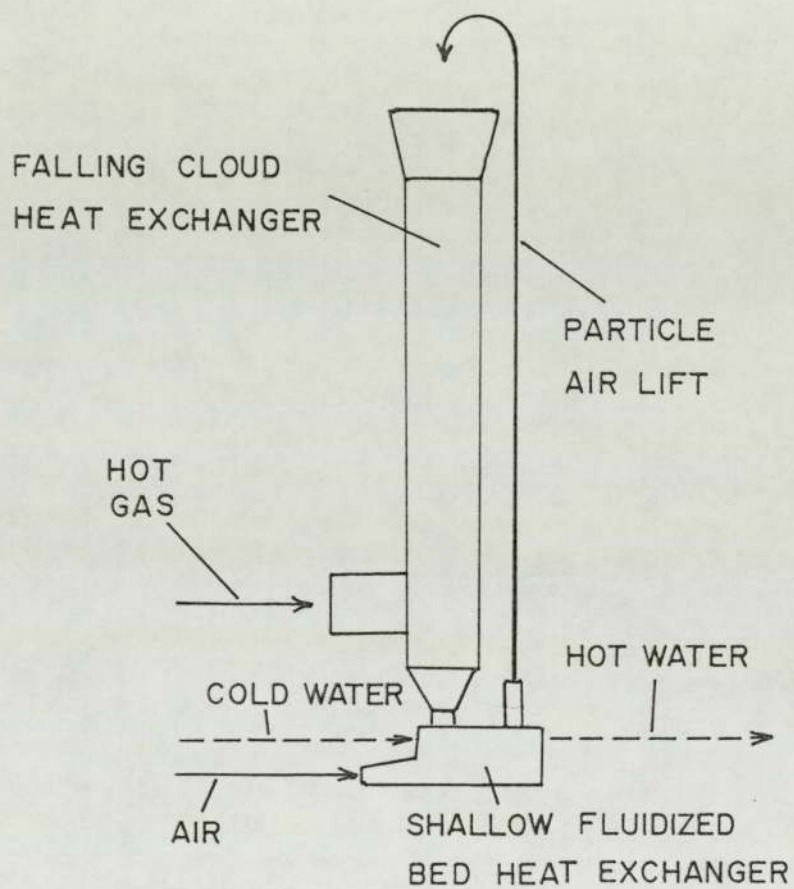
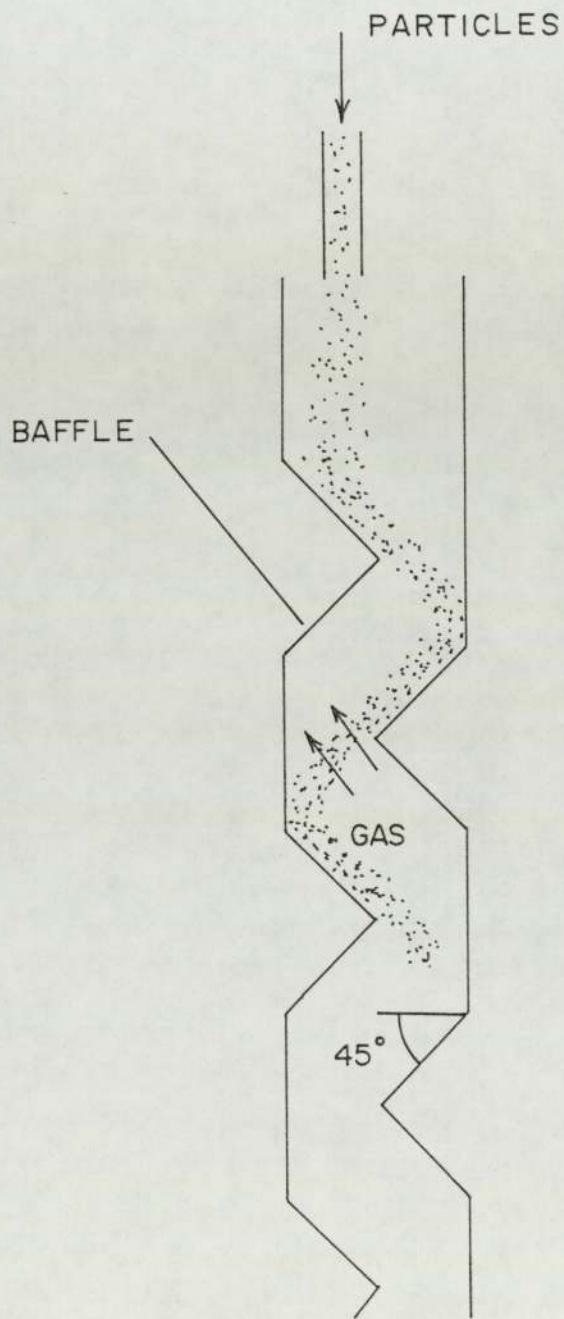


FIGURE 2.26 A ZIG-ZAG CONTACTOR  
from Noordergaaf et al (93)



CHAPTER THREE  
THEORETICAL CONSIDERATIONS  
OF THE HEAT EXCHANGER DESIGN

3.1 INTRODUCTION

The need for a theoretical model of the heat exchanger arises because it is necessary to be able to predict the performance before design and before scaling-up. It is accepted however that models are often in error, and that extrapolations to larger scales are often uncertain. In this chapter it will become apparent that development of an adequate model can only be achieved after making practical measurements. However it will be also shown that the theoretical consideration of different types <sup>of</sup> design is very necessary and helpful to decide the design of apparatus, the important parameters and the kinds of experiments required.

The gas-to-gas heat exchanger in which heat is transferred from the hot gas to the particles and then from the particles to the cold gas by the circulation of particles from the hot gas stream to the cold air stream, and back again, is shown in Figure 3.1. Two separate heat exchanger sections are therefore present, namely the "heater" and the "cooler". We can choose a suitable "heater" or "cooler" system from either a fluidized bed or a dilute-phase streaming bed. However in this chapter we will only discuss gas-to-gas heat exchangers which consists of either single or multiple fluidized beds with particle transport systems.

### 3.2 HEAT TRANSFER MODEL OF SINGLE STAGE FLUIDIZED BED

In this section, the analysis of heat transfer between gas (or air) and particles in a single stage bed, which can be used as "particle heater" or/and "cooler" in the waste heat recovery unit, was developed to evaluate the efficiency.

In most cases the following simplifications can be made in the analysis of the heating and cooling of continuously fed small particles (2, 66).

1. Neglecting the internal resistance of the particle to heat transfer, i.e. assume infinite thermal conductivity, so that the particles are always at uniform temperature.
2. The vertical flow of gas is plug flow.
3. The solids flow is perfect backmixing flow or horizontal plug flow in the case of using a shallow rectangular fluidized bed (69).

Considering the heating of a continuous stream of cold solids by hot gas in a single fluidized bed "heater", if we neglect heat losses to the surroundings, a steady-state heat balance about the whole bed gives

$$Q = (\text{heat gained by solids}) = (\text{heat lost by gas})$$

With  $R_g$  and  $R_s$  as the feed rate of heat capacity (kW/K) of gas and solids, the above heat balance becomes

$$Q = R_s(T_{s,h,out} - T_{s,h,in}) = R_g(T_{g,in} - T_{g,out}) \quad (3.1)$$

The efficiency of heat utilization of solids in this heater is

$$\eta_h = \frac{T_{s,h,out} - T_{s,h,in}}{T_{g,in} - T_{s,h,in}} \quad (3.2)$$

Assuming the solids flow is perfect backmixing flow, i.e. uniform temperature or composition throughout the reactor (34), which is nearly achieved in an ordinary fluidized bed, as shown in Figure 3.2 (a), the temperature of all particles can be considered equal to  $T_{s,h,out}$  in practice. Therefore a heat balance about the whole bed gives

$$Q = h_p S \frac{T_{g,in} - T_{g,out}}{\ln \left( \frac{T_{g,in} - T_{s,h,out}}{T_{g,out} - T_{s,h,out}} \right)} \quad (3.3a)$$

$$= R_s (T_{s,h,out} - T_{s,h,in}) \quad (3.3b)$$

$$= R_g (T_{g,in} - T_{g,out}) \quad (3.3c)$$

From equations 3.2 and 3.3

$$\eta_h = \left[ \frac{R_s}{R_g} \left\{ 1 - \exp \left( \frac{-h_p S}{R_g} \right) \right\}^{-1} + 1 \right]^{-1} \quad (3.4)$$

As mentioned in Section 2.2.7, the actual solids flow in rectangular section fluidized bed is always between plug flow, i.e. uniform in the direction of gas flow but non-uniform lateral composition, and perfect backmixing. As the bed depth decreases *solids flow* ~~it~~ approaches plug flow, which is illustrated in Figure 3.2 (c). Therefore it is important to analyze the condition of horizontal plug flow too. Assuming perfect mixing of particles in vertical plane, a heat balance over the differential element of bed length,  $\delta a$ , as shown in Figure 3.3, gives

$$\delta Q = \frac{h_p S}{A} \frac{(T_{g,in} - T_{g,out})}{\ln \left( \frac{T_{g,in} - T_s}{T_{g,out} - T_s} \right)} \delta a \quad (3.5a)$$

$$= R_s (T_s + \delta T_s) - T_s \quad (3.5b)$$

$$= \frac{R_s}{A} (T_{g,in} - T_{g,out}) \delta a \quad (3.5c)$$

Integrating equation 3.5 between the limits,  $T_s = T_{s,h,in}$  at  $a = 0$  and  $T_s = T_{s,h,out}$  at  $a = A$ , gives McGaw's equation as follows.

$$T_{s,h,out} = T_{g,in} + (T_{s,h,in} - T_{g,in}) \exp \left[ \frac{-R_g}{R_s} \left\{ 1 - \exp \left( \frac{-h_p S}{R_g} \right) \right\} \right] \quad (3.6)$$

Replacing in equation 3.2 gives

$$\eta_h = 1 - \exp \left[ \frac{-R_g}{R_s} \left\{ 1 - \exp \left( \frac{-h_p S}{R_g} \right) \right\} \right] \quad (3.7)$$

Equations 3.4 and 3.5 are the two extremes of the efficiency of single unit "heater", and any real bed must clearly fall between these two results. McGaw (68) has developed a generalised model for heat transfer to and from a shallow crossflow fluidized bed heat exchanger, taking account internal particle resistance to heat transfer, a residence time distribution and a size distribution of particles. His full analytic solution is therefore complicated and requires the evaluation of an ~~infinite~~ <sup>internal</sup> resistance to heat transfer <sup>within the particles. This</sup> may be neglected and the analysis <sup>with small particles,</sup> simplified. A size distribution of particles may be neglected in the case where the size range of the particles is not wide.

*particle*

Only the contribution of  $\lambda$  residence time distribution is unknown,  
*This so it* will be discussed later.

All the parameters in equations 3.4 and 3.7 can be easily found except the gas-to-particle heat transfer coefficient,  $h_p$ . As discussed in Section 2.2.6,  $h_p$  is very difficult to estimate reliably. Firstly we assume to use the particles whose size is just between Group B and Group D, because it seems suitable for the heat exchanger unit as discussed in Section 2.2.2.

Therefore it is assumed  $d_p$  is about 0.6 mm. In Appendix 1, the condition of the calculation for "heater" is shown, and the results are plotted in Figure 3.4, 3.5 and 3.6 from both models of perfect backmixing solids flow and horizontal plug solids flow. From these results following matters are clarified.

1. If Kato's equation (equation 2.11) is used to estimate  $h_p$ , the calculated efficiencies,  $\eta_h$ , of the "heater" when calculated with different depth of bed,  $L_f$ , or alternatively with different gas velocity,  $U$ , are scarcely different.
2. The efficiency,  $\eta_h$ , decreases as the solids flow rate increases.
3. The particles in the bed with complete mixing of solids have wider residence time distribution than with solids plug flow. The efficiency calculated by the solids plug flow model is approximately 10% larger than that of the complete mixing model.

Practically, the wide residence time distribution may give rise to non-uniform particle temperature and is inefficient for heat exchange. However it can be narrowed and greatly improved by multi-cell cross-current contacting such as shown in figure 3.2 (b) (2). For cross-current contacting in the "heater" which consists of a series of equal sized  $M$  cells, the efficiency of heat utilization of solids in the  $i$ -th cell is given by

$$\eta_{h,i} = \frac{T_{s,h,i,out} - T_{s,h,i,in}}{T_{g,in} - T_{s,h,i,in}} = \frac{T_{s,h,i,out} - T_{s,h,i-1,out}}{T_{g,in} - T_{s,h,i-1,out}} \quad (3.8)$$

*are of equal*

and when all cell's size and  $h_p$  are equal, from equation 3.4.

$$\eta_{h,i} = \left[ \frac{MR_s}{R_g} \left[ 1 - \exp\left(-\frac{h_p S}{R_g}\right) + 1 \right]^{-1} \right]^{-1} \quad (3.9)$$

If the efficiency of the "heater",  $\eta_h$ , given by equation 3.2, is rearranged and the intermediate temperatures eliminated, we obtain

$$1 - \eta_h = (1 - \eta_{h,i})^M \quad (3.10)$$

hence from equation 3.9

$$\eta_h = 1 - \left[ 1 - \left[ \frac{MR_s}{R_g} \left( 1 - \exp\left(-\frac{h_p S}{R_g}\right) \right) + 1 \right]^{-1} \right]^M \quad (3.11)$$

Figure 3.7 shows  $\eta_h$  calculated by equation 3.11 <sup>for</sup> in the condition described in Appendix 1 and of  $U = 0.4$  m/sec and  $L_f = 0.04$  m. As the number of cells,  $M$ , increases,  $\eta_h$  increases to approach the value of  $\eta_h$  of horizontal plug solids flow which is estimated by equation 3.7.

### 3.3 HEAT TRANSFER MODEL OF MULTI-STAGE FLUIDIZED BED

No matter what the exit temperature of the beds may be, the efficiency of single-stage operation is low and this prompts the desire for multi-stage contacting with its improved efficiencies.

Figure 3.2 (d),(e) and (f) show practical alternatives for multi-stage contacting, a counter-current and cross-current scheme. Let us evaluate the efficiencies of these schemes in the conditions where the solids flow is perfect backmixing flow or plug flow in each stage.

On the presumption that the solids flow in each stage is perfect backmixing flow as illustrated in Figure 3.2 (d), the efficiency in the j-th bed is given by

$$\eta_{h,j} = \frac{T_{s,h,j,out} - T_{s,h,j,in}}{T_{g,j,in} - T_{s,h,j,in}} = \frac{T_{s,h,j,out} - T_{s,h,j-1,out}}{T_{g,j,in} - T_{s,h,j-1,out}} \quad (3.12)$$

Assuming the solid-gas heat transfer coefficient,  $h_p$ , and the bed size in each stage are equal, for the perfect backmixing solids flow model

$$\eta_{h,j} = \left[ \frac{R_s}{R_g} \left\{ 1 - \exp\left(-\frac{h_p S}{R_g}\right) \right\}^{-1} + 1 \right]^{-1} \quad (3.13)$$

from equation 3.4 and for the horizontal plug flow model

$$\eta_{h,j} = 1 - \exp\left[ -\frac{R_g}{R_s} \left\{ 1 - \exp\left(-\frac{h_p S}{R_g}\right) \right\} \right] \quad (3.14)$$

from equation 3.7. The overall efficiency,  $\eta_h$ , is calculated by equation 3.10, then the relation between  $\eta_h$  and  $\eta_{h,j}$  is

$$\frac{R_s}{R_g} \left( \frac{\frac{R_g}{R_s} - 1}{1 + \frac{R_g}{R_s}} \right) = \left[ \frac{R_s}{R_g} \left( \frac{\frac{R_g}{R_s} - 1}{1 + \frac{R_g}{R_s}} \right) \right]^N \quad \text{for } R_s \neq R_g \quad (3.15)$$

$$\frac{1}{1 - \eta_h} - 1 = N \left( \frac{1}{1 - \eta_{h,j}} - 1 \right) \quad \text{for } R_s = R_g \quad (3.16)$$

Overall efficiency,  $\eta_h$ , is calculated from equation 3.13, 3.14, 3.15 and 3.16 for both models of solids flow. Figure 3.8 shows  $\eta_h$  curves <sup>for a</sup> ~~of~~ counter-current contacting "heater" which consists of series of 1, 3 and 5 beds calculated from the two types of solids flow model.  $\eta_h$  <sup>in</sup> ~~of~~ plug solids flow is always higher than <sup>for the</sup> backmixing flow. The differences of  $\eta_h$  between single stage ~~bed~~ and 3 stages ~~bed~~ are larger than between 3 and 5 stages ~~bed~~ for <sup>the</sup> backmixing and plug flow models. Comparing Figure 3.7 and 3.8, we find, not surprisingly, that counter-current contacting always has a higher efficiency.

In order to narrow the <sup>particle</sup> residence time distribution of ~~particles~~, <sup>a</sup> combination of counter-current and cross-current contacting is also one of the alternative <sup>heater</sup> designs of the "heater". It is shown in Figure 3.2 (e). Assuming the "heater" consists of N stages of counter-current contacting beds which are divided into equal sized M cells, the efficiency of the j-th stage can be given from equation 3.11.

$$\eta_{h,j} = 1 - \left[ 1 - \left[ \frac{MR_s}{R_g} \left\{ 1 - \exp \left( - \frac{h_p S}{R_g} \right) \right\}^{-1} + 1 \right]^{-1} \right]^M \quad (3.17)$$

Then the efficiency of the "heater",  $\eta_h$ , is calculated from

equation 3.15, 3.16 and 3.17. Figure 3.9 and 3.10 demonstrate  $\eta_h$  curves of  $M = 1, 2, 4$  and horizontal plug flow, in the case of  $N = 2$  and  $N = 3$ . We find that there is no significant difference between the curves of  $M = 4$  and horizontal plug flow, which is the most effective contacting. Of course the true efficiency is between horizontal plug flow and backmixing flow models.

### 3.4 THEORETICAL CONSIDERATIONS OF THE DESIGN OF HEAT EXCHANGER

#### 3.4.1 Overall Efficiency of the Heat Exchanger

As described in Figure 3.1, the whole gas-to-gas exchanger consists of two separate sections, "heater" and "cooler". We discussed only the efficiency of the "heater",  $\eta_h$ , in the Section 3.2 and 3.3, because the efficiency of <sup>the</sup> "cooler",  $\eta_c$ , can be considered in the same way, which is defined

$$\eta_c = \frac{T_{s,c,out} - T_{s,c,in}}{T_{a,in} - T_{s,c,in}} \quad (3.18)$$

The heat balance in <sup>the</sup> "cooler" becomes

$$Q = R_s(T_{s,c,out} - T_{s,c,in}) = R_a(T_{a,in} - T_{a,out}) \quad (3.19)$$

In this section we discuss the overall efficiency of the gas-to-gas heat exchanger.

Considering the steady-state heating of <sup>a</sup> continuous stream of cold air by hot gas in <sup>a</sup> gas-to-gas heat exchanger, the efficiency of heat utilization of air in the whole heat exchanger,  $\eta$ , is

$$\eta = \frac{T_{a,out} - T_{a,in}}{T_{g,in} - T_{a,in}} \quad (3.20)$$

Then from equation 3.1, 3.2, 3.18 and 3.19

$$\eta = \frac{R_s}{R_a} \frac{1}{\frac{1}{\eta_h} + \frac{1}{\eta_c} - 1} \quad (3.21)$$

In the special case of  $\eta_h = \eta_c$  and  $R_g = R_a$ ,

$$\eta = \frac{R_s}{R_g} \frac{1}{\frac{2}{\eta_h} - 1} = \frac{R_s}{R_a} \frac{1}{\frac{2}{\eta_c} - 1} \quad (3.22)$$

Figure 3.11 shows the overall efficiency,  $\eta$ , of the gas-to-gas heat exchanger which consists of the <sup>identical</sup> ~~equal designed~~ "heater" and "cooler" of single-stage contacting <sup>sections</sup>  $\eta$  as a function of  $R_s/R_g$  (or  $R_s/R_a$ ).  $\eta$  is calculated by equation 3.11 and 3.22 for multi-cell contacting and by equation 3.7 and 3.22 for solids plug flow.

As  $R_s/R_g$  increases,  $\eta$  increases to approach ~~to~~ 0.5, the maximum efficiency <sup>for</sup> of co-current heat exchanger. This effect of  $R_s/R_g$  can explain the experimental results of Newey's heat exchanger (11) that  $\eta$  increases with faster particle circulation speed. Clearly, as the solids flow approaches plug flow,  $\eta$  increases as shown in Figure 3.11.

Figure 3.12 shows <sup>the</sup> effectiveness,  $\eta$  of the heat exchanger <sub>Λ</sub>

the  
experimented with in present programme, which consists of two identical stages, as a function of  $R_s/R_g$ . The curves are calculated by equations 3.14, 3.15, 3.16, 3.17 and 3.22. Both models of plug and backmixing solids flow models have been computed. It will be seen that the maximum  $\eta$  approximately 0.63, can be obtained at  $R_s/R_g \approx 1.2$  by plug solids flow. Figure 3.13 also shows  $\eta$  for the three-stage contacting heat exchanger, calculated by the same equations. The maximum effectiveness,  $\eta$  is approximately 0.73 at  $R_s/R_g \approx 1.1$ .

#### 3.4.2 Basic Design of the Heat Exchanger

As considered in Section 2.3, the effectiveness of the typical gas-to-gas heat exchanger is in the range 40-70%. The proposed effectiveness of the new competitive heat exchanger in this work should be more than 40%, hopefully 50-80%. From Figure 3.11 to 3.13 it is considered that a counter-current contacting multi-stage device is practicable for a commercial unit. However it is accompanied by a larger pressure drop than a single stage device. Also, as mentioned in Section 2.2.8, it is not easy to maintain a stable downflow of solids and to avoid imbalance among the stages. Achievement of good counter-current contacting therefore requires the design to incorporate features to ensure that good contacting in each stage actually occurs under all operating conditions so as to minimize the number of stages.

the choice of  
McGaw (67) suggested to choose as long a bed as practicable in order to approach a plug solids flow condition in the bed. However, the fluidization in an excessively long bed is not uniform throughout the bed, because the bed depth is different between the two ends of the bed, as shown in Figure 3.14(A).

To avoid this defect the bed may be divided up into several cells by putting some weirs in it as illustrated in Figure 3.14(B). This is <sup>a</sup> combination of counter-current and cross-current contacting, which is probably the most practicable design for industrial use. This design might be improved as shown in Figure 3.14(C), to give a more compact and simple unit. In this case, there is only one gas distributor plate for each stage, inclined slightly to keep the same pressure drop across different cells. We may predict that the gas velocity is the highest through the shallowest part of the bed in each cell, and that channelling will occur if the distributor is inclined excessively.

When we apply the model to the heat exchanger divided into several cells as illustrated in Figure 3.14 (C), several assumptions are implicit in using the equivalent configuration for the theoretical model. Firstly, equating the depth of the bed,  $L_f$ , to that of the median, as illustrated in Figure 3.15, will not be correct, but it is the best approximation that can be made without determining the actual fluidization distribution. Secondly Kato's empirical equation (equation 2.11) (60) has been applied where the fluidization is not uniform. Rios et al (34) measured the heat transfer coefficient between particles and gas in the whirling bed, where the cyclic solids movement illustrated in Figure 2.9 might be similar to that in the cell; however the particle size used is much larger; belonging in Group D.

To the author's knowledge, no one has studied the performance of a shallow fluidized bed having an inclined distributor as a heat exchanger before. It is not possible therefore to quantify the magnitude of the errors produced by the approximations; none-the-less it is highly desirable to develop a workable form of model. The model that has been formulated is therefore semi-empirical. Some errors arise because of the assumed mathematical function

describing the nature of gas flow such as the assumption of plug flow or of backmixing flow, Figure 3.16; others however are due to the uncertainties with which the parameters such as  $h_p$  can actually be determined. The semi-empirical model is, however, adequate for purposes of general predictions of the performance of the heat exchanger.

Taking all the above considerations into account, the proper number of stages predicted is two or three and the number of cells in each stage required may be more than four from Figure 3.9 and 3.10.

### 3.4.3 Prediction of the Time to Reach Steady-State

The model can be used to predict the time taken for the fluidized bed to reach stable temperature under given conditions.

Assuming the solids do not flow, Figure 3.17 shows the model for heat transfer. Plug of gas of mass  $m_g$  passes through the bed during time  $\delta t$ . After <sup>the</sup> plug of gas has passed ~~ed~~ through the bed <sup>the</sup> temperature has risen by  $\delta T_s$ . The heat balance during the differential element of time,  $\delta t$ , gives

$$Q = h_p S \left( \frac{T_{g,in} - T_{g,out}}{\ln \frac{T_{g,in} - T_s}{T_{g,out} - T_s}} \right) \delta t \quad (3.23a)$$

$$= W_b C_s \delta T_s \quad (3.23b)$$

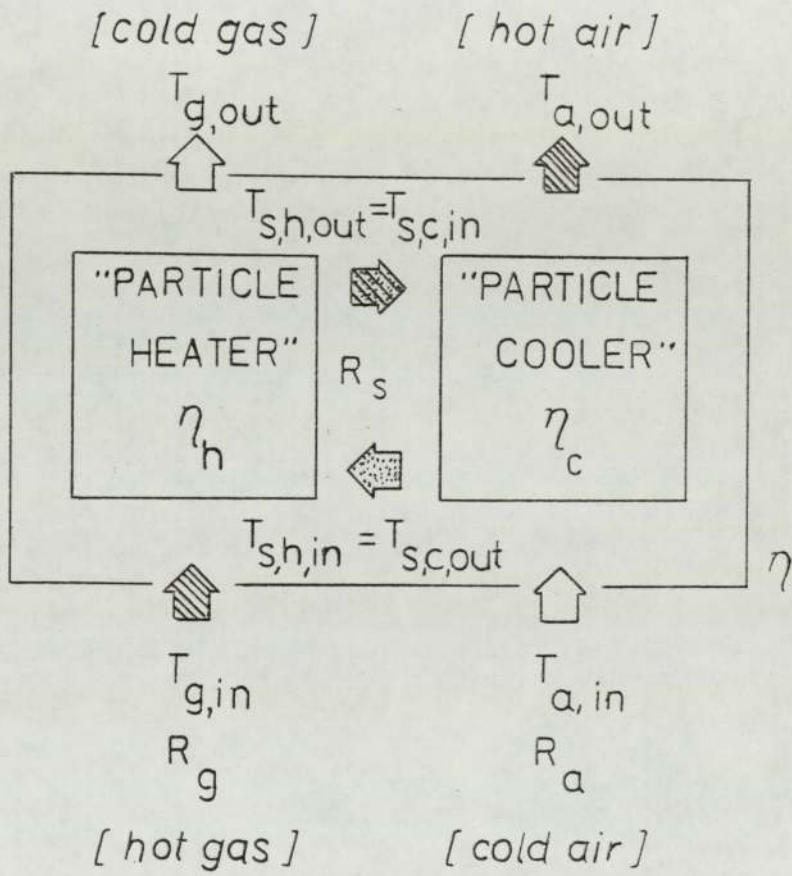
$$= R_g (T_{g,in} - T_{g,out}) \delta t \quad (3.23c)$$

Initially, at  $t = 0$ , the solids are considered to be at the temperature of  $T_{s,0}$ , and the solids temperature becomes  $T_s$  at  $t$ . Then integrating equations 3.23 as shown in Appendix 2 gives

$$\frac{T_s - T_{g,in}}{T_{s,0} - T_{g,in}} = \exp \left[ - \frac{R_g}{W_b C_s} \left\{ 1 - \exp \left( - \frac{h_p S}{R_g} \right) \right\} t \right] \quad (3.24)$$

Hence the rate at which the bed heats up to operating temperature can be predicted for given gas inlet conditions. To estimate the overall heat transfer coefficient between gas and solids in the fluidized bed with <sup>an</sup> inclined distributor,  $h_p$ , it is not exactly proper to apply Kato's empirical equation (equation 2.11) as considered in the Section 4.5. It is very important to know the real heat transfer coefficient from measurement using this model. However assuming the fluidization is uniform through <sup>out</sup> the heat exchanger, Kato's equation may be used to estimate  $h_p$ . Figure 3.18 shows the results for the air inlet temperature of 100 °C with  $U = 0.4$  m/sec,  $\epsilon = 0.45$ ,  $C_s = 1.0$  kJ/kg K, and three different bed depths,  $L_f = 0.02, 0.04$  and  $0.06$  m. The results demonstrate clearly that the major factor in the heating up time is the bed depth because less material has to be heated in shallower beds.

FIGURE 3.1 GAS TO GAS HEAT EXCHANGER



gas (or air)
 solids
 heat

FIGURE 3.2 TYPES OF CONTACTING OF GAS AND SOLIDS

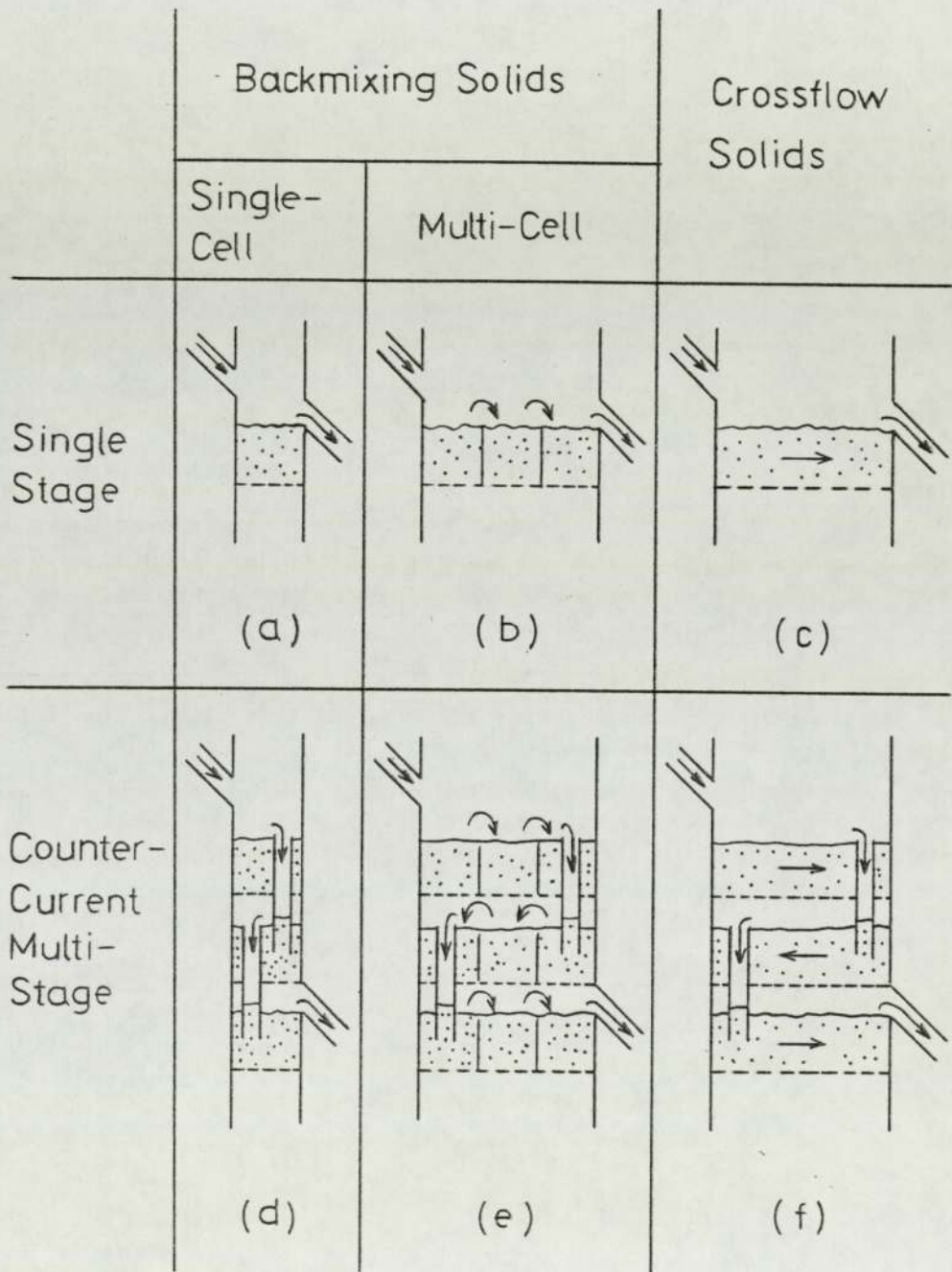


FIGURE 3.3 A HEAT BALANCE OVER THE DIFFERENTIAL ELEMENT OF BED LENGTH

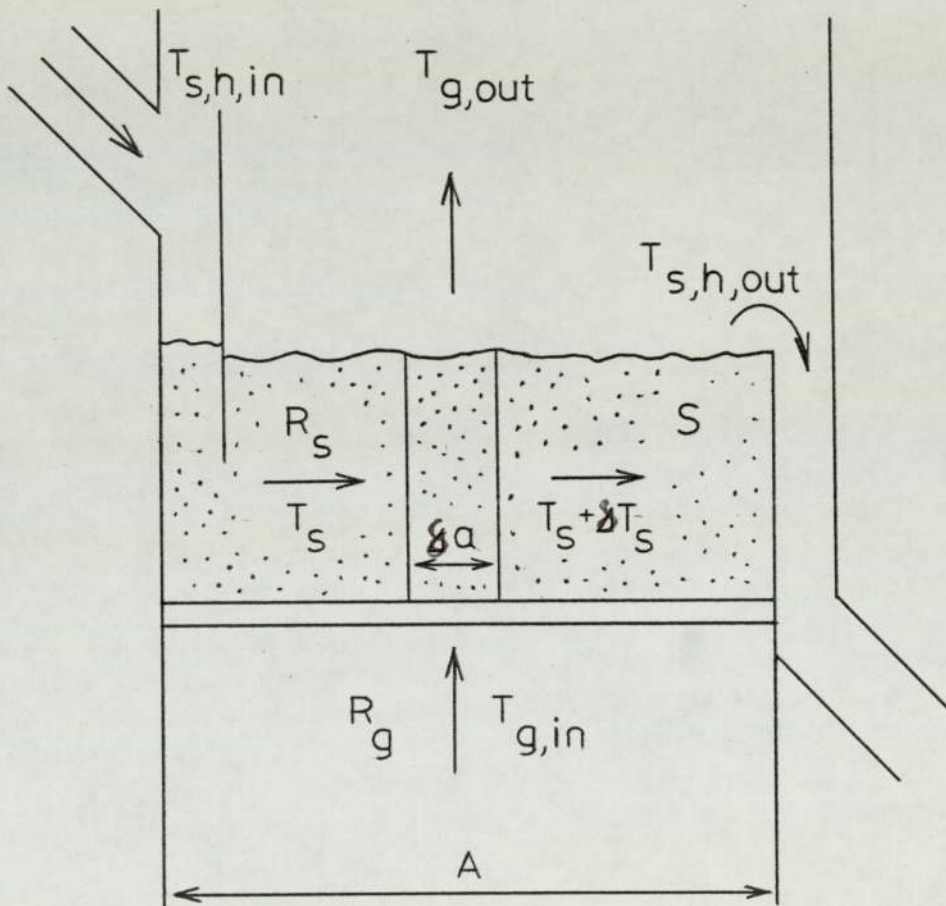


Figure 3.4 Efficiency of perfect backmixing solids flow and horizontal plug solids flow for the "particle heater" as a function of bed depth

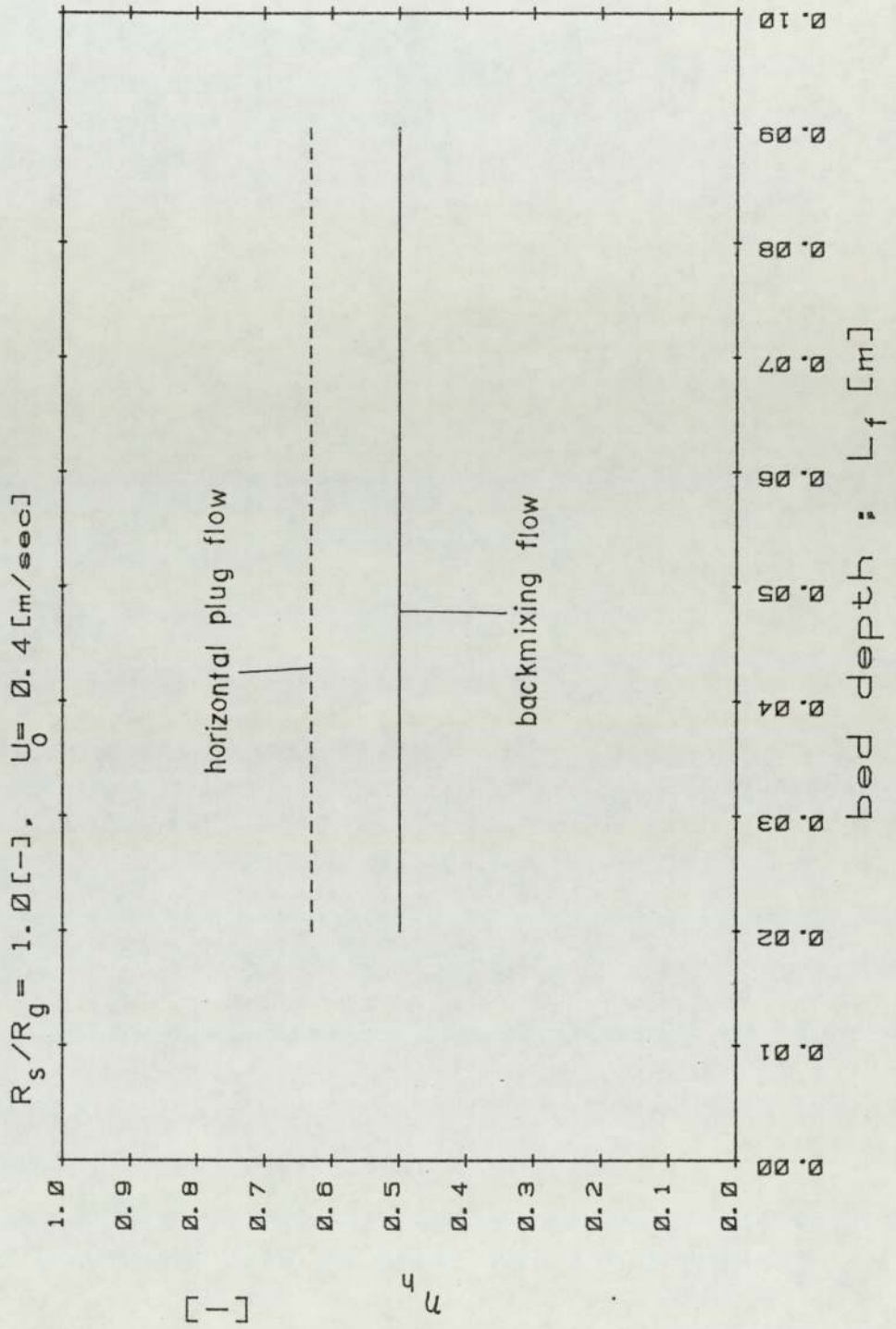


Figure 3.5 Efficiency of perfect backmixing solids flow and horizontal plug solids flow for the "particle heater" as a function of air velocity

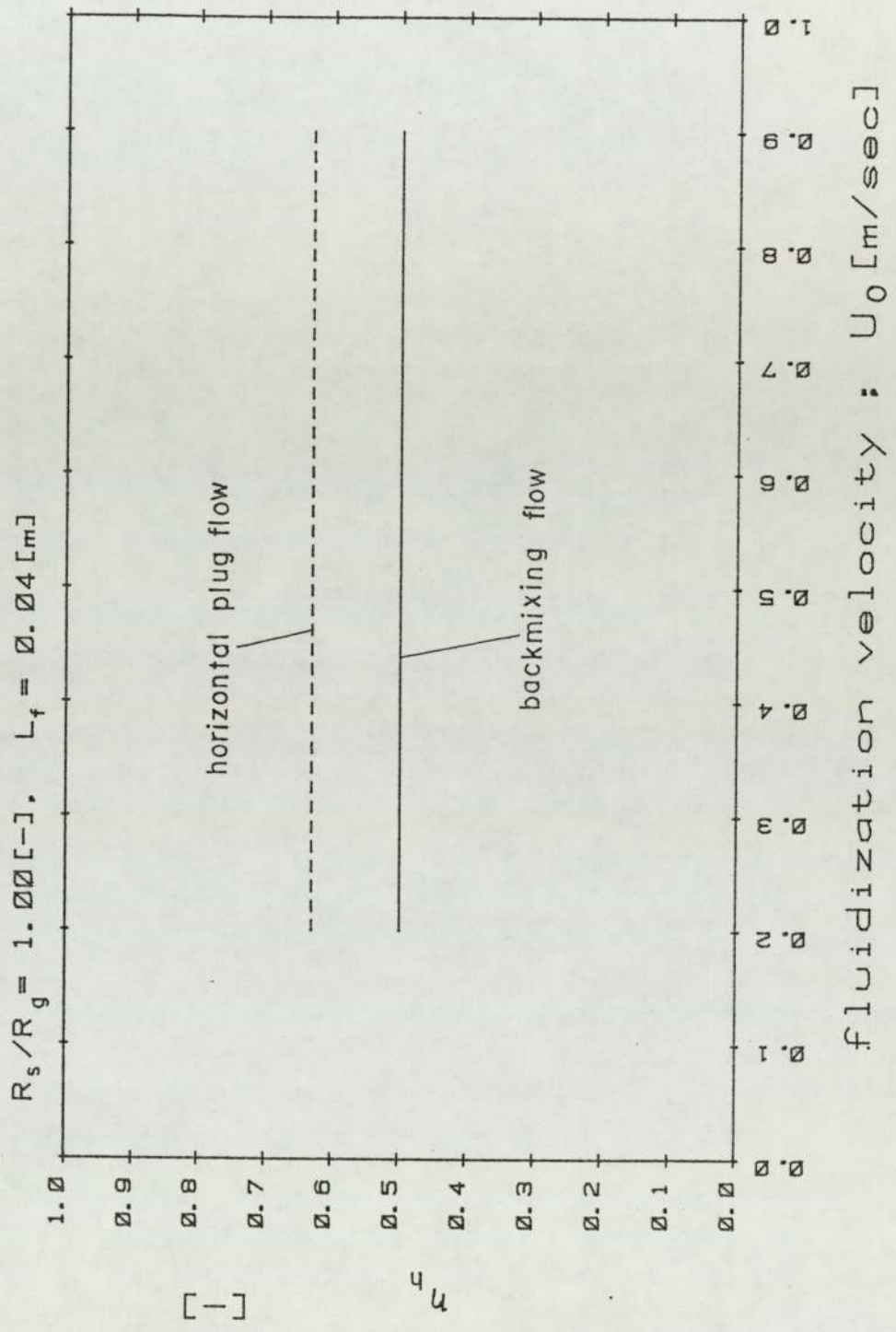


Figure 3.6 Efficiency of perfect backmixing solids flow and horizontal plug solids flow for the "particle heater" as a function of  $R_s/R_g$

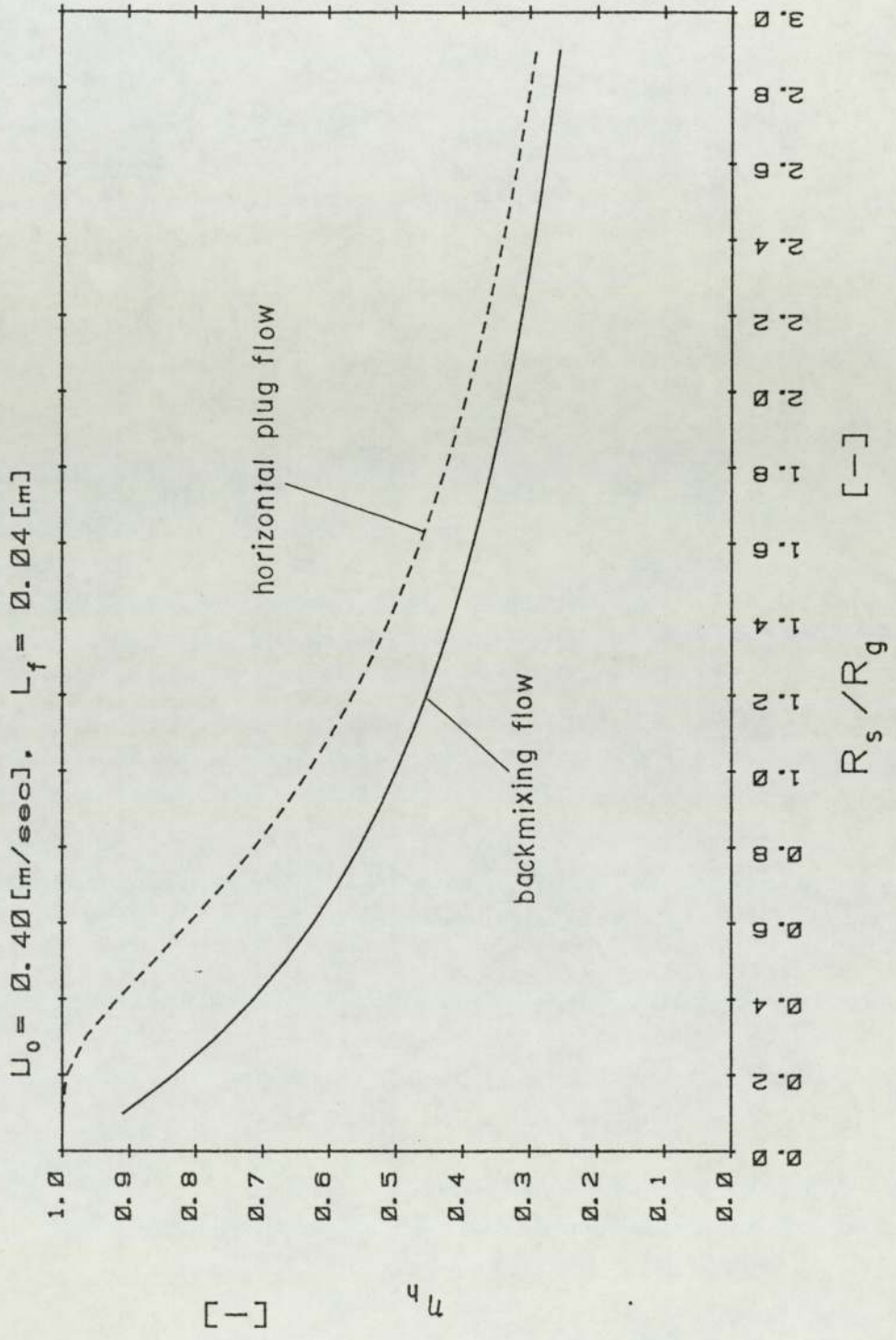


Figure 3.7 Efficiency of cross-current contacting for the single stage

"particle heater" as a function of  $R_s/R_g$

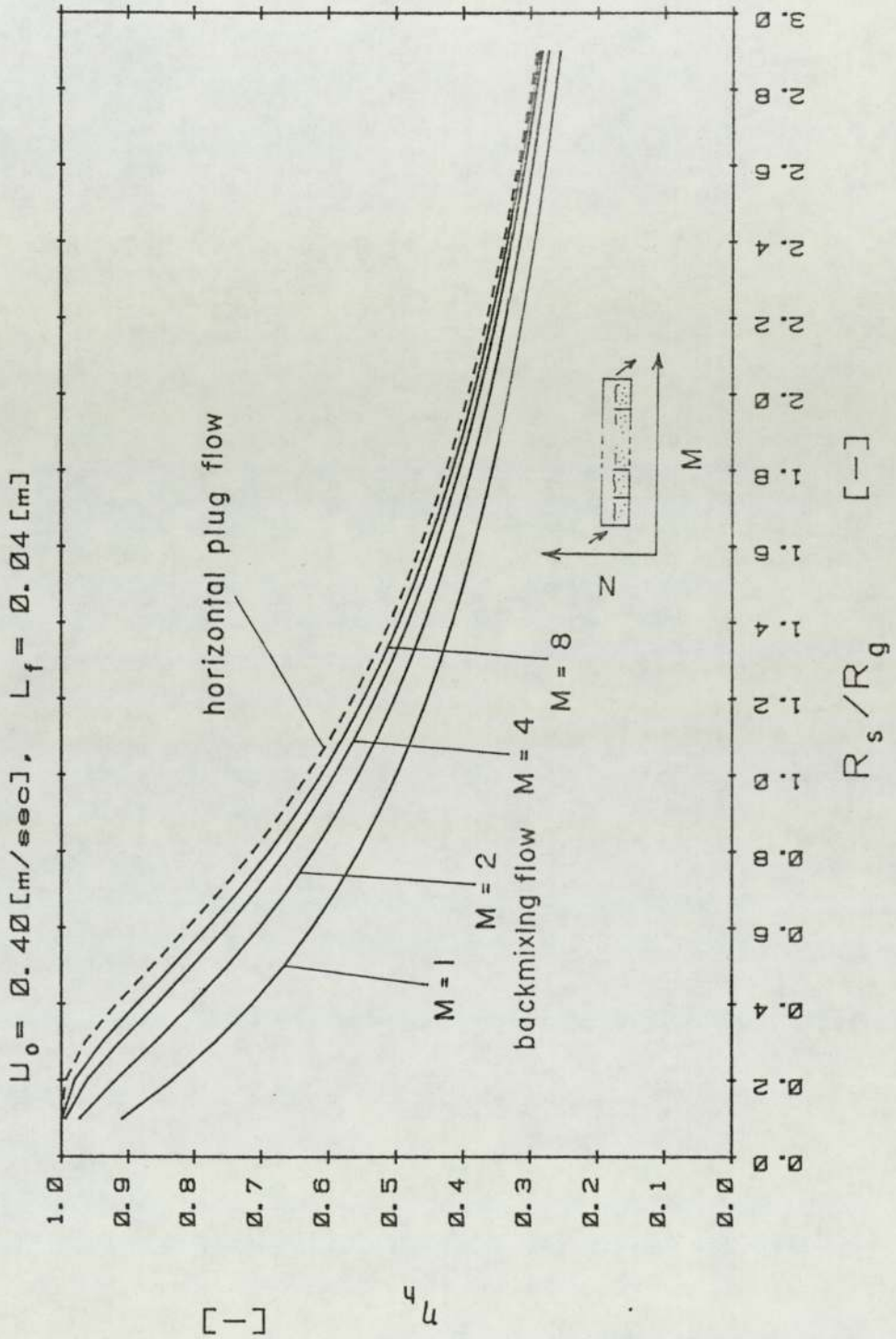


Figure 3.8 Efficiency of counter-current contacting for the "particle heater" as a function of  $R_s/R_g$

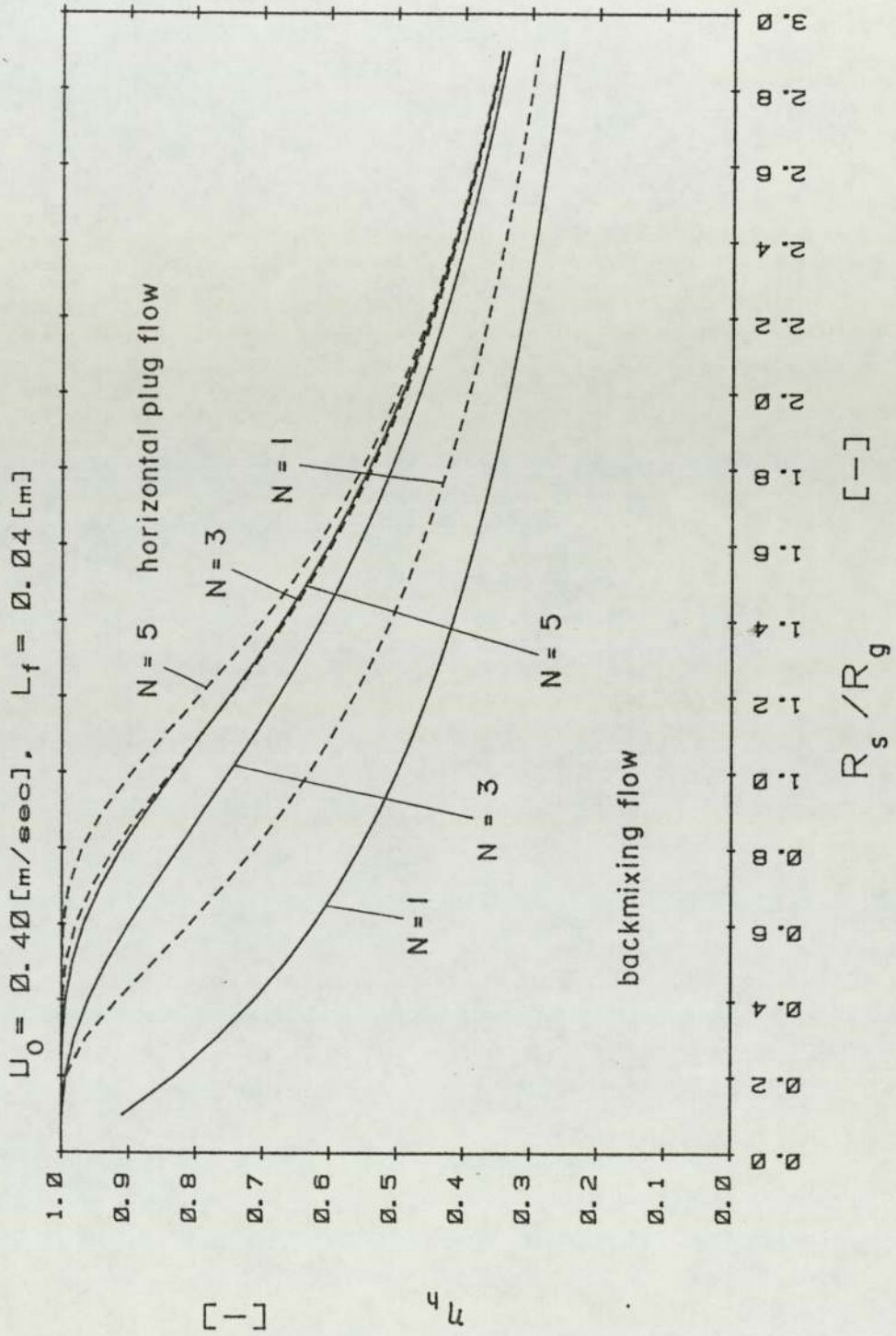


Figure 3.9 Efficiency of the "particle heater" with two-stage beds as a function of  $R_s/R_g$

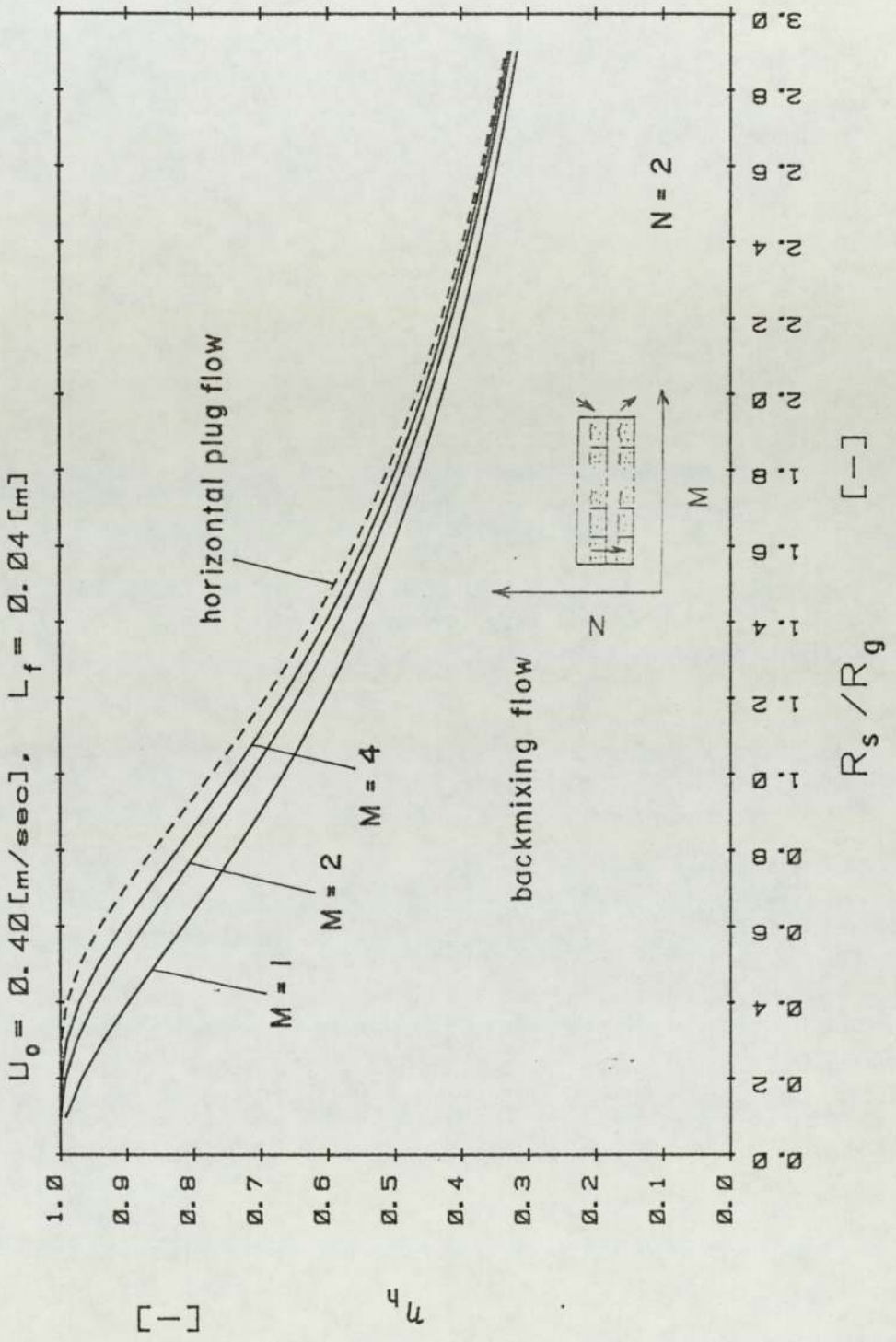


Figure 3.10 Efficiency of the "particle heater" with three-stage beds as a function of  $R_s/R_g$

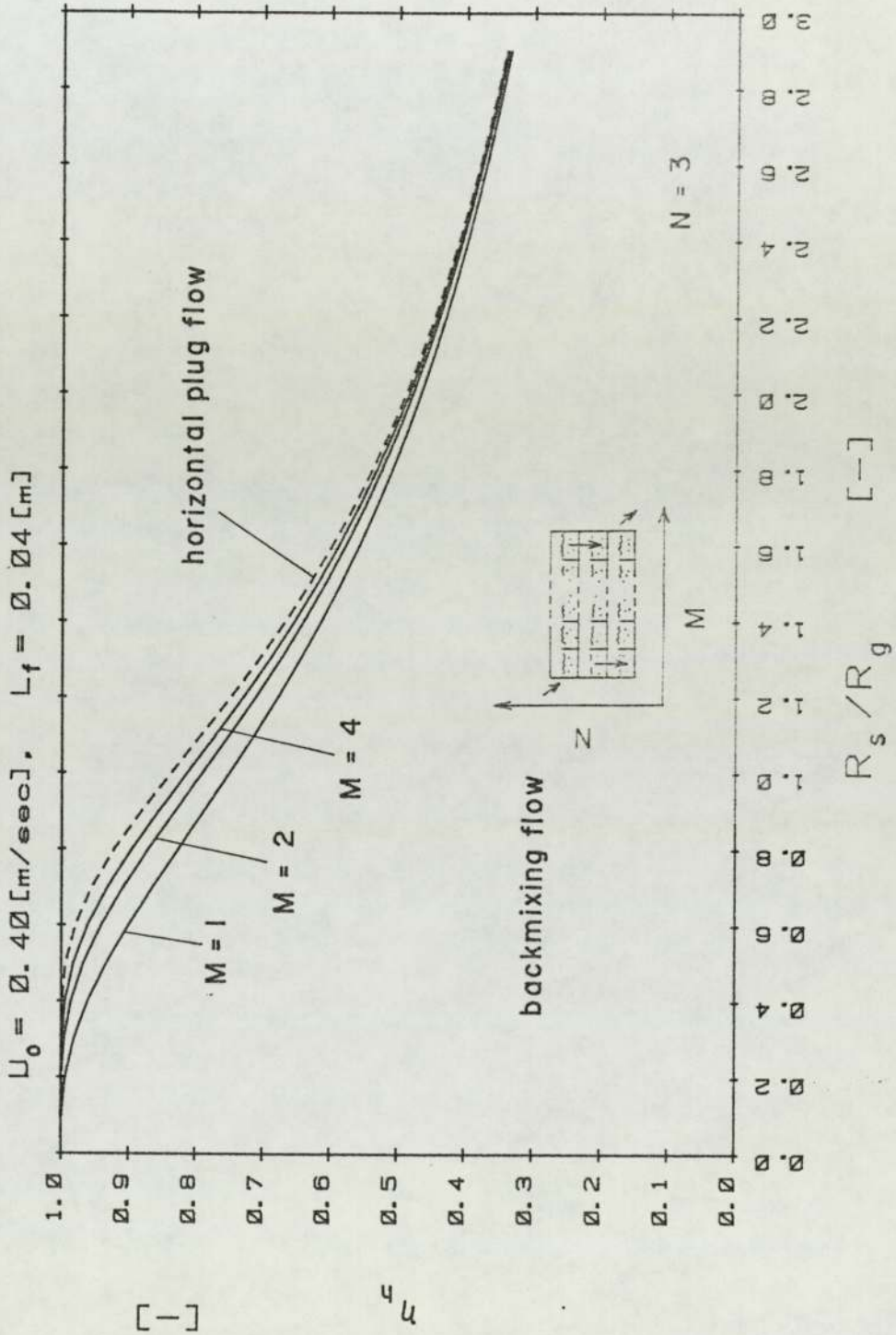


Figure 3.11 Efficiency of the gas-to-gas heat exchanger which consists of equal designed single-stage contacting

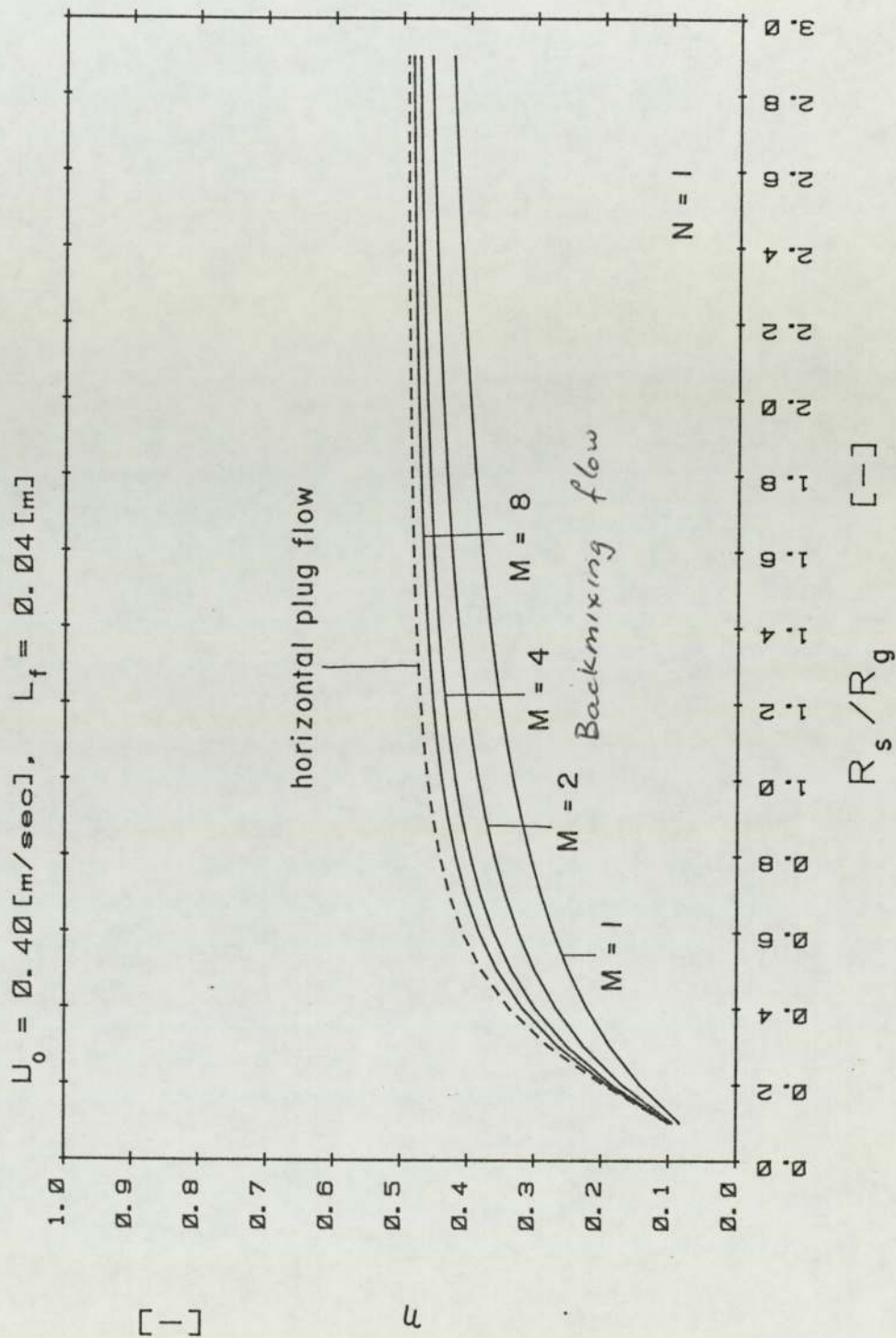


Figure 3.12 Efficiency of the gas-to-gas heat exchanger which consists of equal designed two-stage contacting

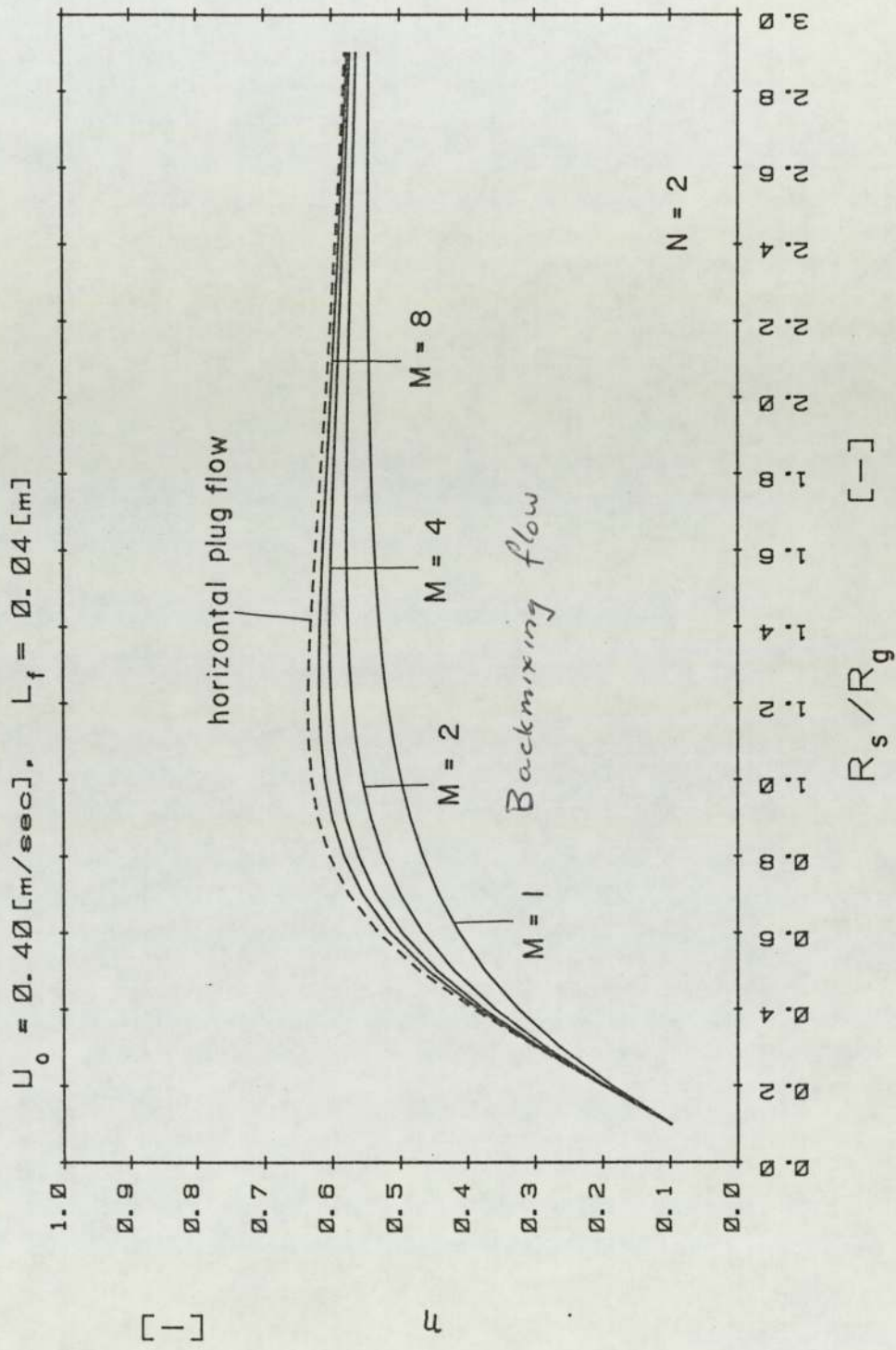


Figure 3.13 Efficiency of the gas-to-gas heat exchanger which consists of equal designed three-stage contacting

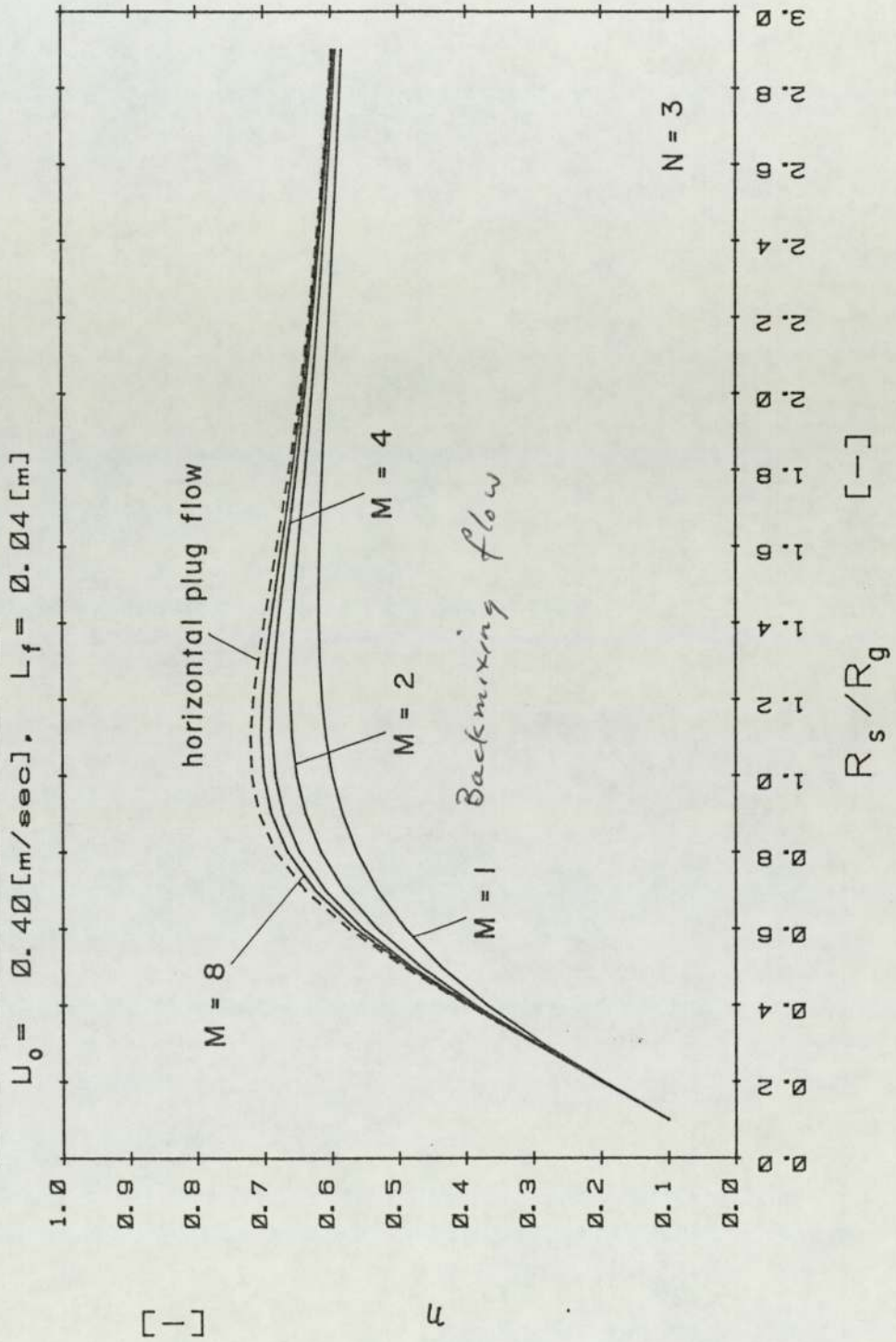


FIGURE 3.14 THREE KINDS OF CONTACTING  
OF GAS AND SOLIDS

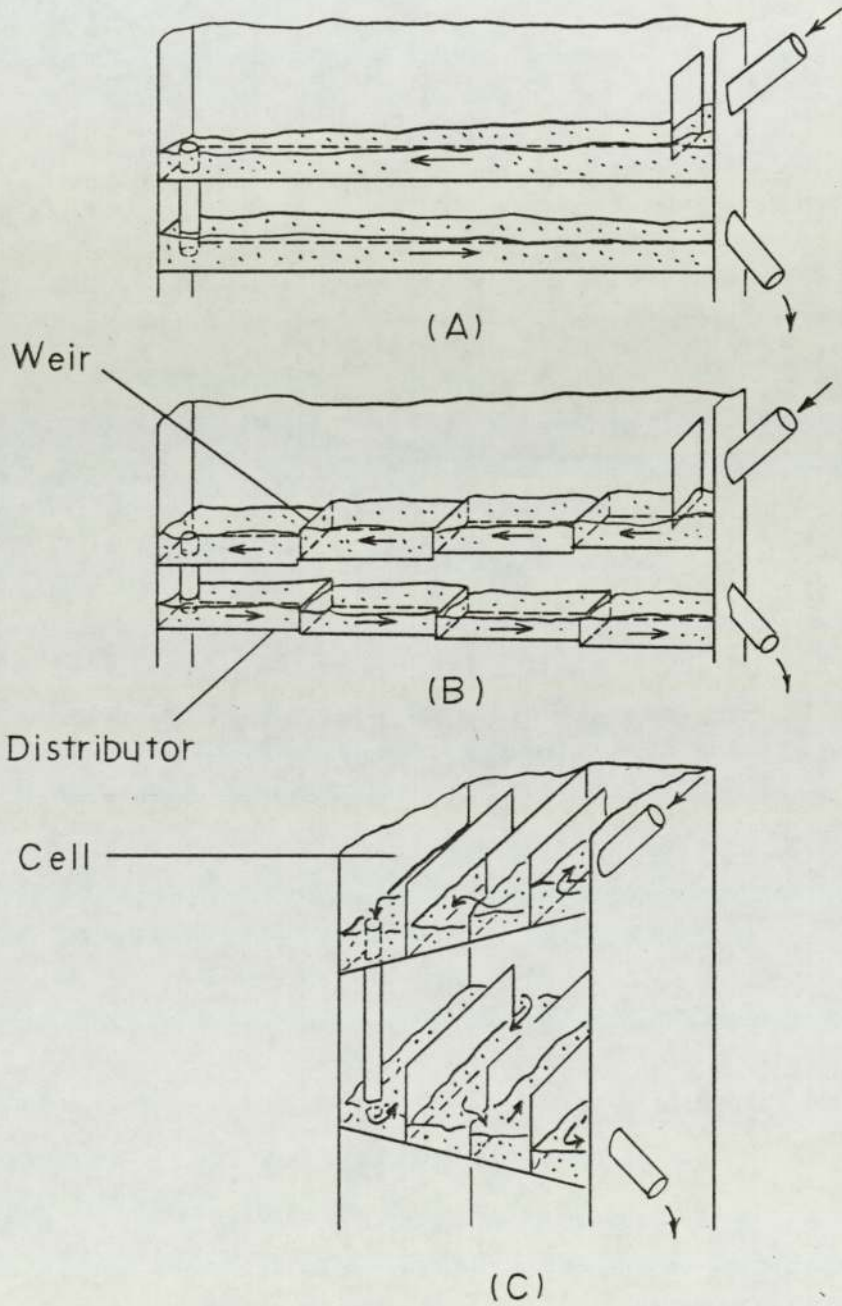


FIGURE 3.15 DEPTH OF BED WITH AN INCLINED DISTRIBUTOR,  $L_f$

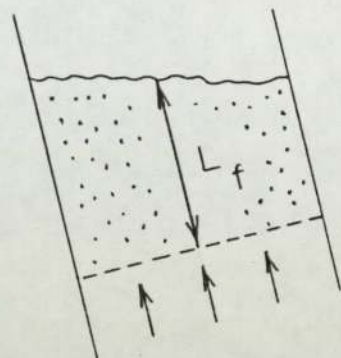


FIGURE 3.16 SCHEMATIC DIAGRAMS OF GAS FLOW PATTERN

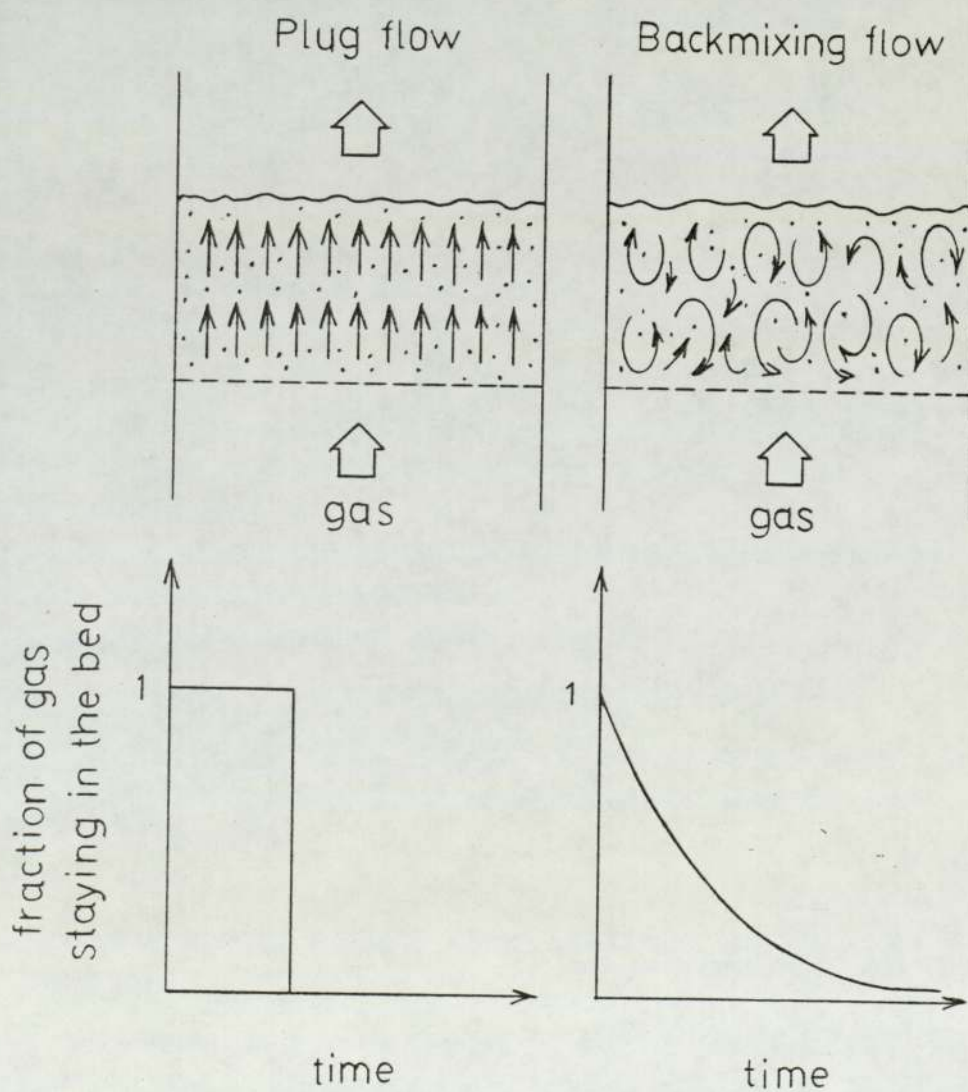


FIGURE 3.17 MODEL FOR HEAT TRANSFER  
BETWEEN THE GAS AND THE BED

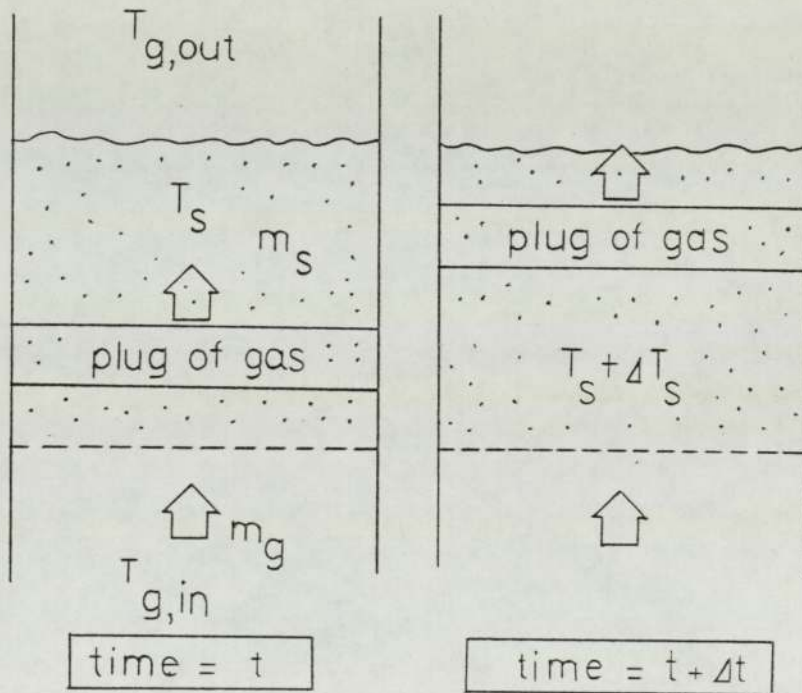
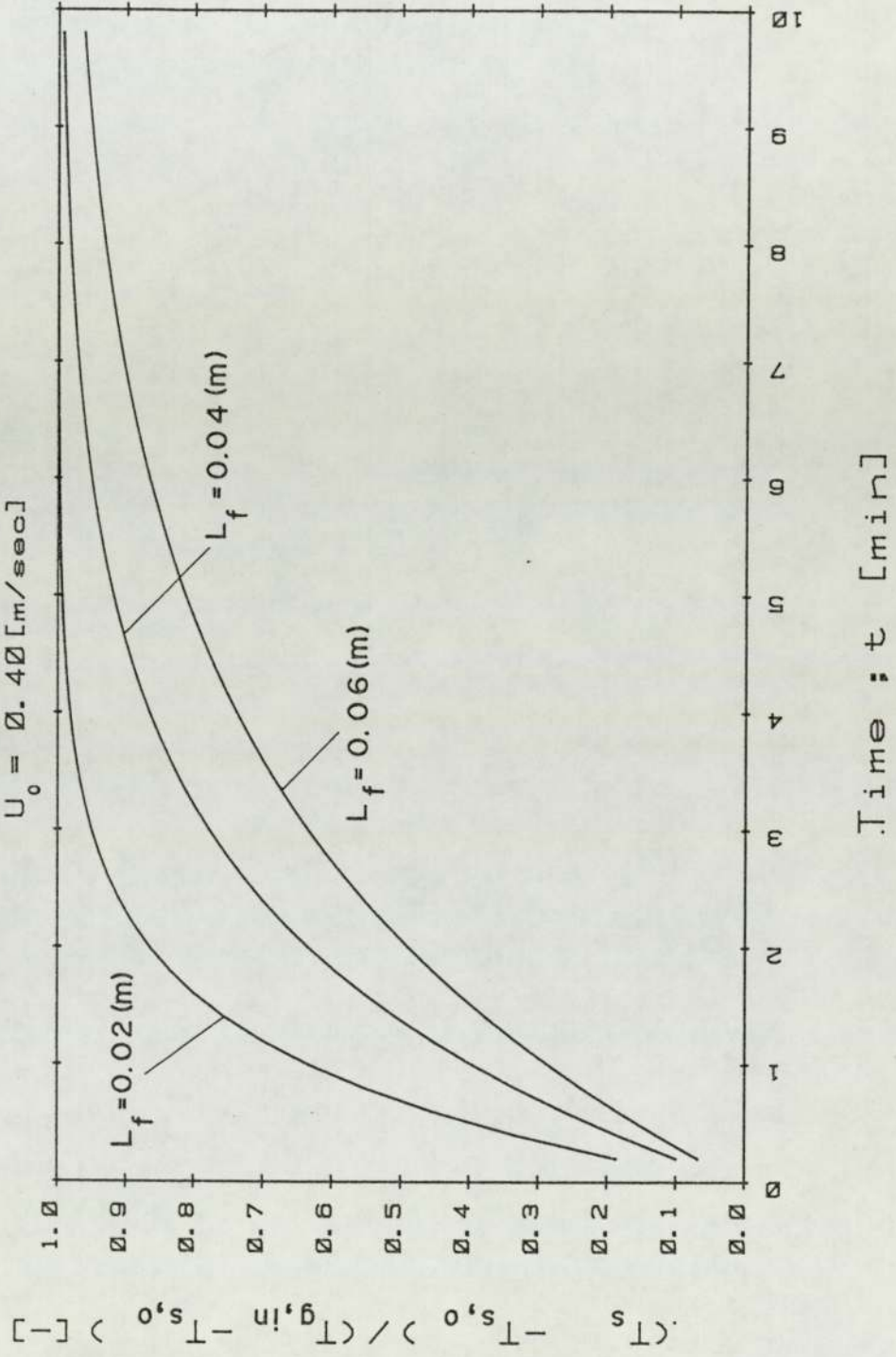


Figure 3.18 Time to reach steady-state



CHAPTER FOUR  
EXPERIMENTAL HEAT EXCHANGER

4.1 INTRODUCTION

This chapter describes the design and construction of the experimental rig which was built to study the ideas explained in Section 3.4. Firstly the aims of the experiments are stated followed by the various constraints placed upon the design of the rig. Then the rig itself is described in detail together with its instrumentation and lastly the experimental procedure is outlined.

4.2 AIM TO THE EXPERIMENTS

Overall the intention was to establish whether a heat exchanger based on the new idea shown in Section 3.4 would actually work. Within this broad scope, several well-defined aims can be specified as follows: —

- (i) to study how the solids movement might be affected by the degree of the inclined gas distributor;
  - (ii) to measure the heat recovery characteristics of the "heater";
- and
- (iii) to obtain sufficient understanding for the design of a complete gas-to-gas heat exchanger.

#### 4.3 DESIGN OF THE EXPERIMENTAL UNIT

There was no knowledge of the movement and flow of solids in the shallow fluidized bed with an inclined gas distributor. Therefore the experimental unit should, as far as practicable, be capable of changing the angle of inclination of the distributor. It had been decided that the angle had to be changed from 0 to 20 degrees. To obtain this wide flexibility, a single-stage bed "heater" was constructed for reasons of simplicity. The "heater" could be divided <sup>in</sup> to 2, 4 or 8 cells by weirs, whose height could also be changed to 2, 4 or 6 cm, as shown in Figure 4.1. After the solids are heated in this bed, they are introduced <sup>in</sup> to fluidized bed "cooler" as shown in Figure 4.2. As discussed in Chapter 3, the solids flow rate is also an important factor for satisfactory operation of this heat exchanger. It is necessary to maintain a stable feeding rate of solids to the "heater", using a vibratory feeder. The cooled particles are lifted up to the top hopper by a vertical pneumatic conveying system and then flow down to the feeder.

The size of the experimental unit was constrained by the amount of fluidizing air available. It had been decided that two existing fans would be used to provide the air to fluidize the "heater" and "cooler"; the performance of these fans therefore limited the area of the bed. ~~The~~ Both fans were of the centrifugal type, namely Secomak type N<sup>o</sup> 492/2. and the performance characteristic is shown in Figure 4.3. The maximum air flow is  $0.2 \text{ m}^3 \text{ sec}^{-1}$ . To be able to attain a fluidizing velocity of  $0.7 \text{ m sec}^{-1}$  at room temperature, the area of the bed ~~could~~ <sup>had to</sup> be less than  $0.3 \text{ m}^2$ . The total area of the bed of the "heater" when constructed was  $0.04 \text{ m}^2$  which ~~can provide~~ <sup>permits</sup> sufficiently large fluidizing velocity for various tests. The

total area of <sup>the</sup> "cooler" was  $0.06 \text{ m}^2$  because the fluidizing velocity ~~was~~ <sup>can be</sup> fixed at about  $2U_{mf}$ .

Thus the basic design of the unit rendered the experimental programme somewhat restricted.

#### 4.4 EXPERIMENTAL UNIT

The experimental unit was assembled at the University from sections fabricated by Aston Services Ltd. Figure 4.4 is a photograph of the complete installation which is shown schematically in Figure 4.5. The air flows generated by the two fans were controlled by gate valves and the flow rate measured by the Rotameters. One air stream was heated electrically, upstream of the plenum chamber located beneath the "heater" distributor. Flow of particles fed from a hopper to the "heater" were controlled by the electrical input to the vibrating feeder. The particles flowed to the "cooler" and were carried to the top hopper by a vertical pneumatic conveying unit. The construction of the heat exchanger and solids conveying unit will now be considered and the metering equipment will be dealt with in Section 4.5.

##### 4.4.1 Fluidized bed "particle heater"

The "particle heater" consists of a square column made of mild steel, 20 cm sides and 16.5 cm high, which can be divided up into 2, 4 or 8 cells by partitions, as shown in Figure 4.1. The height of <sup>the</sup> weirs was alternatively ~~from~~ 2, 4 or 6 cm. The "particle heater" was disposed on the inclined table which angle is variable from  $0^\circ$  to  $20^\circ$  against a horizontal plane. The bed

is filled with particle, which were heated by hot air supplied from an electric heater, a Secomak 15/2, rated at 18 kW. The heated air was forced through the distributor and bed of particles. Figure 4.6 is a photograph of the equipment on the inclined table. Electric heating appeared to be the easiest way of controlling <sup>the</sup> air temperature. Thus a hot air supply and a system to recover heat from it were provided, the recovered heat being retained by the particles, which could then be used to transfer heat to a cold stream of air or gas if desired.

#### Plenum chamber

The heated air enters the lower section of the plenum chamber after having been metered. The plenum acts as a chamber in which the velocity and pressure profiles of the incoming flow are smoothed out partially before the air passes through the distributor. Therefore in the "heater" the plenum is divided into two sections, the upper and the lower section, with a perforated sheet steel as shown in Figure 4.1. The static pressure in the plenum was measured at the 6 mm pressure tapping under the centre of the perforated sheet. The inlet air temperature was determined using a chromel/alumel thermocouples which penetrates the wall of the plenum. The flange on the top of the plenum seals against the underside of the distributor with a gasket.

#### Gas distributor

As already described in Section 2.2.4 the quality or uniformity of fluidization is strongly influenced by the type of gas distributor used. Although the test temperature of the bed is lower than 200° C, dictated by the hot air supply available, the practical operation temperature of the unit in excess of 600° C might be eventually required. So the material of the

distributor should be chosen carefully according to the physical properties. For an inclined fluidized bed, the distributor pressure drop may be a critical factor in obtaining good contacting between solids and gas. From the view point of commercial development the design of the distributor and support plates should also be carefully decided because of the thermal stress and deformation. At temperatures from 500° C to 800° C stainless martensitic chromium steels are suitable for the distributor material because they expand 40% less than stainless chromium-nickel austenitic steels. For higher temperature than 800° C chromium-nickel stainless should be chosen for the distributor and also for its supporting flange, so as to avoid differential thermal distortion between two parts, which can lead to mal-distribution of fluidizing <sup>the</sup> and "channelling" <sup>gas</sup> in the beds.

Before the heat exchanger's performance was determined, the pressure drop characteristics of three kinds of distributors, silicon fibre cloth, perforated sheet and grate bar screen were measured. Their specifications are shown in Table 4.1. The distributors used are square sheets of 20 cm sides with flanges as shown in Figure 4.7.

#### Bed containment

The containment section of the "particle heater" forms the outside wall of the bed and defines the freeboard of the unit as shown in Figure 4.1. It also holds the partitions with weirs in place and the two sloping pipes for the solids entrainment and discharge. The lower flange is sealed on to the top of the distributor with a gasket.

The partitions in the containment separate the bed and freeboard.

The solids flow along the partitions passing over the weirs, which narrows the residence time distribution of the particles in the "heater". A series of interchangeable partitions were made as shown in Figure 4.8. The three different items with the various values of dimension W correspond to a series of weir height of 2, 4 and 6 cm. The number of partitions could also be changed to adjust the solids flow rate and the residence time distribution.

There is no seal between the bottom of the partition and the distributor, <sup>there are</sup> so small <sup>exist</sup> gaps between them which <sup>are</sup> less than 1 mm. Consequently a few particles may transfer to the next cells through the gaps, however we can consider that most particles flow over the weirs because the gap is only about two times larger than the particle diameter. At the higher temperature of practical use there will be no thermal stress between the two parts, which might cause serious distortion there during operation.

As there is some temperature difference between ~~the next~~ two <sup>adjacent</sup> cells, a definite amount of heat will be transferred through the partition between them. In Appendix 3 the heat transfer rate between adjacent cells is considered quantitatively and the analysis concludes that heat insulation is necessary because <sup>comparatively</sup> a large amount of heat will leak between them. Therefore silicon fibre cloth was used for the insulation between the partitions as shown in Figure 4.1.

#### Bed material

The choice of bed material is very important because the functioning of the exchanger strongly depends upon satisfactory gas-to-particle contacting. In Section 2.2.2 it was stated that

Group B particles should fluidize satisfactorily; however it is possible to reduce the size of <sup>the</sup> unit if Group D particles could be used in such a way that <sup>^</sup> good contact efficiency between <sup>the</sup> gas and Group D particles may be improved by circulating solids movement in each cell because of the inclined distributor. In addition the particles need to be resistant to corrosion by hot exhaust gases, to attrition generally and in particular to that induced by thermal cycling. The material must be readily available and as cheap as possible for commercial use. Taking all requirements into account silica sand with a size range of 500 to 710  $\mu\text{m}$  (mean 600  $\mu\text{m}$ ) the most desirable. The basic properties were measured <sup>are given</sup> ~~and shown~~ in Table 4.2.

#### 4.4.2 Fluidized bed "particle cooler"

The aim of the fluidized bed "particle cooler" in this apparatus is merely to cool the particles flowing from the "particle heater", not to test its performance. Therefore the "particle cooler" is an ordinary shallow fluidized bed, which consists of a rectangular column made of mild steel, 40 cm long, 20 cm wide and 16.5 cm high, as illustrated in Figure 4.2. The second Secomak 492/2 fan provides air to fluidize and to cool the particles.

The hot particles flow from the "particle heater" to the "cooler" through an open-ended sloping pipe of heat resistant silicon rubber. To prevent air from flowing between the fluidized beds through the sloping pipe, the pressures in the freeboard of the beds were maintained equal by the outlet air valves. Variations in the exit shape of the sloping pipe were found to strongly influence the flow of solids (2). When the exit shape of the 1 inch diameter pipe as shown in Figure 4.2

is used, we can get smooth solids flow down the pipe.

After the solids were cooled in the bed, they were carried up to the hopper located at the top of the apparatus by pneumatic transport through a 2.5 m long polyethylene pipe. For the test which needed higher solids transporting velocity, the air pressure in the freeboard of the "particle cooler" was raised so as to obtain a larger air velocity for pneumatic transport.

#### 4.4.3 Hoppers and vibratory feeder

Figure 4.5 shows two hoppers and a vibratory feeder, which can feed the cooled particles to the "heater" at steady rates. The two hoppers were square hoppers of 24 cm sides, which were connected by a sloping pipe and <sup>an</sup> open channel bridge. The bridge could be moved manually as illustrated in Figure 4.5 to measure the circulating velocity of solids in the apparatus by sampling them. So as to ensure constant solids flow a brass wire was vibrated in the pipe, because the silica sands have a tendency to adhere to the inside wall due to electrically charging during operation. From the second hopper particles were fed to the "heater" through an enclosed vibratory feeder manufactured by NEI International Combustion Ltd of Derby, photograph of which is shown in Figure 4.9. The controller supplied with the machine enables the amplitude of vibration of the feeder platform to be increased or decreased. Using the silica sand of size range 500  $\mu\text{m}$  to 710  $\mu\text{m}$ , the feed rate was measured and is shown in Figure 4.10.

## 4.5 INSTRUMENTATION

There were four different parameters to be measured on the experimental heat exchanger. These were air flow, solids flow, temperature and pressure and these will be considered in turn.

### 4.5.1 Air flow measurement

The flow meters used for the fluidizing air to the "heater" and the "cooler" were Rotameters manufactured by GEC-Marconi Process Control Ltd. (now Fisher Controls Ltd.) of Croydon. For the fluidizing air flow to the "heater" one Type 65A Rotameter was used to measure the flow and for the air flow to the "cooler" two Type 65A Rotameters mounted parallel were used. The standard curve for a 65A Rotameter for air is shown in Figure 4.11. The air temperature and pressure at the inlet to the Rotameters were measured and the reading was corrected to take account of the difference between operating temperature and pressure and that at which the Rotameter was calibrated.

### 4.5.2 Solids flow measurement

It is difficult to measure the solids flow rate in a pipe from the outside. Therefore a sampling method was used to measure it. As the method explained already in Section 4.4.3 the solids flow was led away from the bridge between two hopper to a beaker and the weight delivered over a measured time was measured. The amount of the sampling weight was limited to between 300g and 600g.

### 4.5.3 Temperature measurement

All the temperature measurements were made using chromel/alumel junction thermocouples supplied by BICC Ltd. The thermo-electric e.m.f. was measured relative to an ice/water bath at  $0^{\circ}\text{C}$ , using a Solartron A200 digital voltmeter which was checked against a standard Weston cell using a potentiometric bridge.

Nine thermocouples were used to measure the temperatures around the system. The air temperatures were measured at the outlet manifold from the Rotameter, in the plenum chamber of the "heater" and at the centre of the outlet manifold from the "heater", these latter being the hot inlet and cooled outlet air temperatures. *using shielded thermocouples* The solids temperatures ~~were~~ *was* also measured in the feeder and at the sloping pipe by which the "heater" and the "cooler" are connected. Four thermocouples were supported from the top of the bed containment of the "heater" and measured the temperatures at four different points about 5mm below the bed surface. As will be described later, these results must be interpreted, bearing in the mind that thermal equilibrium between air and particles might not be attained.

#### 4.5.4 Pressure measurement

The air pressures in the system were measured with a water-filled U-tube manometer which had one limb open to atmosphere. The static pressures in each side of the plenum chamber were measured at their centre, and the Rotameter flow readings were corrected for these pressures and a barometer reading to account for the higher fluid density at the flow meter. The other measurement was the differential pressure between the freeboard spaces of the two beds as this affected the leakage through the sloping pipe between them. Throughout all experiments, attention was paid to minimizing this leakage by maintaining a low differential

pressure.

#### 4.5.5 Bubbling observation

The movement of solids and rising bubbles were observed by using a transparent bed containment, namely, acrylic plastic. The containment was the same size as one cell in the "heater" and it has neither the inlet nor the outlet of solids. A diagram of the containment is Figure 4.12. As the plastic does not withstand high temperature the bed temperature was limited to less than  $100^{\circ}$  C. The visual observations were made with the various angles of inclination of the distributor.

#### 4.6 EXPERIMENTAL PROCEDURE

Having chosen the particle size, the weir height, the distributor and its inclined angle, the following procedure was adopted in the experimental work on the heat exchanger.

1. The hot and cold sides air flow were selected and these were set on the Rotameters.
2. The air heater and the particle feeder were then switched on.
3. The power of the heater was selected so as to heat up the air flow to the temperature  $120-170^{\circ}$  C.

It took about one hour for the heat exchanger to attain a steady-state. (The bed temperature was always monitored by a pen-recorder, so that it could be easily ascertained when a steady-state was established.) To plot a performance curve, the hot air flow was maintained constant; the solids flow rate was varied.

At each solids flow rate all the thermocouple outputs and air pressure were noted once steady-state was reached. The solids flow rate was then changed to the next value and steady-state observations repeated.

In order that meaningful calculations based on the experimental data could be made, it was important to ensure that steady-state had been reached in the experiments. This required that the hot air flow rate, the power supplied, the hot air inlet temperature, the solids flow and the cold air flow had to be held constant.

Table 4.1 Specifications of distributor plates used

sheet type	make	material	hole or slit size (mm)	sheet thickness (mm)	open area (%)
silicon fibre cloth	Chemical & Insulating LTD	silicon	-	-	-
perforated sheet	Hein, Lehmann AG	stainless steel AISI 316	0.15	0.75	2.5
grate bar screen	N.Greening LTD	stainless steel AISI 430	0.125	3.83	4.8

Table 4.2 Basic properties of the bed material

material	$d_p$ (m)	$\rho_s$ (kg/m <sup>3</sup> )	$C_s$ (kJ/kg K)
silica sand	0.0005-0.00071 (mean 0.0006)	2590	1.00

FIGURE 4.1 "PARTICLE HEATER" CONFIGURATION

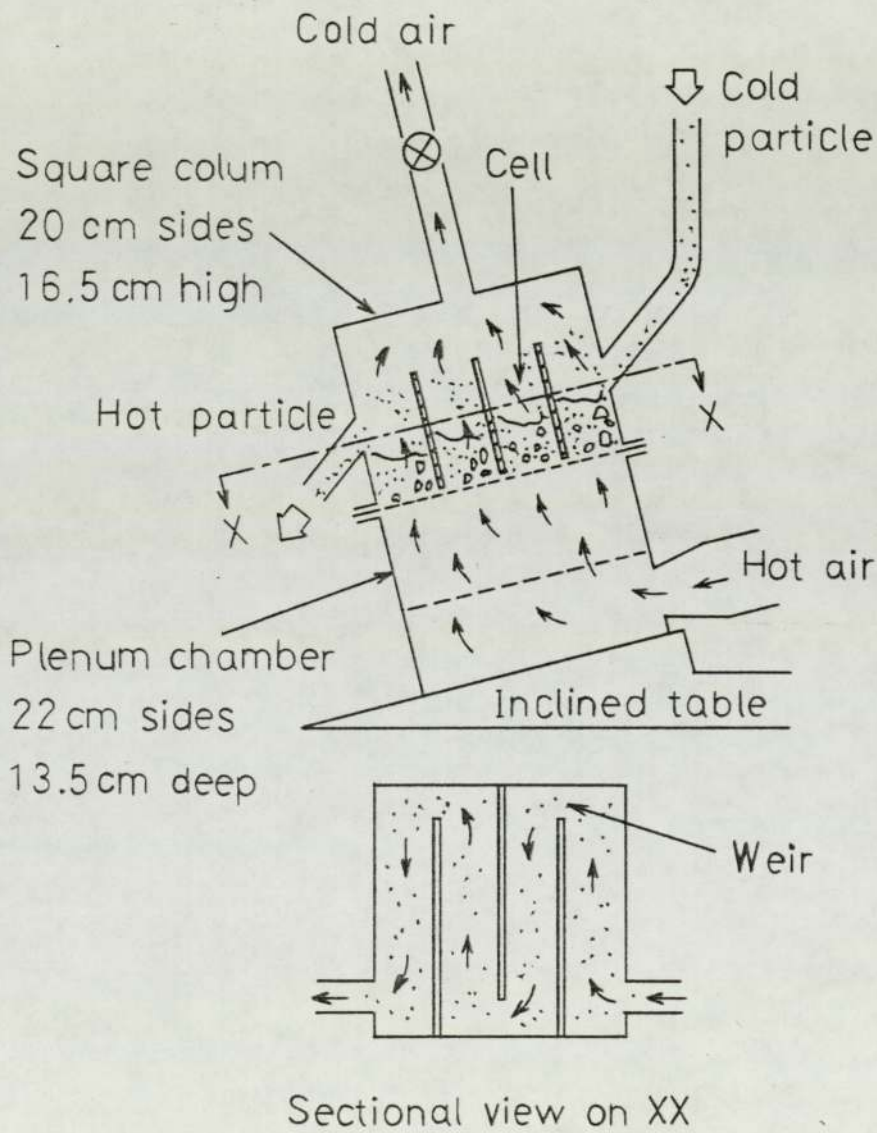


FIGURE 4.2 "PARTICLE COOLER" CONFIGURATION

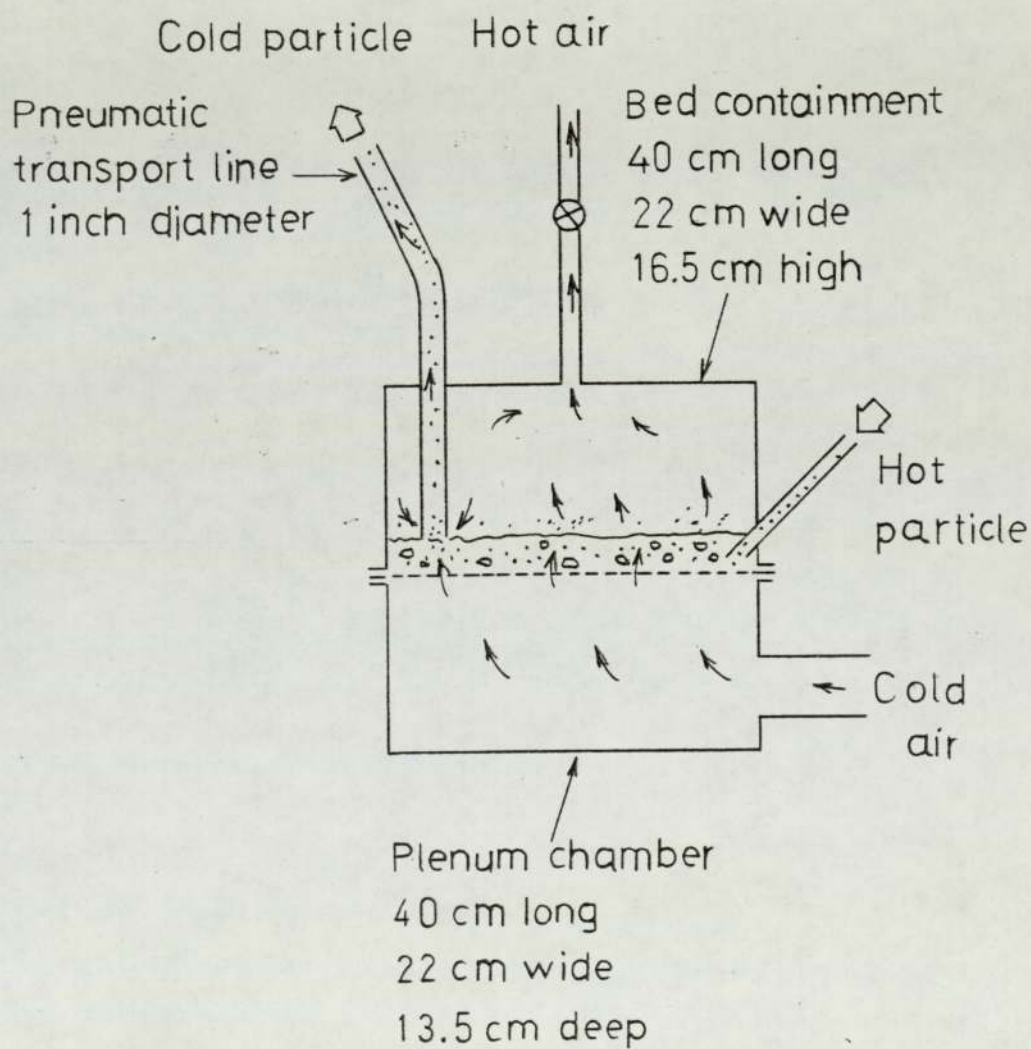


FIGURE 4.3 PERFORMANCE CURVE OF SECMAK  
FAN 49 2/2

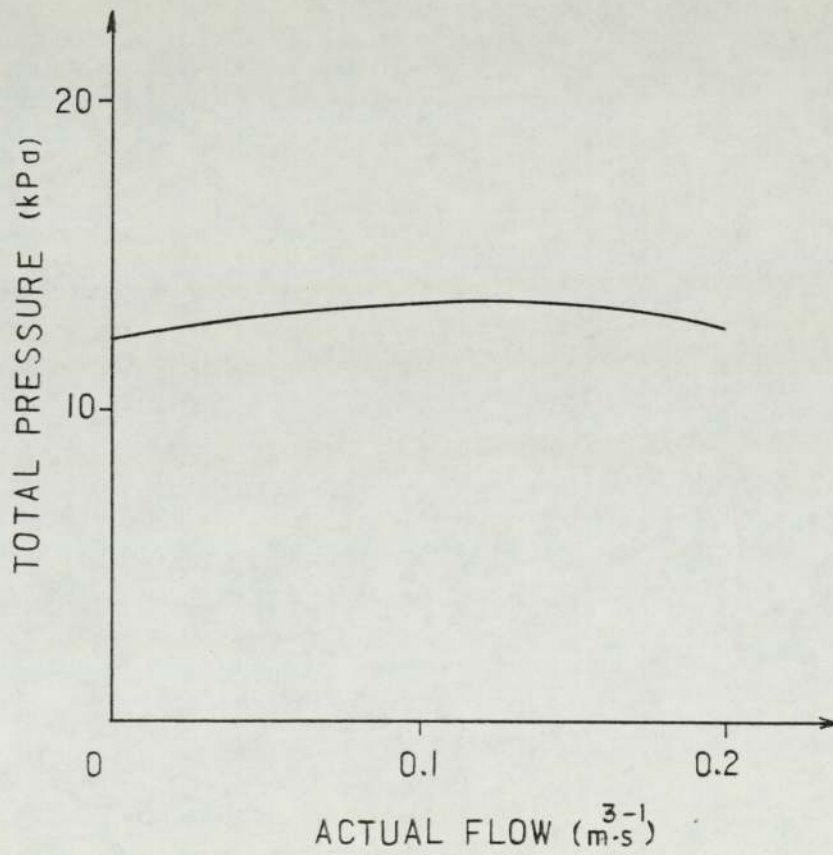


Figure 4.4 Photograph of the complete installation

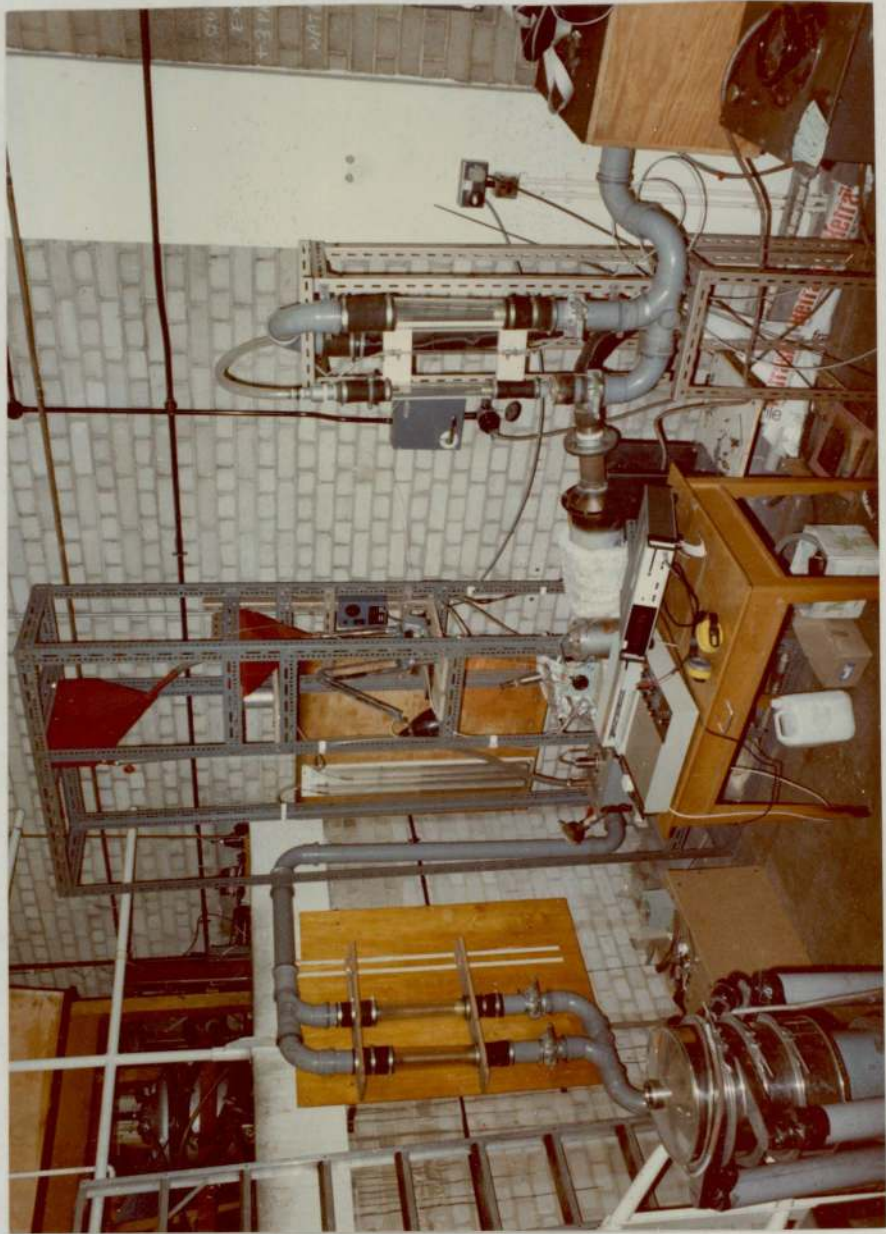


FIGURE 4.5 SCHEMATIC DIAGRAM OF EXPERIMENTAL SYSTEM

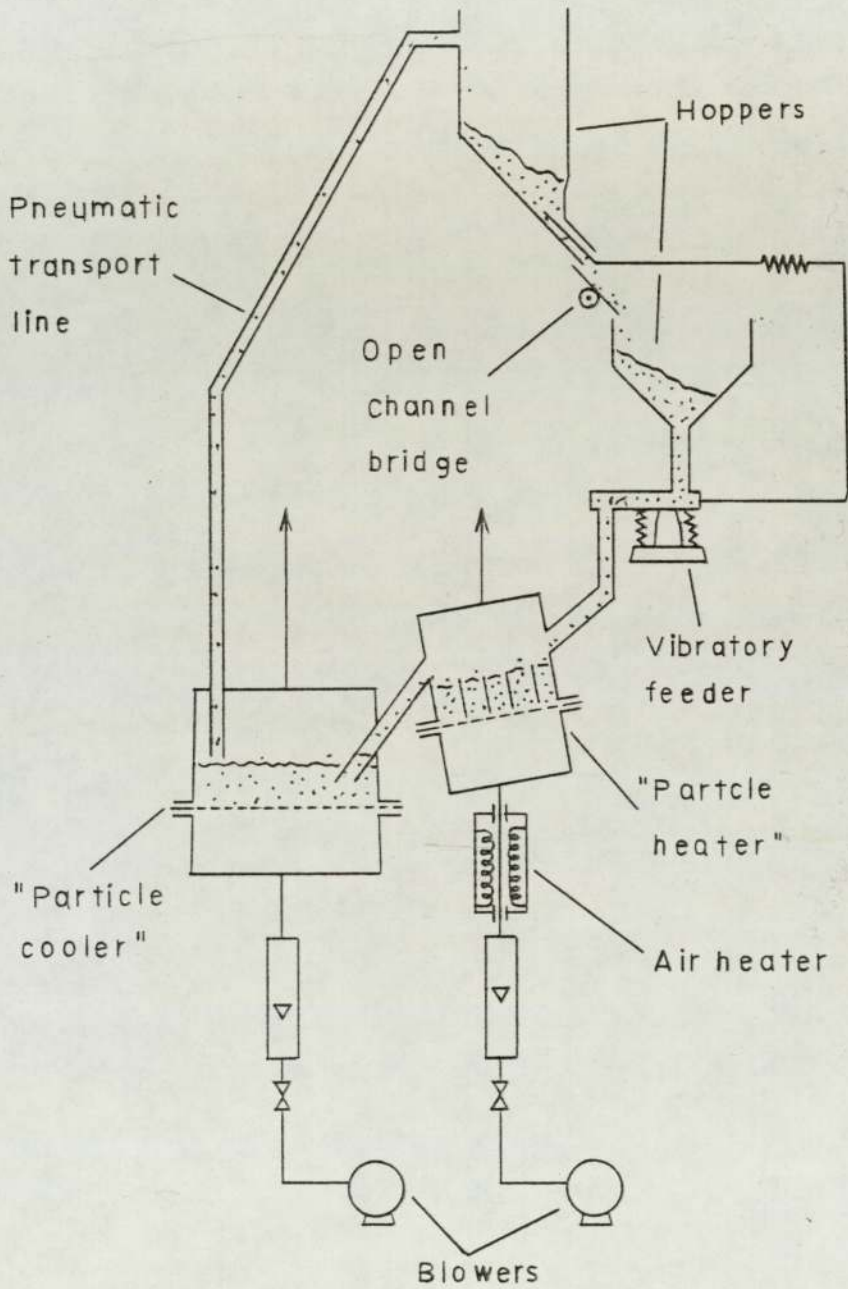


Figure 4.6 Photograph of the equipment on the inclined table

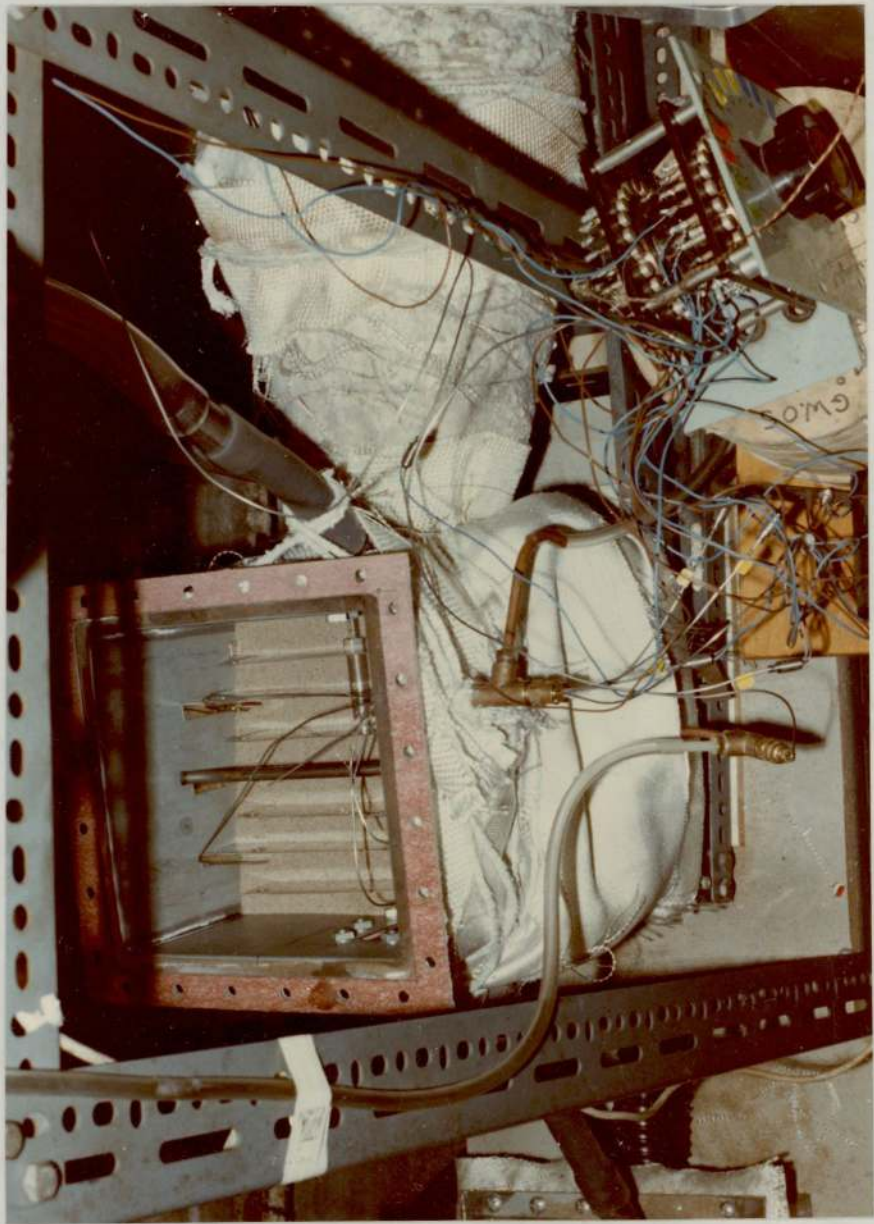


FIGURE 4.7 DIMENSION OF GAS DISTRIBUTOR OF  
"PARTICLE HEATER"

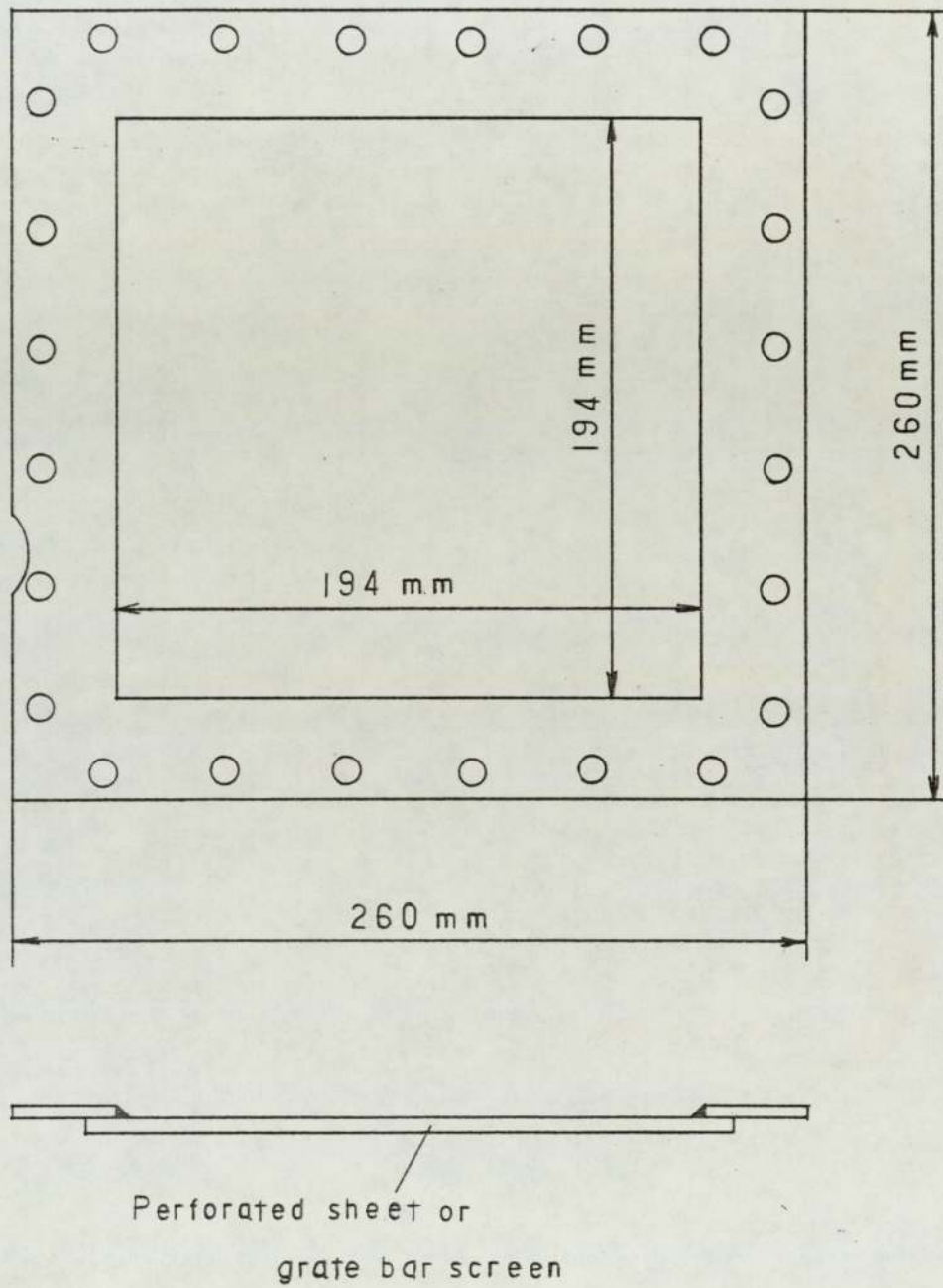
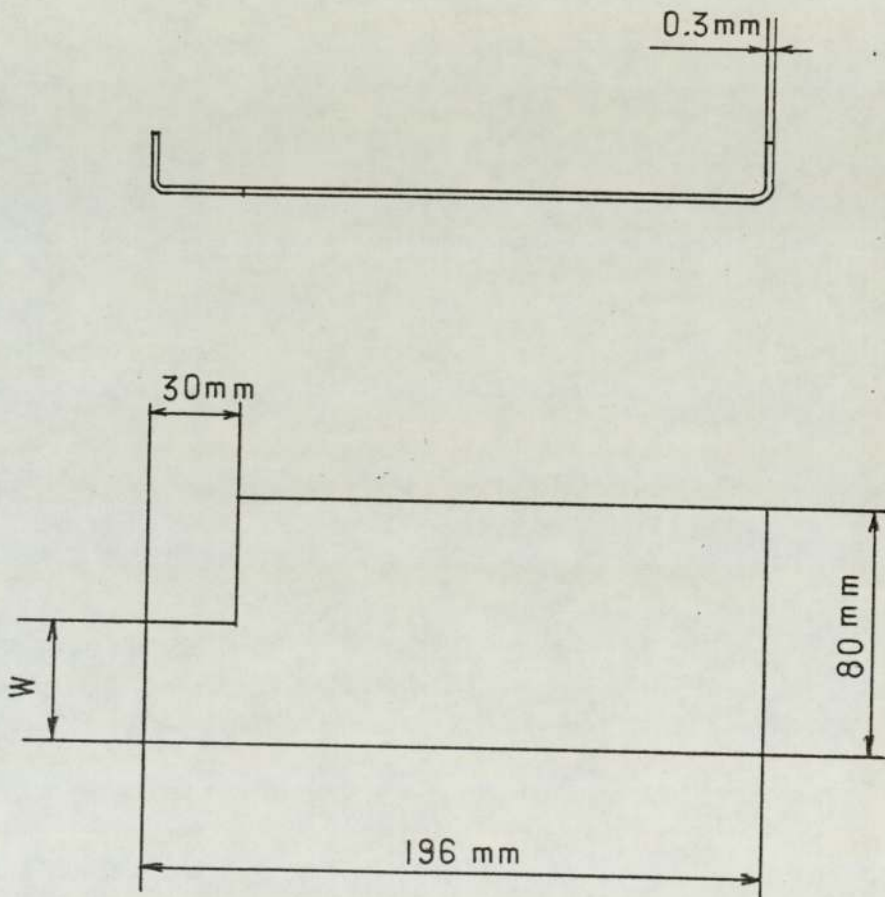


FIGURE 4.8 DIMENSION OF PARTITION



W : Height of weir

Figure 4.9 Photograph of the vibratory feeder



FIGURE 4.10 PARTICLE FEED RATE OF VIBRATORY FEEDER VERSUS CONTROLLER SCALE SETTING

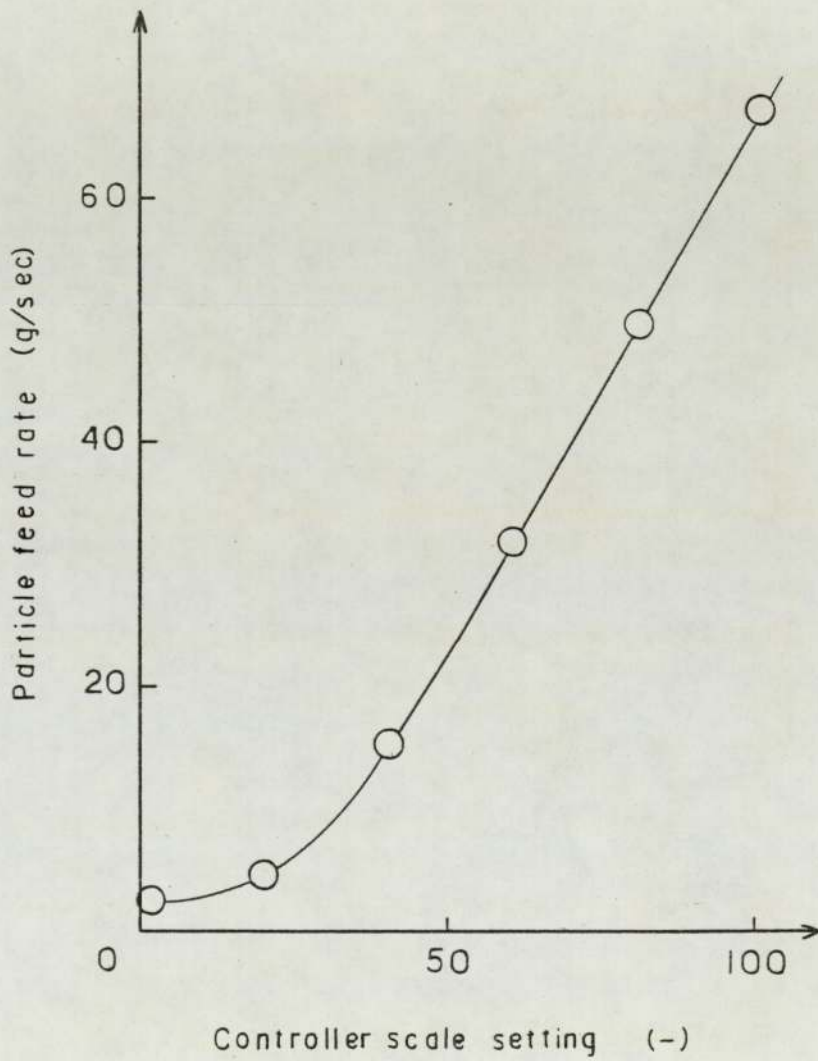


FIGURE 4.11 THE STANDARD CURVE FOR A 65A ROTAMETER

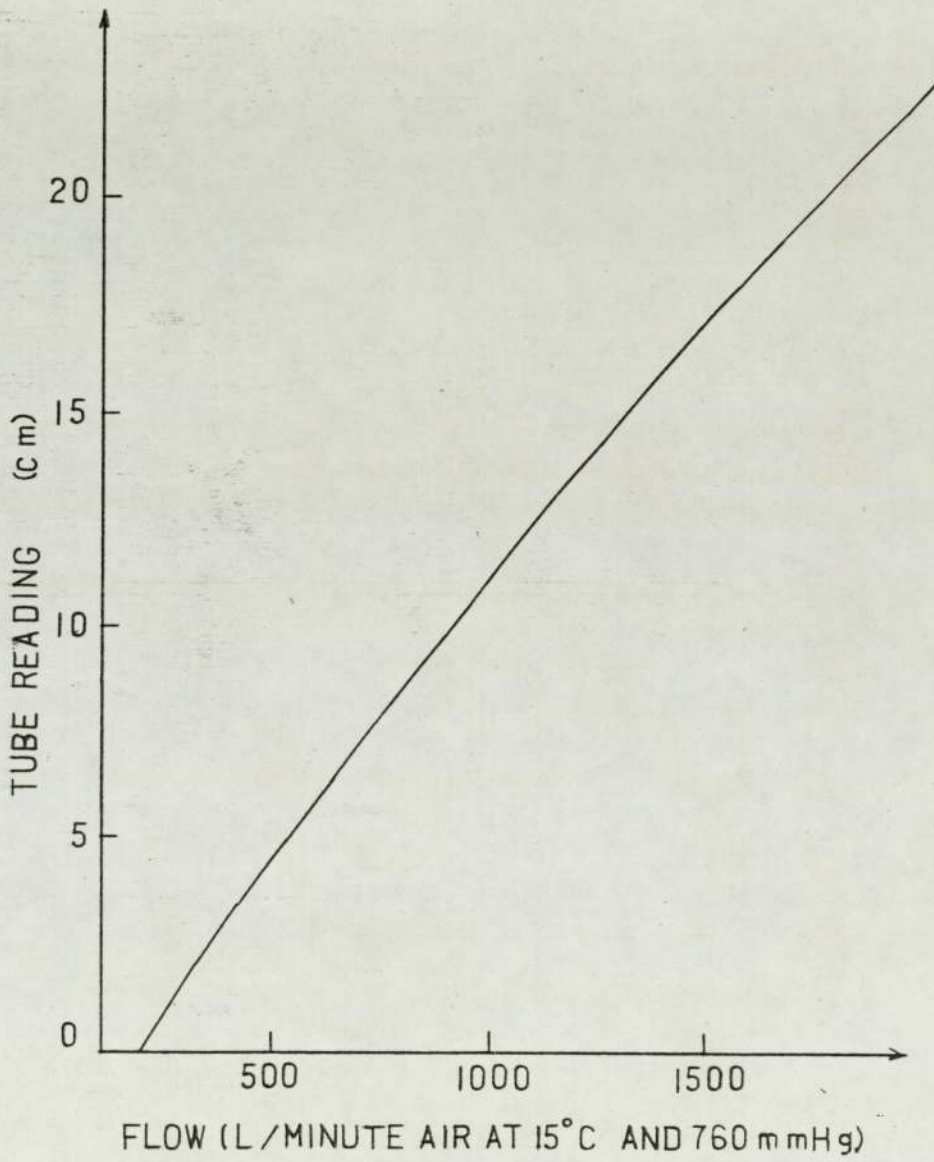
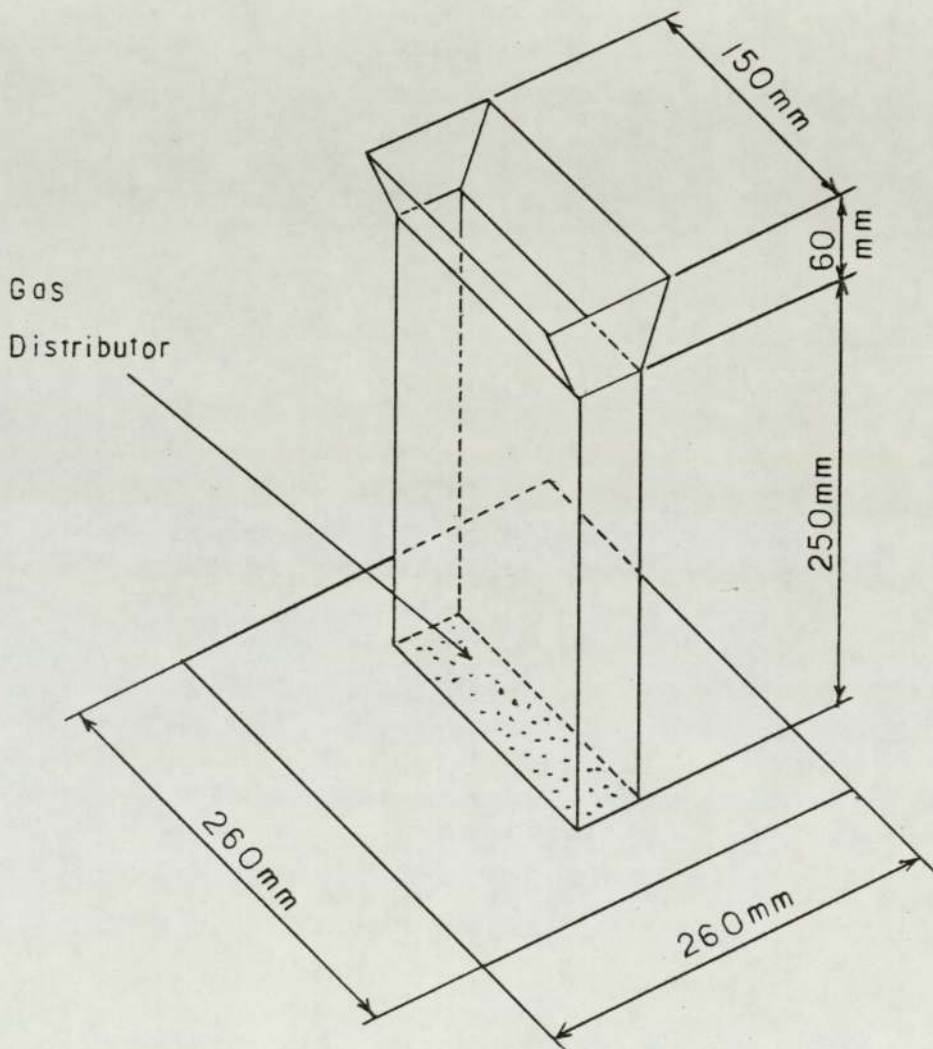


FIGURE 4.12 DIMENSIONS OF TRANSPARENT BED CONTAINMENT



## CHAPTER FIVE

### OPERATIONAL CHARACTERISTICS OF THE EXPERIMENTAL HEAT EXCHANGER

#### 5.1 INTRODUCTION

This chapter describes the work carried out on the experimental heat exchanger, the design of which was detailed in the previous chapter. The aim of the experiments was to find how effectively the "particle heater" performed, not to study the solids circulation systems between the "heater" and the "cooler", <sup>although</sup> ~~because~~ the operational characteristics of shallow beds with an inclined distributor have never been studied for heat exchanger applications. The experiments focused on the efficiency of the "heater" of one stage unit. Multi-stage operation will be evaluated theoretically in Chapter 6 using the results of this one stage unit. Before describing these however, the basic practical properties of the distributor plate, the particles, their movement and the heat transfer between the particles and air will be discussed.

#### 5.2 DISTRIBUTOR PLATE PRESSURE DROP CHARACTERISTICS

The distributor plate used in the heat exchanger was chosen from the three kinds of sheets whose specifications were shown in Table 4.1. The pressure drops across the sheets,  $\delta p_d$ , increases with the air velocity through them and the plots of this characteristic are shown in Figure 5.1. The pressure drop of the silicon fibre cloth is the largest and the perforated sheet pressure drop is

the smallest. The grate bar screen has a pressure drop twice as large as that of the perforated sheet, but the pressure drop across the shallow bed predicted from equation 2.1 is larger than it. The mechanical strength of the silicon fibre cloth was found to be insufficient for use as the distributor for the practical heat exchanger. The grate bar screen and the perforated sheet were therefore chosen for the further experiments.

### 5.3 MINIMUM FLUIDIZING VELOCITY OF THE PARTICLE

The minimum fluidizing velocity,  $U_{mf}$ , of the silica sand used in the heat exchanger was determined in the square column of the "particle heater" as shown in Figure 4.1. This had a horizontal grate bar screen distributor and no partitions. Compressed air at room temperature,  $20^{\circ}\text{C}$ , was used to produce fluidization. The distributor plate characteristic was measured and the pressure drop across the bed,  $\delta p_b$ , was found by subtraction from the total pressure drop. In these experiments the air velocity was gradually increased from zero to well above  $U_{mf}$  and reduced to zero. The resulting graph is shown in Figure 5.2. The determination of  $U_{mf}$  from the pressure drop data has been described earlier with reference to Figure 2.2 and this can be done for Figure 5.2. The value of  $U_{mf}$  with air at  $20^{\circ}\text{C}$  is  $0.28\text{ m sec}^{-1}$ . Below this value of fluidizing velocity the bed would not be fluidized so it is impossible for the heat exchanger to operate below this limit.

## 5.4 FLUIDIZATION IN THE BED ON INCLINED DISTRIBUTOR

Fluidization in a small containment was observed through transparent bed wall as shown in Figure 4.13. The pressure drop and the heat transfer characteristics of the bed were also measured. The inclined angle of the table was changed to  $0^\circ$ ,  $5^\circ$ ,  $10^\circ$ ,  $15^\circ$  or  $20^\circ$ . The total weight of the particles used for the all tests was 400 g.

### 5.4.1 Observation of fluidization

Bubble formation and solids movement in the small bed were observed, changing the inclined angle and fluidizing velocity. Fluidization behaviour changed significantly when the horizontal distributor was changed to an inclined distributor. In the bed with horizontal distributor, the bubbling started at  $U_{mf}$  in the normal manner of the fluidized bed as described in Section 2.2. As the air flow increased beyond  $U_{mf}$  the agitation of bubbling became more violent so that the solids were uniformly fluidized. The photograph of this condition is shown in Figure 5.3. On the other hand, in the bed on <sup>the</sup>  $15^\circ$  inclined distributor the bubbling started at <sup>a</sup> lower superficial velocity than  $U_{mf}$  <sup>and</sup> ~~the~~ all bubbles passing through the shallowest part of the bed. Increasing the air velocity caused most bubbles to rise rapidly through the shallower part like a jet so that ~~the~~ many of the particles were swept upwards and then fell downward to produce a circulation of particles; the upward flow being rapid, the downward flow being slow through the deep part of the bed, as shown in the photographs from Figure 5.4 to 5.6. The change to this fluidization behaviour occurs progressively as the distributor angle of inclination is increased from  $5^\circ$  to  $20^\circ$ . As the angle increases the fluidization tends toward spouting through the shallow part, as shown in the

photographs from Figure 5.7 to 5.9. Figure 5.10 also shows the observation from the top of the "particle heater".

#### 5.4.2 <sup>c</sup> Pressure drop characteristics

The pressure drop across the bed was measured at each angle of the distributor from  $0^\circ$  to  $20^\circ$ . A grate-bar screen distributor was used, and the resulting graph is shown in Figure 5.11. It shows the trend that as the angle increases,  $\delta p_b$  decreases gradually. When the horizontal distributor was used, a sharp change of  $\delta p_b$  curve is seen at  $U = U_{mf}$  because the fluidization starts suddenly everywhere in the bed at this point. On the other hand, as the angle increases the change from packed bed to fluidized bed becomes smoother because the bubbling starts from the shallowest part of the bed and spreads gradually over the other part. This is reflected in the rate of change of pressure drop in Figure 5.11 with the inclined distributors. As the large fraction of the bubbles pass through the shallow part the bed, with the more inclined distributor, this one has the lower  $\delta p_b$ .

Pressure distribution was measured in the beds by an 1 mm diameter pipe with pressure tap at its top. The pressure tap can be immersed anywhere in the bed and the pressure is read at the U-tube manometer. Figure 5.12 shows the pressure distribution in the beds with the distributor inclined at angles  $0^\circ$  and  $15^\circ$ . In the bed with the horizontal distributor the isobaric lines were also horizontal, parallel to the surface and the distributor. However with the  $15^\circ$  inclined distributor the isobaric lines were not horizontal because the large fraction of the air flows through the shallower part.

### 5.4.3 Heat transfer between solids and air

The experiments in Section 5.4.1 and 5.4.2 suggest that the fluidization in the inclined distributor bed is not equal everywhere, being similar in a whirling bed (34) or a spout-fluid bed (94). It might not be proper to apply Kato's empirical equation (equation 2.11) to estimate the heat transfer coefficient,  $h_p$ , in this condition. To find the heat transfer characteristics, unsteady-state experiments were carried out. Hot fluidizing air, about  $95^{\circ}$  C, heated up the particles from room temperature and the exit air temperature was measured with time as described in Section 4.6.

Figure 5.14 shows the experimental results of the dimensionless exit air temperature change from the horizontal distributor bed with heating time. From the result, the air-to-particle heat transfer coefficient,  $h_p$ , can be estimated assuming that the air flow through the bed is plug flow and that heat also transfers between the bed and the distributor. The bed-to-distributor heat transfer coefficient,  $h_d$ , was assumed to be equal to  $h_w$  and was estimated  $220 \text{ W/m}^2 \text{ sec. K}$  from <sup>Zubrodsky's</sup> equation 2.7 as detailed in Appendix 3. The logic diagram for the computer simulation of <sup>the</sup> exit air temperature is shown in Figure 5.13 and the simulated result is shown in Figure 5.14,  $h_p$  being estimated by Kato's equation. Comparing the experimental and the simulated curves they show good agreement.

Figure 5.15 shows the comparison of  $T_{g,out}$  change of the horizontal and  $15^{\circ}$  inclined distributor bed. Between the two experimental curves no significant difference can be seen, even though their fluidizing behaviors are utterly different as described in Section 5.4.1 and 5.4.2. In <sup>the</sup> inclined distributor bed the majority of air flows in the rapid bubbles through the

shallower part of the bed, which does not cause good contacting between air and particles there. However, <sup>the</sup> bubbles' movement enhances the solids circulation in the bed and the contact between air and particles in <sup>the</sup> freeboard.

Gas outlet temperatures,  $T_{g,out}$ , were measured for different air velocities in the  $15^\circ$  inclined distributor bed and all results are shown in Figure 5.16. Assuming that ~~the~~ all particles contact with <sup>the</sup> air, that the air flow is plug flow, whose velocity is equal to the superficial velocity,  $U_f$ , and that the bed depth is equal to the average depth, the exit air temperature was calculated by the same computer simulation logic as shown in Figure 5.13, although the fluidization was quite different. The curves calculated are also shown in Figure 5.16,  $h_p$  and  $h_d$  being estimated by Kato's equation and <sup>Zabrodsky's</sup> equation 2.8. The calculated curves seem to be in good agreement with the experimental results.

## 5.5 SOLIDS FLOW RATE THROUGH THE "HEATER"

The efficiency of the gas-to-gas heat exchanger depends on the ratio of the heat capacity flow of the gases and solids. Then it is important to know the limits of their flow rate ranges. The gas flow rate range can be predicted from the  $U_{mf}$  and  $U_T$ . However the maximum flow rate of solids through the "particle heater" or "cooler" cannot be predicted from any other works. In this section the maximum flow rate of solids was measured in the inclined "heater", which was not heated by hot air.

*during cold operation*

The maximum solids flow rate,  $M_{s,max}$ , must be affected by some ~~variables of the~~ properties of <sup>the</sup> solids, the flow condition of <sup>the</sup> gas

and the geometric properties of the bed. As the aim of the experiments was to find how the "particle heater" performed, the experiments focused on only a few essential factors such as air superficial velocity, the inclined angle of the bed and height of weir.

Figure 5.17 shows the maximum solids flow rate through the "particle heater" divided <sup>into</sup> 4 cells, whose weirs are 2 cm high. The bed temperature was room temperature, about 25° C, and  $U_{mf}$  in the horizontal bed is 28 cm/sec. If the solids feeding rate exceeds the maximum solids flow rate measured here, the bed height in the nearest cell from <sup>the</sup> particle inlet increases gradually and fluidization stops in the cell. The maximum flow rate increases with inclining the bed from 0° to 5°, because it makes particles jump beyond the weirs rapidly. However, in the bed on a 10° inclined distributor only the shallower part in ~~the~~ each cell tends to fluidized and the flow rate decreases. It can be also seen that increasing the fluidizing velocity enhances the solids flow. Figure 5.18 shows the maximum solids flow rate in the bed divided <sup>into</sup> 4 cells with 4 cm high weirs. It shows that the "heater" with higher weirs can operate larger <sup>at a</sup> inclined angle.

The operation of the gas-to-gas heat exchanger requires that the solids flow in the heat exchanger <sup>is maintained at</sup> the proper flow rate as discussed in Chapter 3. For example if the heat exchanger consists of two one-stage beds,  $R_s/R_g$  should be more than 1. Figure 5.19 show the operating condition of the "heater", whose distributor size is 20 cm x 20 cm and where the temperature of ~~the~~ air is room temperature. From Figure 5.19 proper solids feeding rate and fluidizing velocity can be decided for the gas-to-gas heat exchanger and it will help to scale-up to industrial size.

## 5.6 HEAT RECOVERY PERFORMANCE

The measure of the performance of <sup>the</sup> particle "heater" is its efficiency,  $\eta_h$ , which is defined in equation 3.2. The experimental procedure which was used to obtain the performance curves is described in Section 4.6.

So as to gain the maximum efficiency in each operating condition, insulated partitions were employed for this experiment. One partition consists of two stainless steel plates <sup>with</sup> and silicon fibre cloth sandwiched between them. The temperature of <sup>the</sup> outlet solids from the "heater",  $T_{s,o}$ , was measured at the point about 5 mm below the bed surface near the outlet. The temperature reading during the fluidization does not change after stopping the hot air to the "heater", which confirms that  $T_{s,o}$  can be measured there.

The complete set of experimental data is given in Table 5.1. The range of the experimental variables of hot air flow,  $U_f$ , and the heat capacity flow ratio,  $R_s/R_a$ , is shown in Figure 5.20. The range was limited by the maximum particle flow rate through the "heater" and through the pneumatic transport pipe from the "cooler" to the top hopper. The various trends which can be seen in the large amount of data will be considered in turn following a general review of the data.

### 5.6.1 General review of the data

It is important to look first at the data qualitatively and comment upon their accuracy and consistency. Table 5.1 shows the heat lost from <sup>the</sup> air flow, the heat gained <sup>by the</sup> solids flow and their balance, which is the sum of the heat loss from the

"particle heater" and experimental error. The mean of the balance is 0.0629 kW and the standard deviation  $\sigma_n$  is 0.0833 kW. If <sup>it is</sup> <sup>ed that</sup> assuming the heat loss is constant in the series of experiments, the loss is 0.0629 kW and it is less than 5% of the heat transferred from air to solids. Then <sup>the</sup> standard deviation of the experimental error is 0.0833 kW. ~~The~~ Both are considered to be small enough to discuss the experimental data without reference to them.

### 5.6.2 Effect of the heat capacity flow ratio

As analysed in Section 3.2 the heat capacity flow ratio of solids and air,  $R_s/R_a$ , is an important factor for the heat exchanger operation. The performance characteristics of the "particle heater" shown in Figure 5.21 are for several different operating conditions. It can be seen that  $R_s/R_a$  affects the  $\eta_h$  and that there ~~are~~ <sup>is</sup> no significant difference <sup>between</sup> among the different operating conditions such as the distributor and the inclined angle. From the calculated curves shown in Figure 3.7 the horizontal plug flow model and the backmixing flow in 4 series cells were plotted in Figure 5.21. Although  $h_p$  was estimated by Kato's equation, the performance characteristics measured tend to agree with the curve of the plug flow model within  $\pm 4.5\%$ .

### 5.6.3 Effect of the distributor and the inclined angle

Figure 5.21 shows that there is no significant difference <sup>in</sup> ~~of~~  $\eta_h$  between the two types of distributor, perforated sheet and grate bar screen. As the pressure drop <sup>with the</sup> of grate bar screen is larger than <sup>with</sup> the perforated sheet, it was observed that the fluidization in the bed <sup>with</sup> the grate bar screen distributor was more uniform than with the perforated sheet distributor. Then the efficiency

of the "heater" with the grate bar screen might be slightly greater than the perforated sheet.

Figure 5.21 shows also that there is no difference between the performance with ~~two inclined angle~~,  $10^\circ$  and  $15^\circ$  *angles of inclination.*

#### 5.6.4 Effects of the flow rates of solids and air

We note from Figure 5.21 that the plug flow model seemed to give predictions of heat exchanger efficiency which corresponded ~~the~~ most closely to the measured performance. This does not necessarily mean that the solids flow was, in reality, plug flow. However the effects of the flow rates of solids and air were re-examined, comparing the calculated results from the model and the experimental data. Figure 5.22 shows the effect of solids flow rate in the condition of air flow from 25 g/sec to 36 g/sec. Figure 5.23 shows the effect of air flow rate for  $M_s$  from 18 g/sec to 25 g/sec. ~~The~~ Both Figure 5.22 and 5.23 show that the plug flow model gives predictions sufficient for initial design purposes.

### 5.7 SUMMARY OF OVERALL PERFORMANCE OF THE "PARTICLE HEATER"

The work on the experimental unit shows conclusively that the "particle heater" functions as a gas-to-solids heat exchanger. Performance may be predicted sufficiently well by a model which assumes both solids and gas flows are almost perfect plug flows (Section 3.2). The observation of bed behaviour in a single cell clarified the movement of solids circulating, which is affected by the angle of inclination and fluidizing velocity. These two

factors influence the maximum solids flow limit. In the given operating range the ratio of the feed rates of solids and air heat capacity,  $R_s/R_g$ , is the major factor to change the efficiency,  $\eta_h$ , as discussed the calculated results from the solids plug flow model in Section 3.2.

Table 5.1 Experimental results of the "particle heater"

Test	Distributor type	Inclination angle (deg)	Air mass flow (g/sec)	Particle mass flow (g/sec)	Particle $R_s$ $\frac{R_s}{R_g}$ (-)	Temperature ( $^{\circ}C$ )			Heat (kW)		$\eta_h$	
						$T_{g,in}$	$T_{g,out}$	$T_{s,h,in}$	Air heat loss	Solids heat gain		Balance (-)
1			24.9	18.5	0.74	127	69	29	1.46	1.26	0.20	0.69
2			33.9	22.1	0.64	123	80	32	1.49	1.53	-0.04	0.76
3			31.6	24.1	0.76	134	80	35	1.73	1.65	0.08	0.69
4			29.4	20.6	0.69	134	81	30	1.59	1.56	0.03	0.73
5			28.0	19.7	0.70	133	82	32	1.44	1.38	0.06	0.69
6			28.3	18.0	0.63	132	83	31	1.39	1.32	0.07	0.72
7			30.2	21.8	0.72	124	77	32	1.43	1.38	0.05	0.69
8			30.8	21.1	0.68	122	77	30	1.38	1.36	0.02	0.71
9			31.1	18.8	0.60	120	79	29	1.29	1.31	-0.02	0.60
10		10	25.2	19.3	0.76	146	87	33	1.50	1.49	0.01	0.68
11			25.5	19.5	0.76	143	86	33	1.46	1.48	-0.03*	0.69
12			21.3	15.2	0.71	166	96	34	1.50	1.34	0.15	0.67
13			21.6	17.0	0.78	166	91	35	1.63	1.41	0.22	0.64
14			23.5	18.7	0.79	152	90	35	1.47	1.47	-0.01	0.67
15	Grate		23.7	20.1	0.84	152	90	36	1.49	1.54	-0.05	0.66
16	bar		24.2	20.0	0.82	151	89	34	1.53	1.55	-0.03	0.67
17	screen		24.0	18.3	0.75	153	90	33	1.53	1.49	0.04	0.68
18			23.8	17.0	0.71	154	93	33	1.47	1.45	0.02	0.71
19			29.2	18.4	0.62	134	82	31	1.51	1.40	0.11	0.74
20			32.0	26.1	0.81	130	80	33	1.61	1.73	-0.11	0.68
21			32.0	23.0	0.71	130	82	32	1.56	1.61	-0.05	0.71
22			26.4	21.7	0.81	139	79	30	1.59	1.61	-0.02	0.68
23			26.1	18.0	0.68	140	81	29	1.55	1.44	0.12	0.72
24		15	25.9	15.6	0.60	138	81	27	1.49	1.30	0.20	0.75
25			23.5	21.0	0.88	154	84	37	1.64	1.54	0.11	0.63
26			24.0	21.2	0.88	152	83	37	1.67	1.52	0.15	0.62
27			23.9	17.8	0.74	147	83	30	1.55	1.44	0.11	0.69
28			22.1	16.5	0.74	152	82	28	1.54	1.39	0.15	0.68
29			22.6	19.5	0.86	156	86	36	1.60	1.49	0.11	0.64
30			19.9	14.3	0.71	164	92	35	1.44	1.30	0.14	0.70
31		20	28.5	19.9	0.69	135	76	27	1.70	1.52	0.18	0.70
32	Perforated sheet	10	31.6	25.8	0.81	131	80	34	1.64	1.59	0.05	0.63
33			31.7	23.6	0.74	134	84	33	1.60	1.56	0.04	0.66

4 cells used here

\* produced by rounding error

FIGURE 5.1 PRESSURE DROP ACROSS DISTRIBUTOR  
PLATE

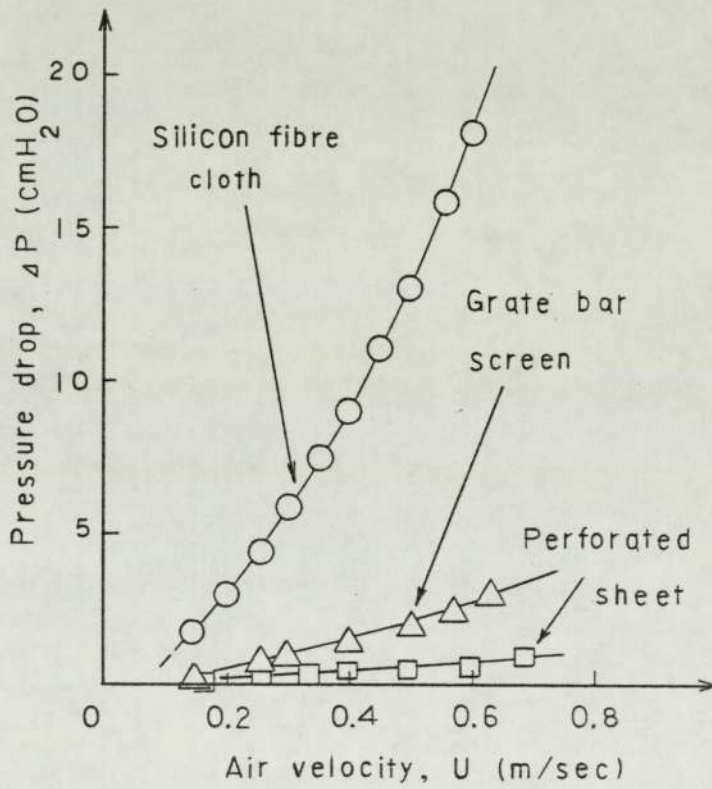


FIGURE 5.2 PRESSURE DROP ACROSS BED

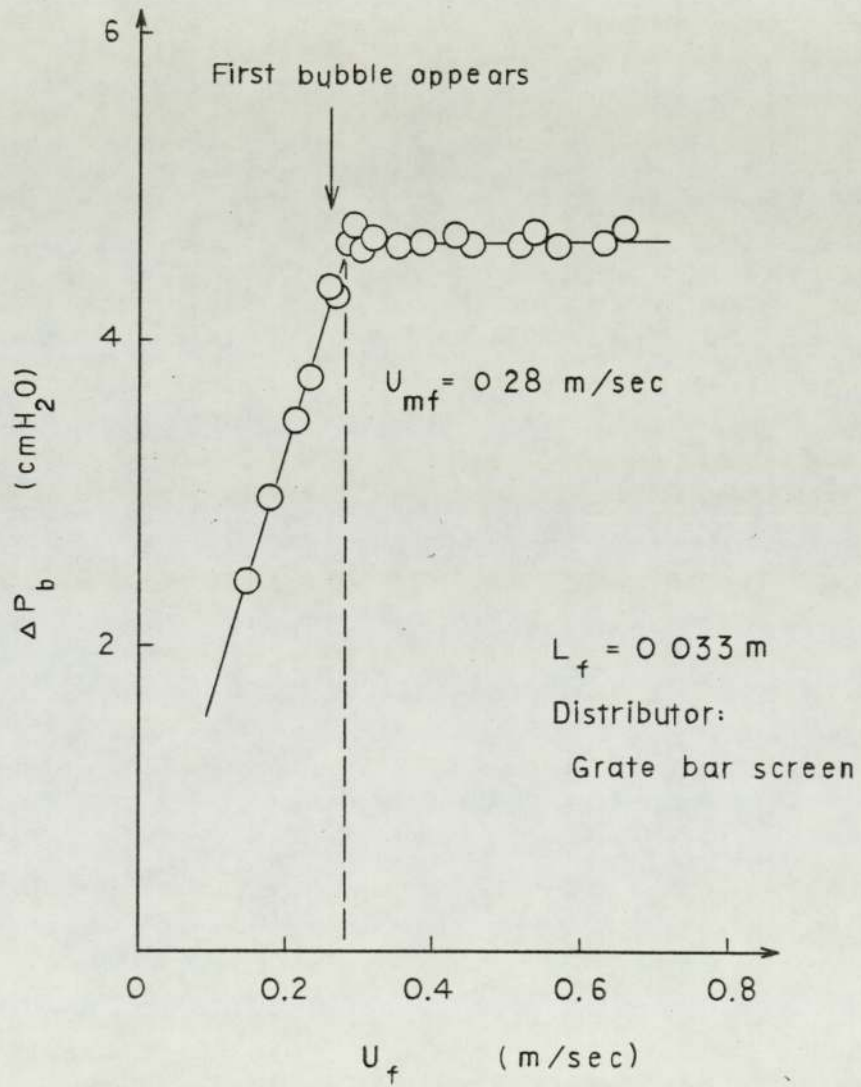


Figure 5.3 Photograph of fluidization  
in the bed with horizontal distributor:

$$U = 2 U_{mf}$$



Figure 5.4 Photograph of fluidization  
in the bed with 15° inclined distributor:

$$U = 2 U_{mf}$$



Figure 5.6 Photograph of fluidization  
in the bed with 15° inclined distributor:  
 $U = 3 U_{mf}$



Figure 5.5 Photograph of fluidization  
in the bed with 15° inclined distributor:  
 $U = 2.5 U_{mf}$



Figure 5.7 Photograph of fluidization  
in the bed with 5° inclined distributor:

$$U = 2 U_{mf}$$



Figure 5.8 Photograph of fluidization  
in the bed with 10° inclined distributor:

$$U = 2 U_{mf}$$

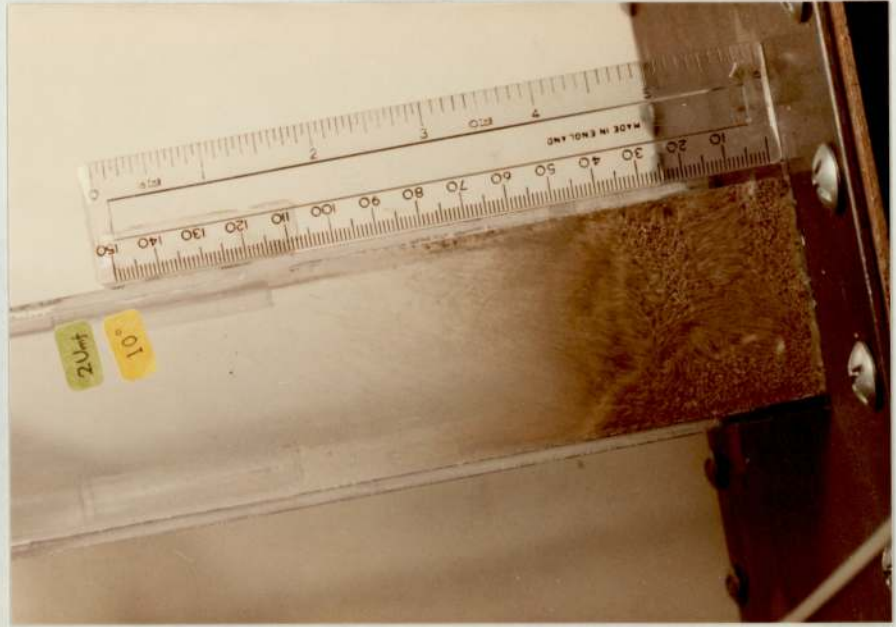


Figure 5.9 Photograph of fluidization  
in the bed with  $20^\circ$  inclined distributor:

$$U = 2 U_{mf}$$



Figure 5.10 Photograph of fluidization in the "particle heater":  
Weir height,  $W = 2$  (cm); (inclination angle)  $= 7.5^\circ$ ;  $U = 2 U_{mf}$

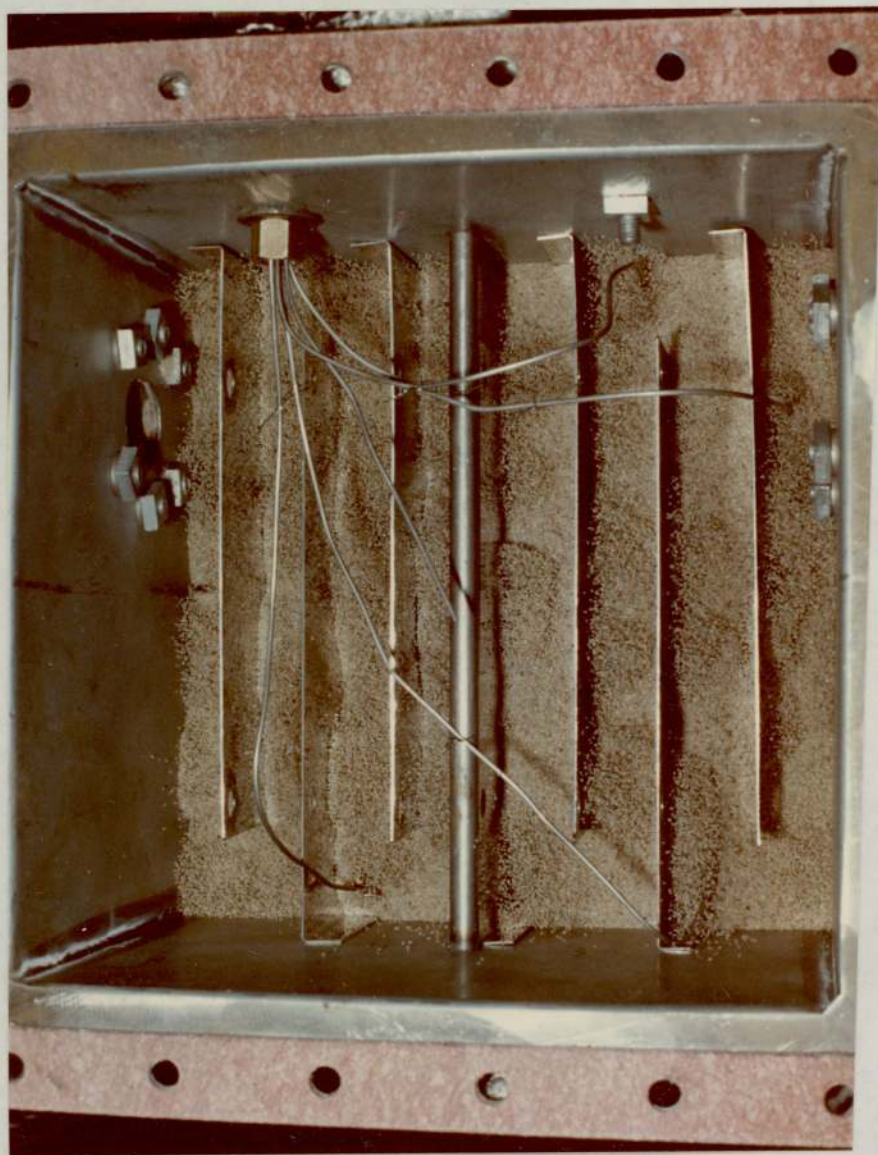


FIGURE 5.11 PRESSURE DROP ACROSS THE BED ON INCLINED DISTRIBUTOR

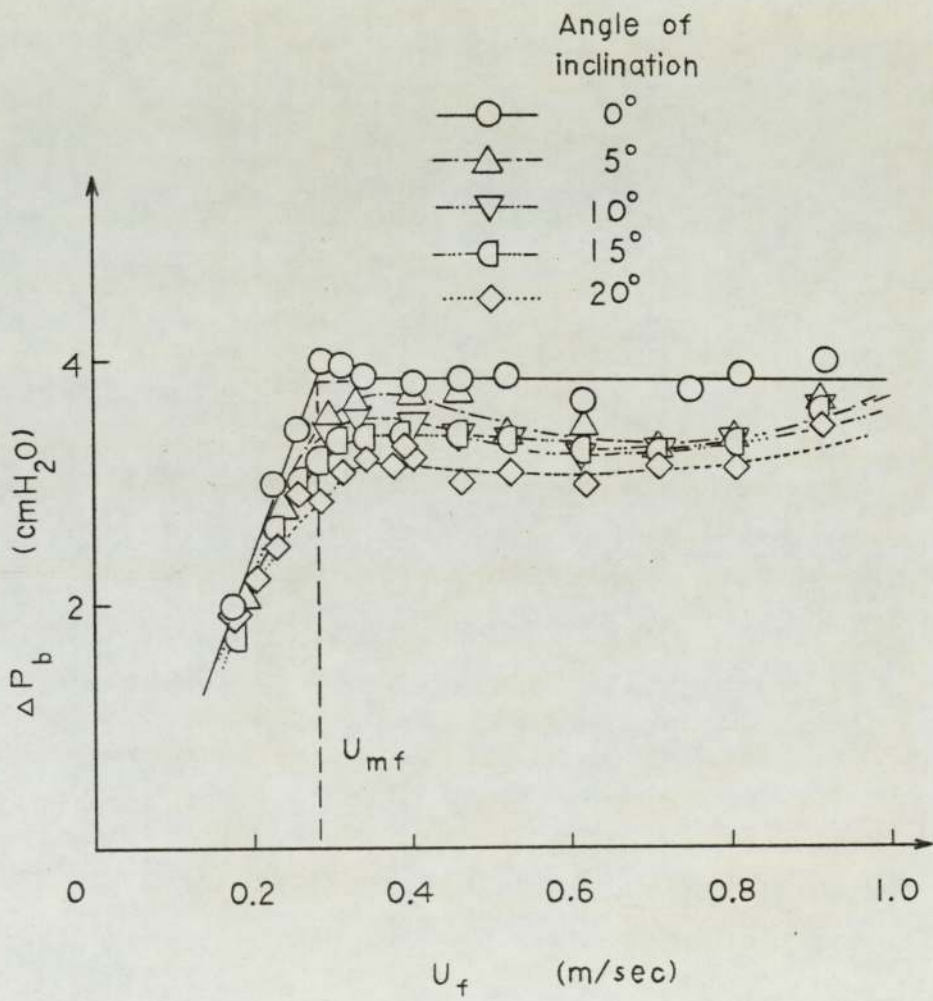


FIGURE 5.12 PRESSURE DISTRIBUTION IN  
BED

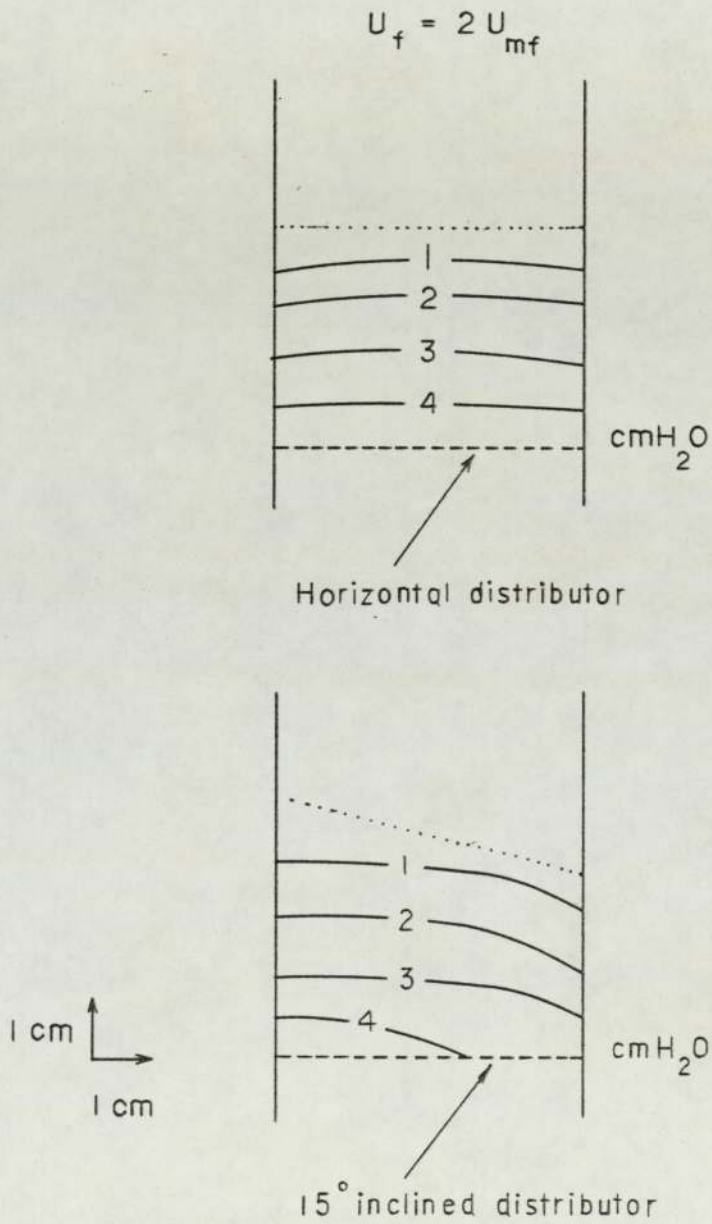


Figure 5.13 Logic diagram for computer simulation of unsteady-state experiments

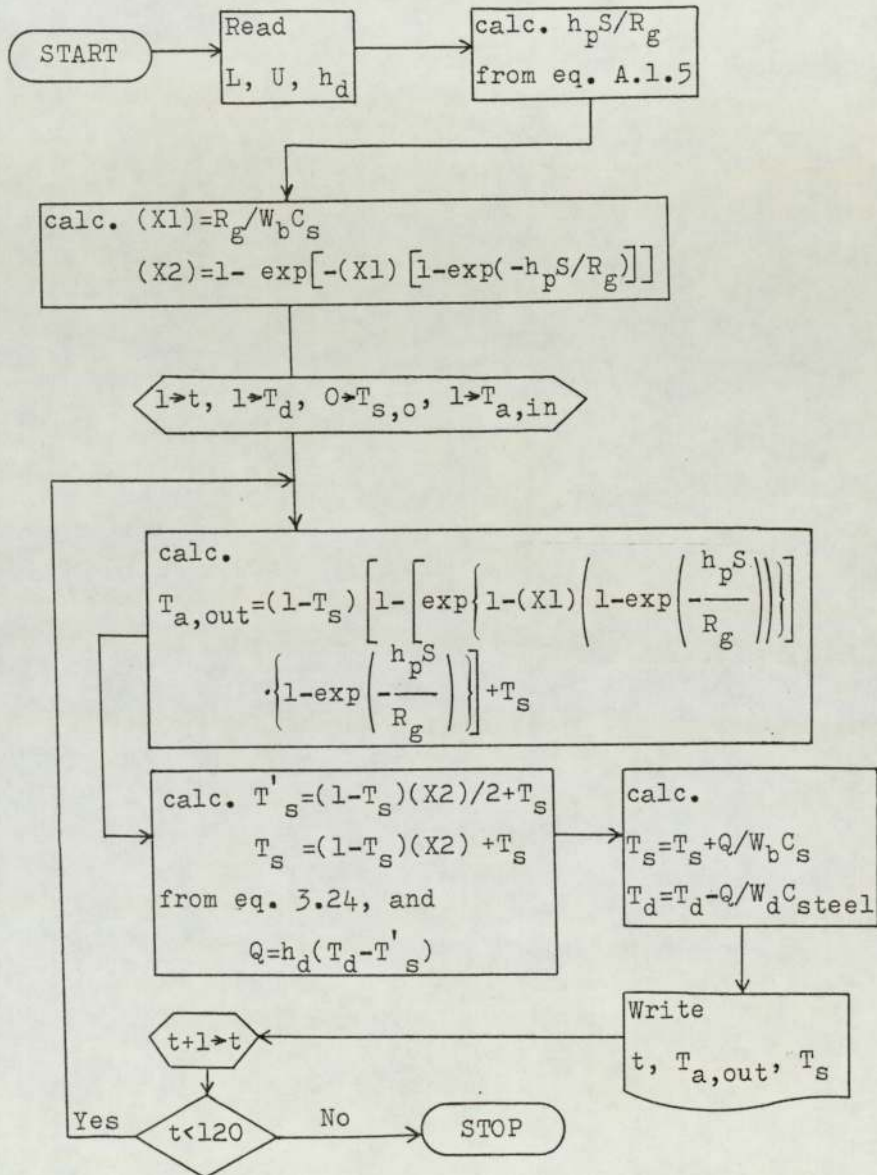


FIGURE 5.14 DIMENSIONLESS EXIT AIR TEMPERATURE CHANGE FROM THE HORIZONTAL DISTRIBUTOR BED

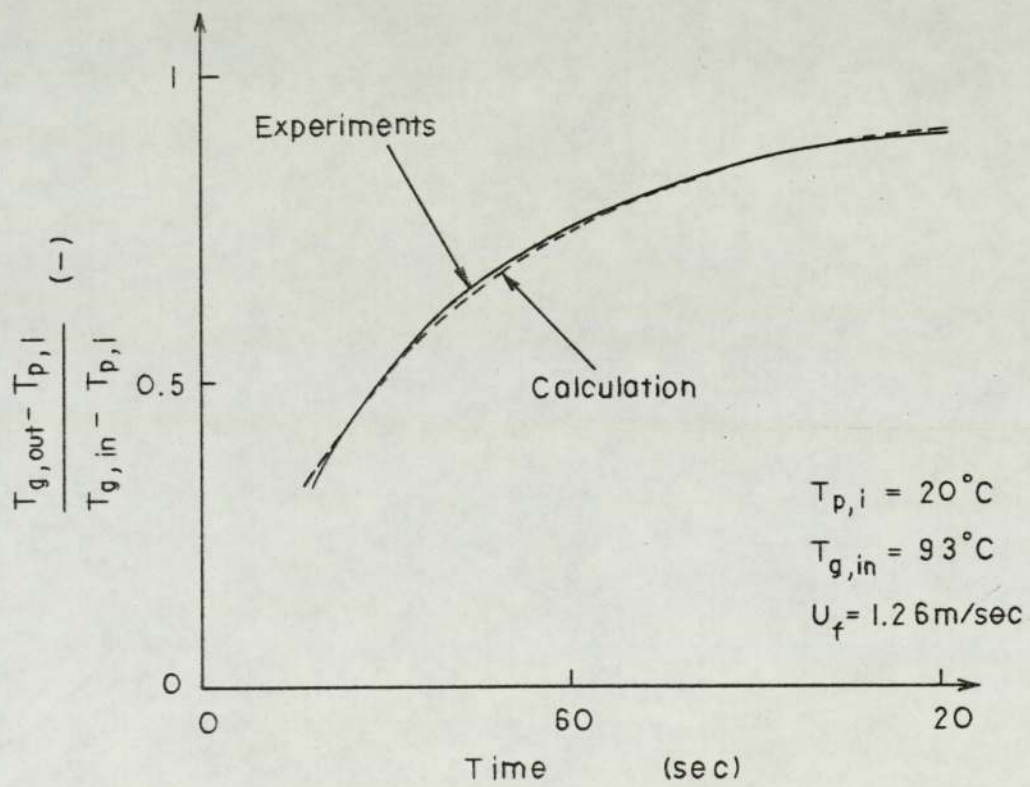


FIGURE 5.15 DIMENSIONLESS EXIT AIR TEMPERATURE CHANGE FROM THE HORIZONTAL AND INCLINED DISTRIBUTOR BEDS

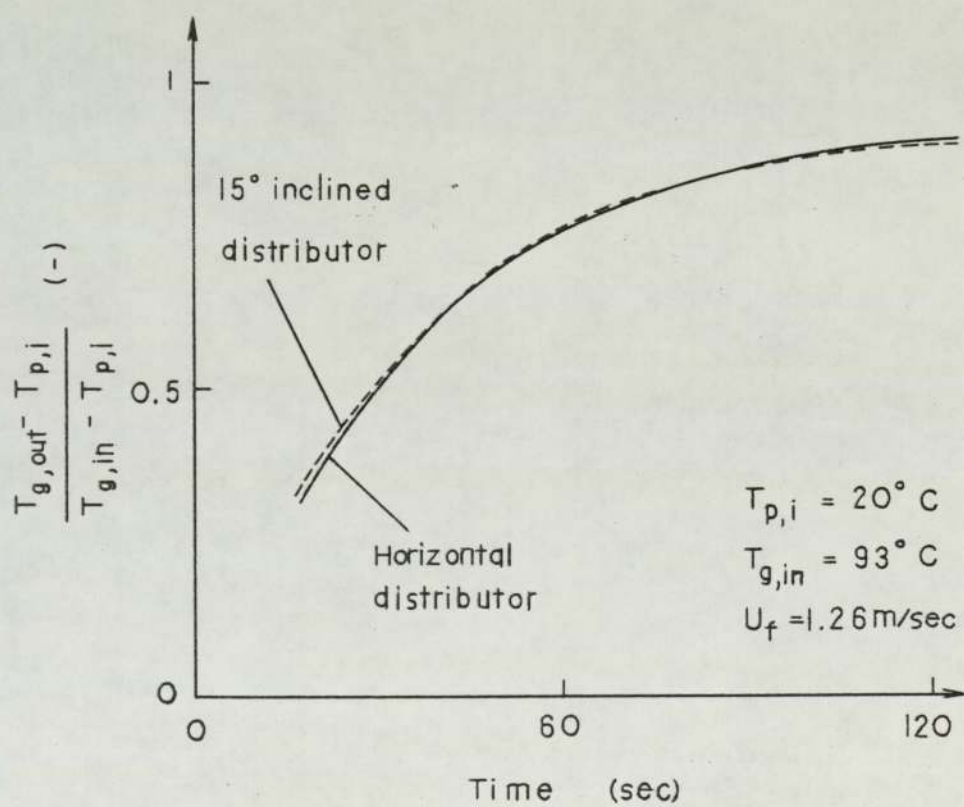


FIGURE 5.16 DIMENSIONLESS EXIT AIR TEMPERATURE CHANGE FROM THE INCLINED DISTRIBUTOR BED

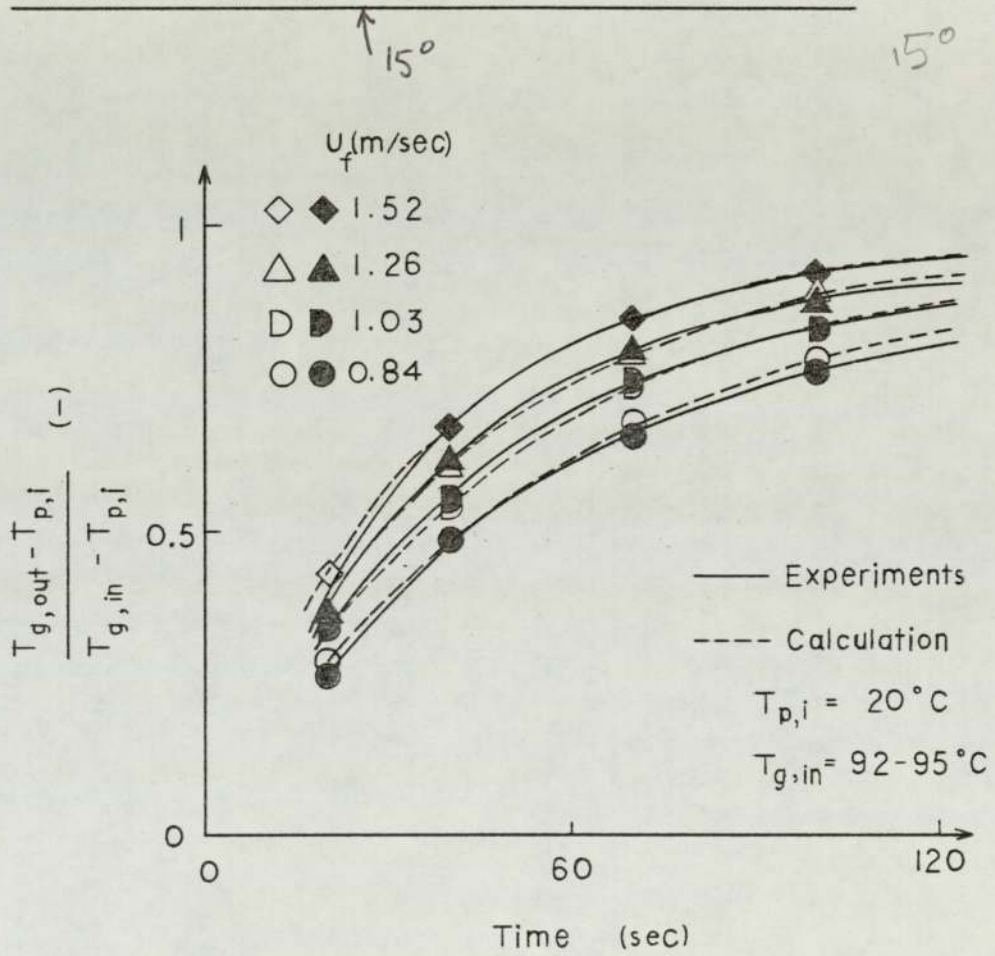


FIGURE 5.17 MAXIMUM SOLIDS FLOW RATE VERSUS INCLINED ANGLE

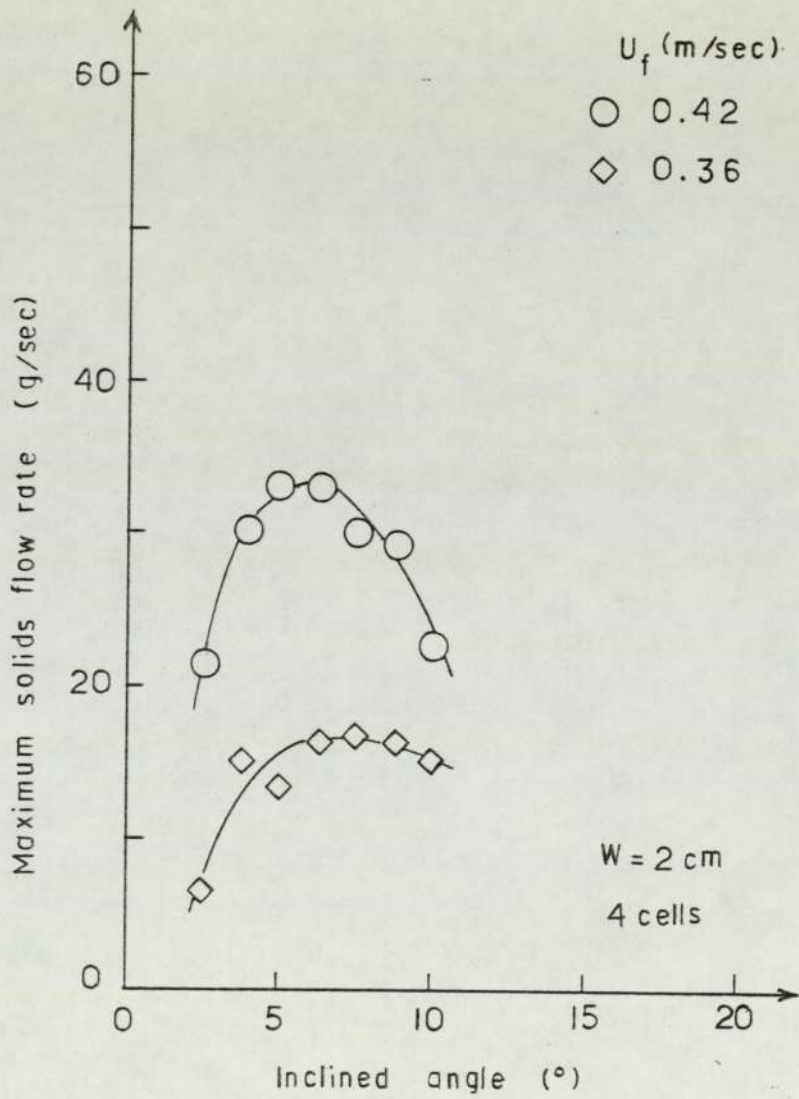


FIGURE 5.18 MAXIMUM SOLIDS FLOW RATE VERSUS INCLINED ANGLE

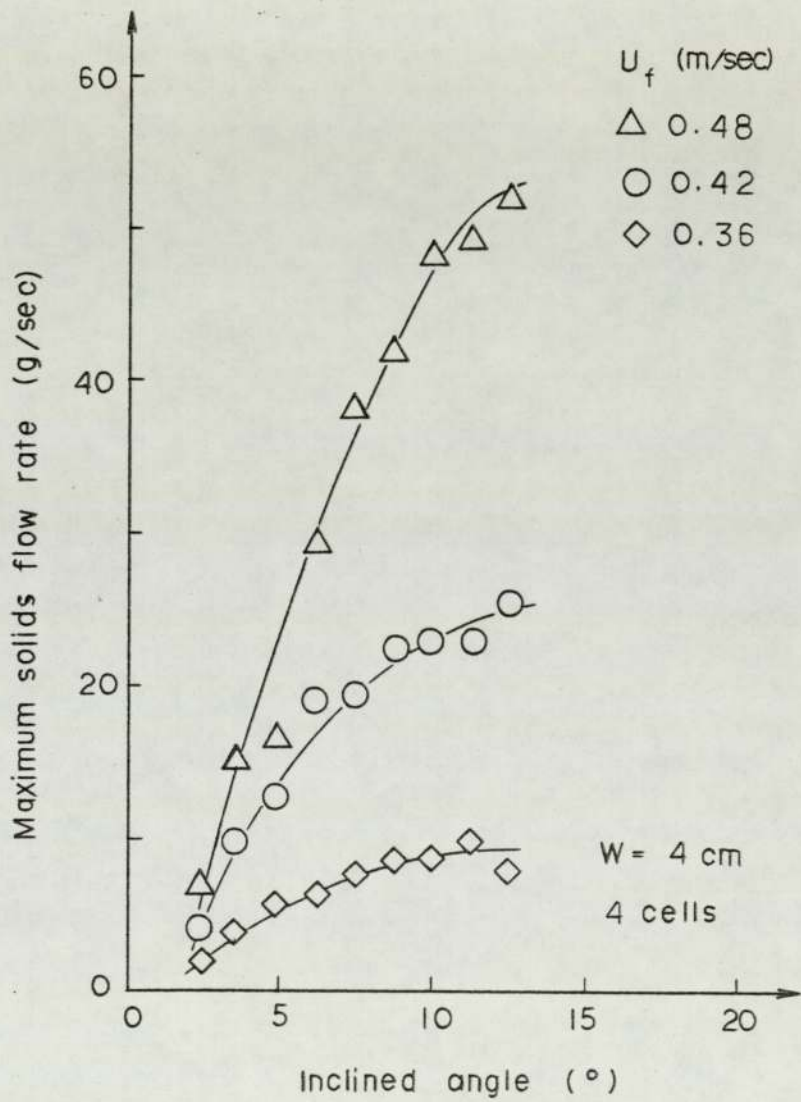


FIGURE 5.19 AN EXAMPLE OF OPERATING CONDITION OF "HEATER"

$T_{q,in} = 20^{\circ}\text{C}$ , 4 cells,  $W = 4\text{ cm}$ , Inclined angle =  $10^{\circ}$

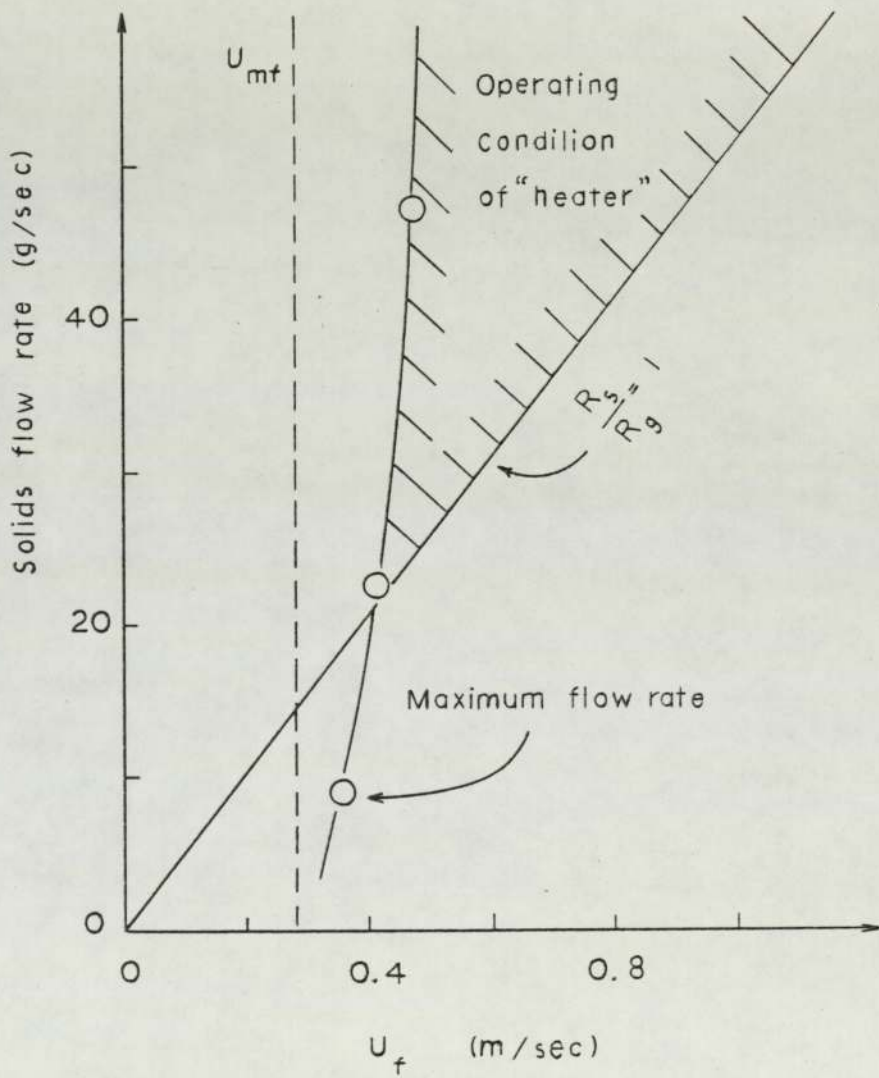


FIGURE 5.20 RANGE OF THE EXPERIMENTAL VARIABLES

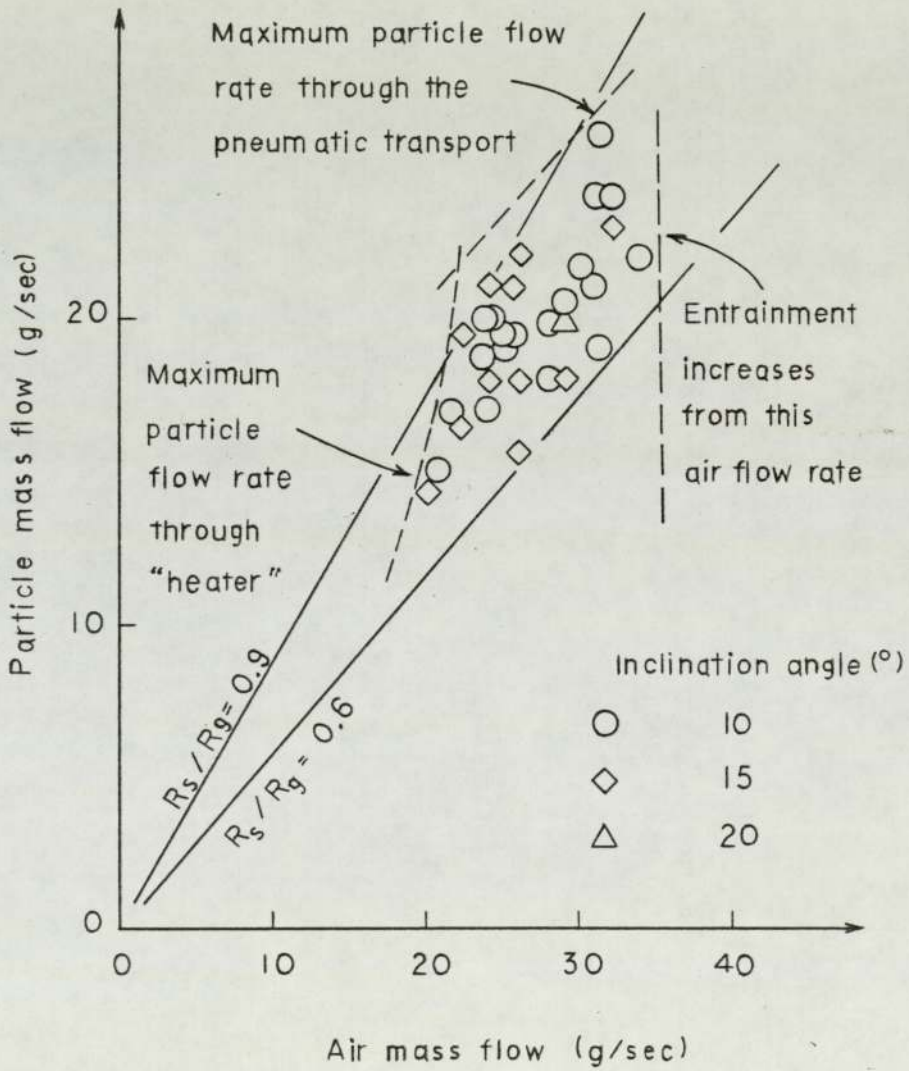


FIGURE 5.21 PERFORMANCE CHARACTERISTICS OF THE "PARTICLE HEATER"

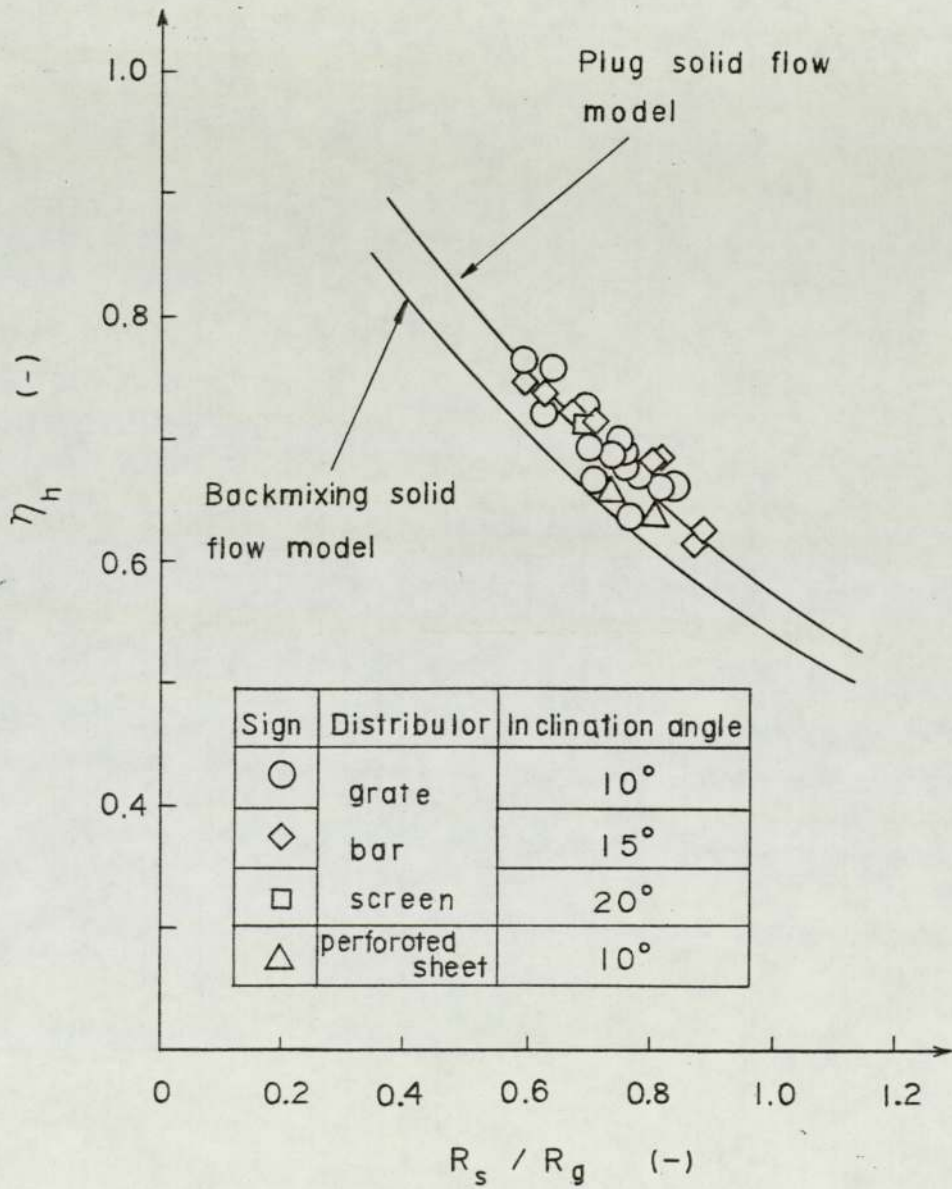


FIGURE 5.22 EFFECT OF THE AIR FLOW RATE

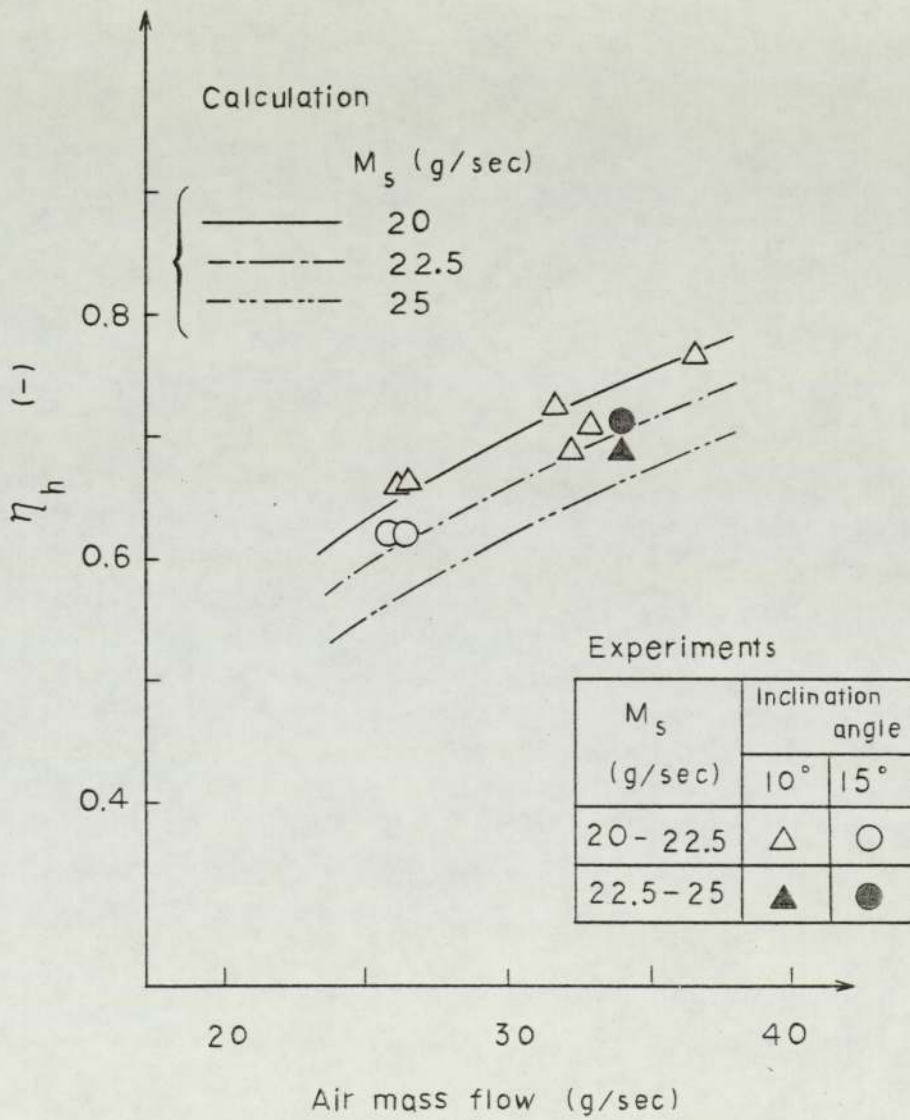
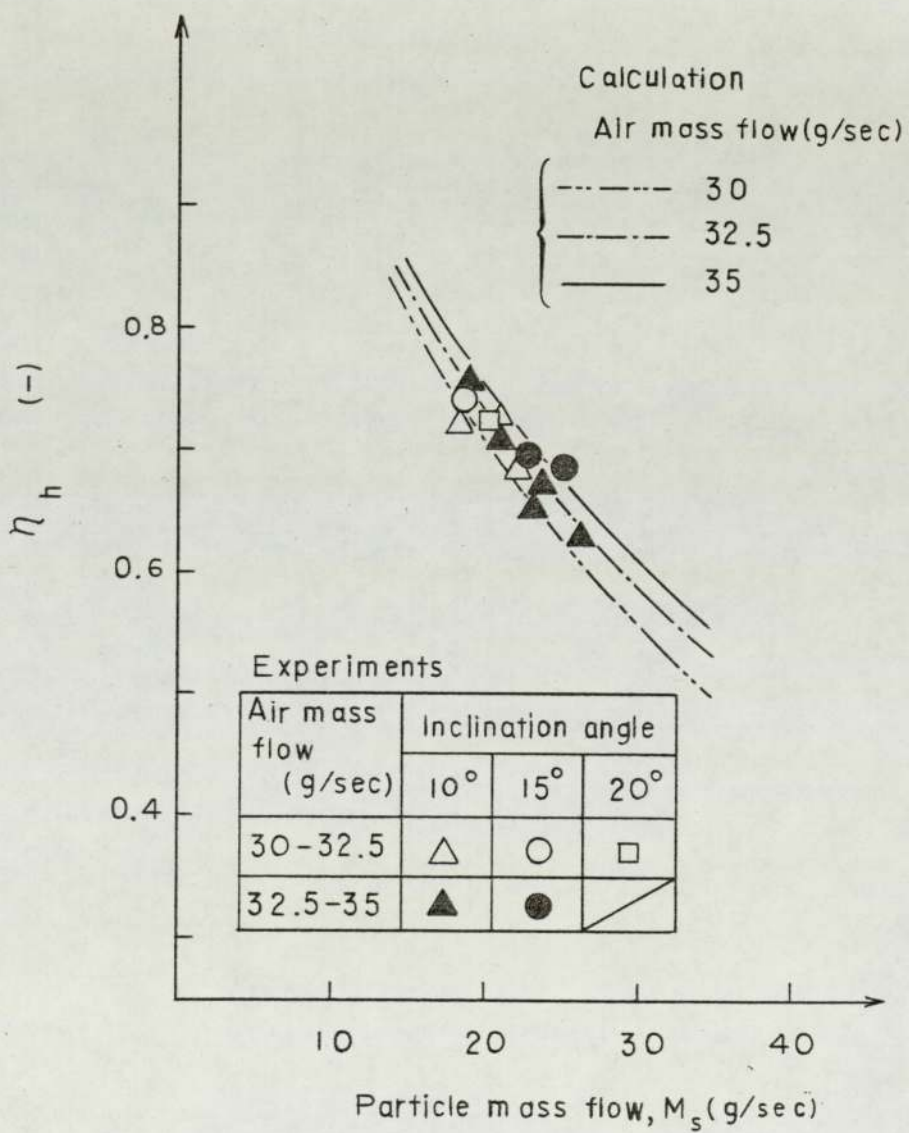


FIGURE 5.23 EFFECT OF THE SOLIDS FLOW RATE



CHAPTER SIX  
ASSESSMENT OF THE FLUIDIZED BED  
GAS-TO-GAS HEAT EXCHANGER

6.1 INTRODUCTION

The intention of this chapter is to collate all the information presented earlier on the review of literature, the theoretical model and the experimental work. The assessment of this information will lead to two distinct areas for discussion, the design criteria for larger units and recommendation for further work.

6.2 DESIGN CRITERIA FOR LARGE UNITS

The experimental work has demonstrated that the "particle heater" built in accordance with the ideas presented in Section 3.4.2 operates satisfactorily. The experimentally observed performance of the "particle heater" corresponds closely to that predicted on the assumption that the solids flow through it is perfect plug flow over the whole range of the fluidizing conditions examined. However it is necessary to build a larger multi-stage bed heat exchanger to demonstrate satisfactory functioning of all the elements if the system is to be used for industrial applications. Such elements are solids transport between the beds and between the heat exchanger and for example, a heat storage system. Before discussing the further work, it is important to extract sufficient information from the data obtained during this study so as to

define the criteria which are essential for the prediction of the performance of a larger unit. In this section the principles adopted for scaling-up the heat exchanger design are described.

The starting points of the design are the values of the hot and cold gas inlet temperatures and their flow rates, together with their fluctuations with operating time, which are sometimes important factors. From the above conditions the areas of the distributors of the "particle heater" and "particle cooler", the range of solids flow rate and the size of heat storage, if it is required, can be determined by setting the actual fluidizing velocity at some value, as the flow chart illustrated in Figure 6.1. The full set of recommended design values is given in Table 6.1. The dimensions of each cell will depend upon the gas flow rates and the temperature, however the section of the cell should be rectangular in order to make the solids flow in a near plug-flow fashion. The angle of inclination of the distributor must be decided from the maximum solids flow rate required.

The material of particle was recommended silica sand in Table 6.1, however its resistance to high temperature may not be higher than about  $900^{\circ}$  C for continuous operation and its ability to withstand cyclic thermal shock without breaking is not always very high. If the particle is to be heated higher than  $900^{\circ}$  C, alumina is a more suitable particle material and it is claimed that its resistance to thermal shock is greater. If alumina is to be used, then the particle size may have to be different from that given in Table 6.1 because alumina density is larger than that of silica sand.

Lastly, it is clear that the "particle heater" can be used for other applications such as particle dryers, particle coolers, for sizing or solids-to-solids heat exchange. For these applications

the design values of the design parameters might have to be different from those in Table 6.1; this matter is however beyond the chosen scope of this thesis.

### 6.3 FURTHER WORK

Further studies on the heat exchanger will fall into one of two categories. One will be to test a larger size heat exchanger operating at higher temperatures; the other will be to gain better understanding about the interaction between the fluidizing gas and the bed material. The two groups will be discussed in turn, and the other aspects which merit more study will be suggested.

#### 6.3.1 Larger size heat exchanger operating at higher temperature

The next stage of the development of the heat exchanger into a commercial product is the construction of a prototype of typical industrial size, which should consist of multi-stage "heater" and "cooler" beds and the solids transporting system. The technical aims of the operation of the prototype are to study the effects of prolonged thermal cycling on the size and shape of particles, the life of partitions and distributor, solids transport and the quality of fluidization. It is reasonable to expect that all these will be influenced by the larger size and higher operating temperature of the prototype compared with the present small experimental unit. The design of the solids transport system needs particularly careful consideration if pneumatic conveying, downcomer and non-mechanical valves are to achieve the smooth operation, high performance, flexibility against the change of gas flow rates and temperatures and be reliable under such

service conditions. The predictions of the theoretical model ~~will~~ <sup>need</sup> also <sup>to</sup> be evaluated against actual performance and improved to aid the design of a full range of production units. In the industrial prototype the hot gas stream would be exhaust gases from a gas burner. These can be used to study effects of contamination of the hot gas stream on particles and distributors as well as gaining experience of using a gas of differing physical properties from air. Contamination is a serious problem for some applications. It might be necessary to develop the maintenance technique of the distributor for such applications. Much will depend upon the kind of the application to decide what further development and studies are required.

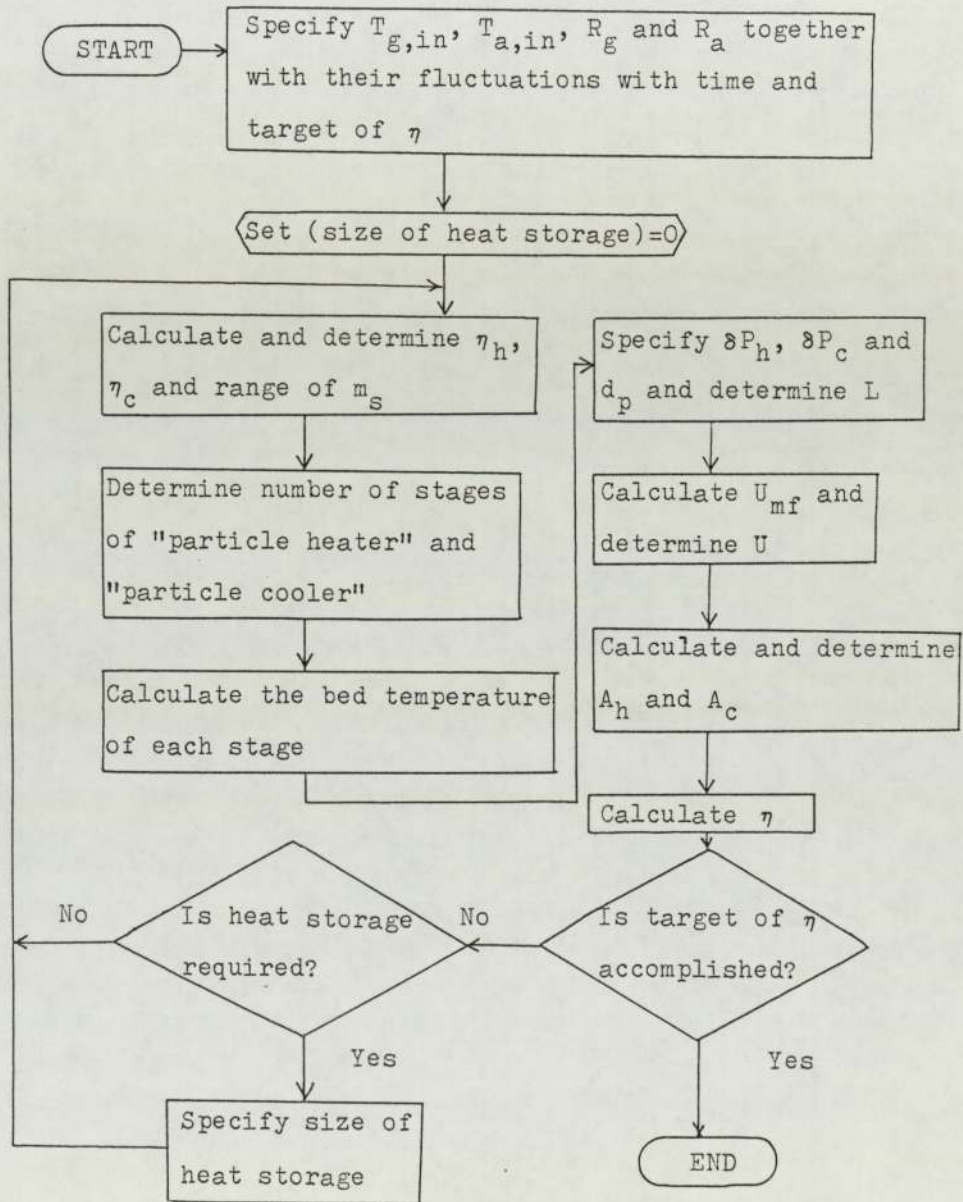
#### 6.3.2 Advancing basic understanding

The principal area of basic understanding which <sup>was</sup> beyond the scope of the present work was the interaction and the heat transfer between the fluidizing gas and the bed material. This is a complicated phenomenon, which has received limited study. The circulating movement of particles in the cell observed in the experimental work reported here are determined by many factors, but particularly by the size of the cell, the inclination of the distributor and the fluidizing velocity. The heat transfer might not only be under the influence of the particle circulation but also be influenced by the number of the particles in the freeboard.

Table 6.1.1 Recommended design values for large gas-to-gas heat exchanger

Item	Recommendation
Particle	Material Silica sand (at lower temperature than 900° C)
	Size $d_p = 0.5 - 0.7$ mm
	Material Stainless steel
	Type Perforated sheet or grate bar screen
Gas distributor	Pressure 0.5 - 5 cm H <sub>2</sub> O drop
	Angle of inclination 5° - 20° (according the range of solids flow rate) to the horizontal
Fluidizing velocity	$U_0 = 1.5 - 6 U_{mf}$
Height of weir	$W = 4$ cm
Number of cells in each stage	4 or more

Figure 6.1 Flow chart for scaling-up the heat exchanger design



## CHAPTER SEVEN

### CONCLUSIONS

#### 7.1 CONCLUSIONS

A single-stage fluidized bed apparatus with inclined distributor has been developed as the "particle heater" for a gas-to-gas heat exchanger and the effects of some design and operating parameters have been evaluated. The conclusions are as follows:

- (i) Sufficiently rapid transport of solids through the "particle heater" fluidized bed is achieved by inclining the distributor by  $10^{\circ}$  --  $20^{\circ}$  to the horizontal and returning the cooled solids to the top of the slope mechanically to give continuous circulation of solids. In practice, a  $10^{\circ}$  inclination is sufficient for the solids to flow readily for the weirs 4 cm high and the cells 4 cm wide. An inclination greater than  $20^{\circ}$  may lead to too large solids flow or to partial fluidization.
- (ii) The maximum solids flow rate is affected by the fluidizing velocity, the angle of the inclination of the distributor and the dimension of cell. The maximum flow rate increases with the fluidizing velocity but decreases with the height of weirs. The maximum flow rate also increases with the inclination from  $0^{\circ}$  and decreases beyond a certain angle.
- (iii) The gas-to-particle heat transfer coefficient in the bed with inclined distributor seems to be nearly equal to that in the ordinary fluidized bed with horizontal distributor, although the most bubbles were observed passing through only the shallower part of bed. It may be that

the rapid circulation of particles caused by the bubbles rising yields gas-to-particle contact as good as a bed with horizontal distributor.

- (iv) From the unsteady-state experiments carried out, these values of the gas-to-particle heat transfer coefficient may be estimated by Kato's empirical equation.
- (v) Some aspects of the performance of the "particle heater" and gas-to-gas heat exchanger, which will be constructed by combining the "particle heater" with a "particle cooler", can be predicted from the simple theoretical model developed in Chapter 3.
- (vi) The model predicted that the efficiency of the "particle heater" is strongly dependent on the heat capacity ratio of solids and gas flows and the gas-to-particle heat transfer coefficient. The measured performance of the "particle heater" tends to agree with values calculated from the horizontal solids plug flow model within  $\pm 4.5\%$ , if Kato's equation is used to estimate coefficient.
- (vii) The analysis concludes that a number of the beds arranged in stages is required to give sufficiently large of heat transfer rate between two gas streams.
- (viii) The pumping power to fluidize and circulate the solids is smaller than that required to fluidize multi-stage beds with horizontal distributors containing the same volume of solids.
- (ix) The heat exchanger seems particularly suited to those waste heat recovery applications in which both the temperatures and the flow rates of two gases changes with time, because the solids flow rate can be controlled so as to maintain the maximum performance. Storage of heat in hot solids may be combined with this type of heat exchanger, so as to accommodate large changes of heat supply and demand rates.

(x) A set of recommended design values for a large prototype is presented and further studies on the heat exchanger are proposed.

Appendix 1

DESIGN CONDITION OF THE FLUIDIZED BED "HEATER"

It is required to calculate the efficiency of heat utilization of solids in one "heater" of single stage fluidized bed, where the solids flow is assumed to be a perfect backmixing flow or a horizontal plug flow. From Kato's equation (equation 2.32),

$$\text{Nu} = \frac{h_p d_p}{\lambda} = 0.59 \text{Re}^{1.1} \left( \frac{d_p}{L_f} \right)^{0.9} = 0.59 \left( \frac{d_p U_o \rho_g}{\mu_g} \right)^{1.1} \left( \frac{d_p}{L_f} \right)^{0.9} \quad (\text{A.1.1})$$

Assuming the particles are spherical, the total surface area of bed particles, S, is

$$S = (\text{Number of particles in a bed}) \times (\text{Surface area of one particle})$$

$$= \left[ \frac{AL_f(1 - \epsilon)}{\frac{4}{3}\pi \left(\frac{d_p}{2}\right)^3} \right] \times \left[ 4\pi \left(\frac{d_p}{2}\right)^2 \right]$$

$$= \frac{6AL_f(1 - \epsilon)}{d_p} \quad (\text{A.1.2})$$

Heat capacity flow of gas,  $R_g$ , is

$$R_g = AU_o \rho_g C_g \quad (\text{A.1.3})$$

Then from equations A.1.1, A.1.2 and A.1.3

$$\frac{h_p S}{R_g} = \frac{3.54 \lambda (1 - \epsilon) (U_o \rho_g L_f)^{0.1}}{C_g \mu_g^{1.1}} \quad (\text{A.1.4})$$

For the air at 100° C,  $\lambda = 0.0316$  (W/m K),  $\rho_g = 0.946$  (kg/m<sup>3</sup>),  $C_g = 1.01$  (kJ/kg K),  $\mu_g = 2.17 \times 10^{-5}$  (kg/m sec) and assuming  $\epsilon = 0.45$ , equation A.1.4 becomes

$$\frac{h_p S}{R_g} = 8.14 (U_o \times L_f)^{0.1} \quad (\text{A.1.5})$$

From equation 2.4, minimum fluidizing velocity,  $U_{mf}$ , can be estimated by

$$U_{mf} = \left( \frac{\mu_g}{d_p \rho_g} \right) \frac{Ar}{1400 + 5.22 \sqrt{Ar}} \quad (\text{A.1.6})$$

where 
$$Ar = \frac{g d_p^3 (\rho_p - \rho_g) \rho_g}{\mu_g^2}$$

assuming the solid particle is silica sand,  $d_p = 0.0006$  (m) and  $\rho_p = 2590$  (kg/m<sup>3</sup>),  $Ar = 10660$  then  $U_{mf} = 0.216$  (m/sec)

Appendix 2

INTEGRATION OF EQUATION 3.23

It is required to integrate equations 3.23. This is shown in Figure A1.  $\delta t$  = time for mass  $m_g$  of gas to pass through bed, during which time we assume no particle flow, but that the particles mix <sup>o</sup>throughly so that there is no temperature gradient in the bed. This mass of gas  $m_g$  raises the bed temperature by  $\delta T_s$  hence

$$R_g (T_{g,in} - T_{g,out}) \delta t = m_s C_s \delta T_s \quad (A.2.1)$$

where  $R_g = m_g C_g$ . Heat transfer across solids-to-gas interface during time  $\delta t$  is the same amount  $Q$ . So that equations 3.23 are obtained.

From equation 3.23.a and 3.23.b

$$h_p S (T_{g,in} - T_{g,out}) \delta t = m_s C_s \ln \left( \frac{T_{g,in} - T_s}{T_{g,out} - T_s} \right) \delta T_s \quad (A.2.2)$$

from which

$$\exp \left[ \frac{h_p S}{m_s C_s} (T_{g,in} - T_{g,out}) \frac{\delta t}{\delta T_s} \right] = \frac{T_{g,in} - T_s}{T_{g,out} - T_s} \quad (A.2.3)$$

from equation 3.23.b and 3.23.c

$$\frac{1}{m_s C_s} (T_{g,in} - T_{g,out}) \frac{\delta t}{\delta T_s} = \frac{1}{R_g} \quad (A.2.4)$$

or

$$T_{g,out} = - \frac{m_s C_s \partial T_s}{R_g \partial t} + T_{g,in} \quad (A.2.5)$$

From equation A.2.3, A.2.4 and A.2.5

$$\frac{1}{T_s - T_{g,in}} \partial T_s = - \frac{R_g}{m_s C_s} \left[ 1 - \exp\left(-\frac{h_p S}{R_g}\right) \right] \partial t \quad (A.2.6)$$

Integrating equation A.2.6

$$\int_{T_{s,o}}^{T_s} \frac{dT_s}{T_s - T_{g,in}} = - \frac{R_g}{m_s C_s} \left[ 1 - \exp\left(-\frac{h_p S}{R_g}\right) \right] \int_0^t dt \quad (A.2.7)$$

Then

$$\ln\left(\frac{T_s - T_{g,in}}{T_{s,o} - T_{g,in}}\right) = - \frac{R_g}{m_s C_s} \left[ 1 - \exp\left(-\frac{h_p S}{R_g}\right) \right] t \quad (A.2.8)$$

It gives equation 3.24

Appendix 3

CONSIDERATION OF THE HEAT TRANSFER RATE BETWEEN ADJACENT CELLS

It is required to compare the heat transfer rates between adjacent cells through the partitions without insulation and between gas and solids. If they are of similar magnitude, it is necessary to insulate the partitions in order to prevent a large amount of heat from transferring between cells. This leakage of heat might reduce the performance of <sup>the</sup> heat exchanger to a level of single-cell contacting.

Firstly we should predict the heat transfer coefficient between bed and wall,  $h_w$ . Assuming the bed temperature is  $100^\circ \text{C}$  and  $U_o = 3U_{mf}$ , from Appendix 1

$$\begin{aligned} U_o &= 3 \times 0.216 = 0.65 \text{ (m/sec)} \\ \mu_g &= 2.17 \times 10^{-5} \text{ (kg/m sec)} \\ \rho_g &= 0.946 \text{ (kg/m}^3\text{)}, \quad d_p = 0.0006 \text{ (m)} \end{aligned}$$

Then

$$\text{Re} = \frac{d_p \rho_g U_o}{\mu_g} = 17, \quad \text{Re}_{mf} = \frac{d_p \rho_g U_{mf}}{\mu_g} = 5.7$$

From Zabrodsky's equation  $h_w$  can be predicted, because (50)

$$\text{Ar} = 10660, \text{ (< 26000)} \quad \text{from Appendix 1}$$

and

$$\text{Re}_{mf} = 5.7, \text{ (< 12.5)}$$

From equation 2.8 taking  $\lambda = 0.0316 \text{ (W/m K)}$  and  $\rho_s = 2590 \text{ (kg/m}^3\text{)}$

$$\begin{aligned} h_{w,\max} &= 35.8 \times 2590^{0.2} \times 0.0316^{0.6} \times 0.0006^{-0.36} \\ &= 313 \text{ (W/m}^2\text{K)} \end{aligned}$$

This gives about as accurate an answer as one can hope for if we take a realistic value as being about 70% of  $h_{W,max}$ , then we obtain

$$h_W = 0.7 h_{W,max} = 220 \text{ (W/m}^2\text{sec)}$$

Figure A2 shows model for heat transfer between two cells. The heat flow from cell 1 to cell 2,  $Q_{1-2}$ , can be expressed by

$$Q_{1-2} = A_W \frac{h_W}{2} (T_{b1} - T_{b2}) \quad (\text{A.3.1})$$

if the thermal resistance through the partition without insulation is neglected, where  $A_W$  is the area of heat exchange surface and  $T_{b1}$  and  $T_{b2}$  are the temperatures of cells. The surface area of the heat exchange section in one partition of the "particle heater",  $A_W$ , is

$$A_W = 0.008 \text{ (m}^2\text{)} \quad \text{for } L_f = 0.04 \text{ (m)}$$

then

$$Q_{1-2} = 0.008 \times \frac{220}{2} \times (T_{b1} - T_{b2}) = 0.88(T_{b1} - T_{b2}) \quad (\text{A.3.2})$$

On the other hand, the heat removed from the gas by the solids in one cell,  $Q_{g-s}$ , can be expressed by

$$Q_{g-s} = h_p S \delta T_m \quad (\text{A.3.3})$$

where  $\delta T_m$  is the mean temperature difference between gas and solids. From equation A.1.5

$$h_p S = 8.14 R_g (U_o L_f)^{0.1} = 8.14 A U_o \rho_g C_g (U_o L_f)^{0.1} \quad (\text{A.3.4})$$

For one cell 4 cm wide,  $A = 0.008 \text{ (m}^2\text{)}$

Then from equation A.3.4

$$h_p S = 0.028 \text{ (kW/K)}$$

From equation A.3.3

$$Q_{g-s} = 0.028 \times 1000 \times \delta T_m = 28 \delta T_m \quad (\text{A.3.5})$$

From equations A.3.2 and A.3.5

$$\frac{Q_{1-2}}{Q_{g-s}} = 0.031 \frac{(T_{b1} - T_{b2})}{\delta T_m} \quad (\text{A.3.6})$$

Considering that  $(T_{b1} - T_{b2}) / \delta T_m$  is about 1 or less than 1

$$Q_{1-2} < Q_{g-s}$$

however  $Q_{1-2}$  and  $Q_{g-s}$  might be of similar magnitude because the correlations for heat transfer are not <sup>always</sup> accurate. Therefore we should insulate the partitions between cells.

FIGURE A1. MODEL FOR HEAT TRANSFER ACROSS SOLIDS TO GAS INTERFACE DURING TIME  $\delta T$

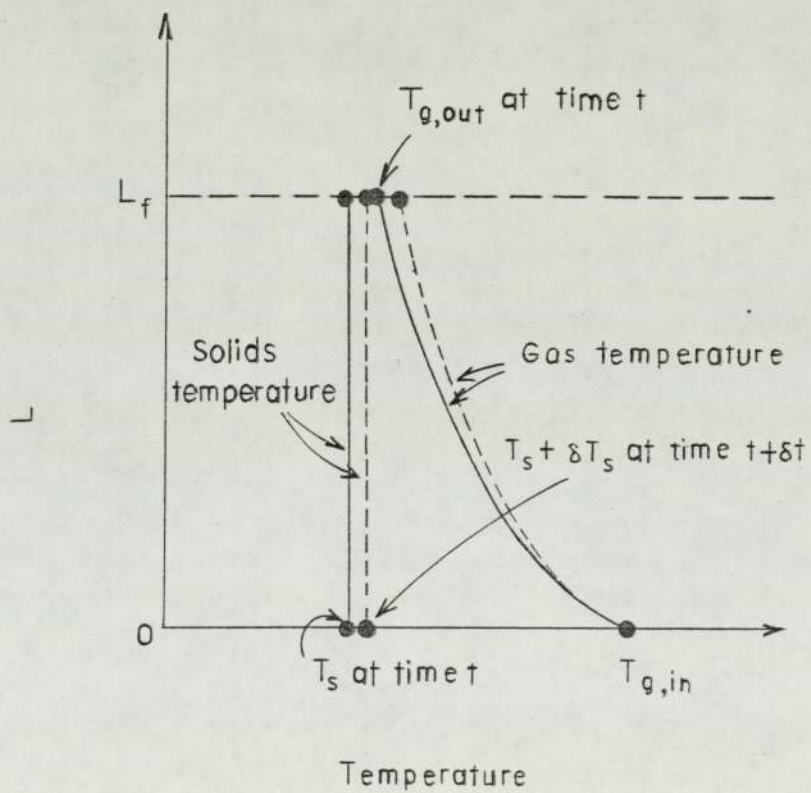
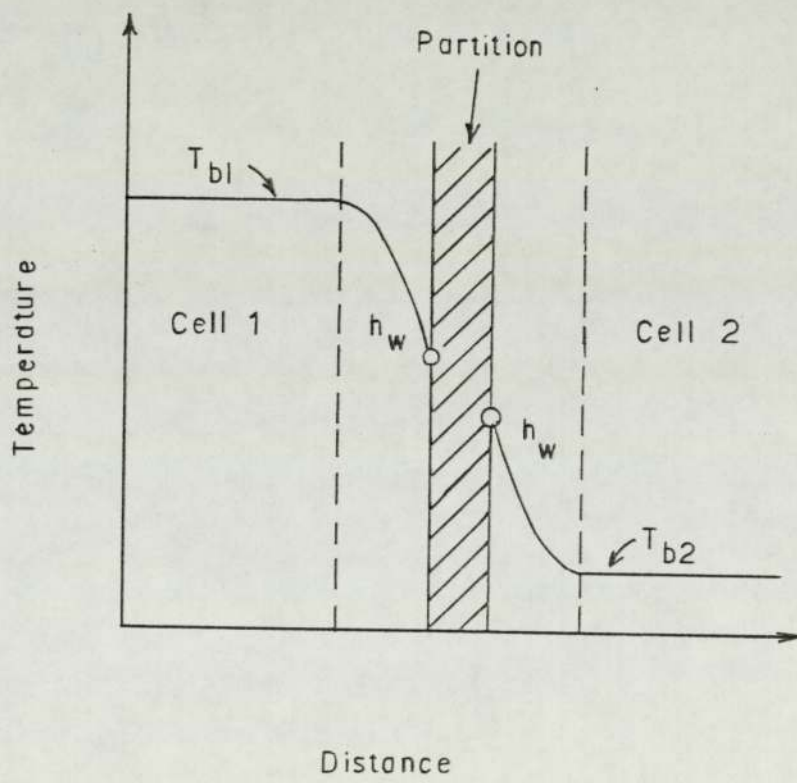


FIGURE A2. MODEL FOR HEAT TRANSFER BETWEEN ADJACENT CELLS



#### LIST OF REFERENCES

1. Robinson, G.A., U.S. Patent 212 508, (1879)
2. Kunii, D. and Levenspiel, O., "Fluidization Engineering", Wiley, N.Y., (1969)
3. Jahnig, C.E., Campbell, D.L. and Martin, H.Z., "History of Fluidized Solid Development at Exxon", pp.3-24 in Fluidization, Plenum, N.Y., (1980)
4. Reynoldson, R.W., "Controlled Atmosphere Fluidized Beds for the Heat Treatment of Metals", Heat Treatment of Metals", 4, 92-100, (1976)
5. Pechey, R., "Fluidised Bed to Heat Prospects", Process Eng., Jan., 38-41, (1982)
6. Davidson, J.F. and Harrison, D., "Fluidization", Academic, London, (1971)
7. Virr, M.J., "A Marine Fluidized Bed Waste Heat Boiler", Trans. Intern. Marine Engrs., 91, 1-12, (1979)
8. Bergougnou, M.A., Botterill, J.S.M., Howard, J.R., Newy<sup>e</sup>, D.C., Salway, A.G. and Teoman, Y., "High Temperature Heat Storage", pp.61-64 in Future Energy Concepts, IEE, (1981)
9. Virr, M.J., "Fluidized Bed Waste Heat Recovery and Equipment", in Combustion Engineering Association Conf., (1977)
10. Elliott, D.E. and Virr, M.J., British Patent 1500 231, (1978)
11. Newey, D.C., "Some Technical and Commercial Aspects of Fluidised Bed Gas-to-Gas Heat Exchanger", PhD thesis, University of Aston in Birmingham, (1981)
12. Newey, D.C. and Howard, J.R., "The Development of a Novel Fluidized Bed Gas-to-Gas Heat Exchanger", Heat Recovery Systems, 3, 35-40, (1983)

Partridge

13. Row, P.N., <sup>A</sup>Partridge, B.A. and Lyall, F., "Cloud Formation around Bubbles in Gas Fluidized Beds", Chem. Eng. Sci., 19, 973-985, (1964)
14. <sup>Staub</sup>Stub, F.W. and Canada, G.S., "Effect of Tube Bank and Gas Density on Flow Behavior and Heat Transfer in Fluidized Beds", Proc. 2nd Eng. Found. Conf., 339-344, Cambridge Univ., (1978)
15. Zenz, F.A., "Two-Phase Fluid-Solid Flow", Ind. Eng. Chem., 41, 2801-2806, (1949)
16. Mathur, K.B. and Epstein, N., "Spouted Beds", Acad., N.Y., (1974)
17. Ergun, S and Orning, A.A., "Fluid Flow Through Randomly Packed Columns and Fluidized Beds", Ind. Eng. Chem., 41, 1179-1184, (1949)
18. Goroshko, V.D., Rozenbaum, R.B. and Todes, O.M., "Approximate Hydraulic Relationships for Suspended Beds and Hindered Fall", Izvestiya VUZov, Neft' i Gaz, no.1, 125-131, (1958)
19. Thorley, B., Saunby, I.B., Mathur, K.B. and Osberg, G.L., "An Analysis of Air and Solid Flow in a Spouted Wheat Bed", Can. J. Chem. Eng., 37, no.5, 184-192, (1959)
20. Leva, M., "Fluidization", McGraw-Hill Book, N.Y., (1959)
21. Geldart, D., "Types of Gas Fluidization", Pow. Tech., 2, 285-292, (1973)
22. Rowe, P.N., "Gas-Solid Reaction in a Fluidized Bed", Chem. Eng. Progr., 60, no.3, 75-80, (1964)
23. Rowe, P.N. and Partridge, B.A., "Particle Movement Caused by Bubbles in a Fluidized Bed", pp.135-142 in Proceedings of Symposium on Interaction between Fluid and Particles, London, Inst. Chem. Eng., (1962)
24. Massimilla, L. and Westwater, I.W., "Photographic Study of Solid Gas Fluidization", AIChE, 6, no.1, 134-138, (1960)

25. Verloop, J., de Nie, L.H. and Heertjes, P.M., "The Residence Time of Solid in Gas-Fluidized Beds", *Pow. Tech.*, 2, 32-42, (1968/9)
26. Heertjes, P.M., de Nie, L.H. and Verloop, J., "Transport and Residence Time of Particles in a Shallow Fluidized Bed", pp.476-490 in *Proc. Intern. Symp. Fluidization*, Netherlands Univ., Amsterdam, (1967)
27. Rowe, P.N., Partridge, S.A., Cheney, A.G., Henwood, G.A. and Lyall, E., "Mechanisms of Solid Mixing in Fluidized Bed", *Trans. Inst. Chem. Eng.*, 43, 271-286, (1965)
28. May, W.G., "Fluidized-Bed Reactor Studies", *Chem. Eng. Progr.*, 55, no.12, 49-56, (1959)
29. Hayakawa, T., Graham, W. and Osberg, G.L., "A Resistance Probe Method for Determining Local Solid Particle Mixing Rates in a Batch Fluidized Bed", *Can. J. Chem. Eng.*, 42, 99-103, (1964)
30. Gabor, J.D., "Lateral Transport in a Fluidized-Packed Bed", *AIChE*, 11, 127-129, (1965)
31. Mathur, K. and Gishler, P., "A Study of Application of the Spouted Bed Technique to Wheat Drying", *J. Appl. Chem.*, 5, 624-636, (1955)
32. Lefroy, G.A. and Davidson, J.F., "The Mechanics of Spouted Bed", *Trans. Instn. Chem. Engrs.*, 47, T120, (1969)
33. Baxerres, J.L. and Gibrt, H., French Patent, ANVAR N°7634846, (1976)
34. Rios, G.M., Baxerres, J.L. and Gibrt, H., "Potential Improvement in the Field of Large Particle Fluidization", *Int. Fluidization Conference*, 529-536, Plenum, N.Y., (1980)
35. Perry, R.H. and Chilton, C.H., "Chemical Engineers' Handbook", 5th Ed., McGraw-Hill, Tokyo, (1973)
36. Shirai, T., "Ryudoso", Kagakugijyustusha, Tokyo, (1977)

37. Werther, J., "Influence of the Distributor Design on Bubble Characteristics in Large Diameter Gas Fluidized Beds", 7-12, "Fluidization", Cambridge Univ. (1978)
38. Takeda, K., "Quality of Fluidized Bed", Kagaku Kogaku, 21, 125-129, (1957)
39. Agarwal, J.C., Davis, W.L. and King, D.T., "Fluidized-Bed Cool Dryer", Chem. Eng. Progr., 58, no.11, 85-90 (1962)
40. Mickley, H.S. and Trilling, C.A., "Heat Transfer Characteristics of Fluidized Bed", Ind. Eng. Chem., 41, 1135-1147, (1949)
41. Leva, M., "A Correlation of Heat-Transfer Film Coefficients in Fluidized System", 421-425, in proc. General Discussion on Heat Transfer, London, I.N.E., A.S.M.E., (1951)
42. Dow, W.M. and Jakob, M., "Heat Transfer Between a Vertical Tube and a Fluidized Air-Solid Mixture", Chem. Eng. Progr., 47, no.12, 637-648, (1951)
43. Heerden, G. van, Nobel, N. and Krevelen, D.W. van, "Studies on Fluidization. — Heat Transfer", Chem. Eng. Sci., 1, 51-66 (1951): "Mechanism of Heat Transfer in Fluidized Bed", Ind. Eng. Chem., 45, 1237-1242, (1953)
44. Wen, C.Y. and Leva, M., "Fluidized-Bed Heat Transfer: a Generalized Dense-Phase Correlation", AIChE J., 2, 482-488, (1956)
45. Leva, M., Weintranb, M. and Grummer, M., "Heat Transmission through Fluidized Bed of Fine Particles", Chem. Eng. Progr., 45, no.9, 563-573, (1949)
46. Leva, M. and Grummer, M., "A Correlation of Solid Turnover in Fluidized System", Chem. Eng. Progr., 48, no.6, 307-313, (1952)
47. Toomey, R.D. and Johnstone, H.F., "Heat Transfer between Beds of Fluidized Solids and the Walls of the Container", pp.51-63 in Chem. Eng. Progr. Symp. Ser., 49, no.5, N.Y. AIChE, (1953)

48. Wender, L. and Cooper, G.T., "Heat Transfer between Fluidized Solids Beds and Boundry Surface - Correlation of Data", *AIChE*, 4, 15-23, (1958)
49. Bartholomew, R.M. and Katz, D.L., "Heat Transfer from the Wall of a Tube to a Fluidized Bed", pp.3-10 in *Chem. Eng. Progr. Symp. Ser.*, 45, no.4, N.Y., AIChE, (1952)
50. Botterill, J.S.M. and Teoman, Y., "Fluid-Bed Behaviour at Elevated Temperatures", pp.93-100 in *Proc. Int. Fluidization Conference*, Plenum, N.Y., (1980)
51. Zabrodsky, S.S., "Hydrodynamics and Heat Transfer in Fluidized Bed", The M.I.T. Press, (1966)
52. Levenspiel, O. and Walton, J.S., "Bed-Wall Heat Transfer in Fluidized System", pp.1-13 in *Chem. Eng. Progr. Symp. Ser.*, 50, no.9, N.Y., AIChE, (1954)
53. Mickley, H.S. and Fairbanks, D.F., "Mechanism of Heat Transfer to Fluidized Beds", *AIChE*, 1, 374-384, (1955)
54. Ranz, W.E. and Marshall, W.R., "Evapolation from Drops", *Chem. Eng. Progr.*, 48, no.4, 173-180, (1952)
55. Frantz, J.F., "Fluid-to-Particle Heat Transfer in Fluidized Beds", *Chem. Eng. Progr.*, 57, no.7, 35-42, (1961)
56. Walton, J.S., Olson, R.L. and Levenspiel, O., "Gas-Solid Film Coefficients of Heat Transfer in Fluidized Coal Beds", *Ind. Eng. Chem.*, 44, 1474-1480, (1952)
57. Heertjes, P.M. and McKibbins, S.W., "The Partial Coefficient of Heat Transfer in a Drying Fluidized Bed", *Chem. Eng. Sci.*, 5, 161-167, (1956)
58. Kato, K. and Wen, C.Y., "Gas-Particle Heat Transfer in Fixed and Fluidized Beds", pp.100-108 in *Chem. Eng. Progr. Symp. Ser.*, 66, no.105, N.Y., AIChE, (1970)
59. Chang, T.M. and Wen, C.Y., "Particle to Particle Heat Transfer in Air Fluidized Beds", pp.491-506 in *Proc, Int. Symp. Fluidization*, Netherlands Univ. Press, Amsterdam, (1967)

60. Kato, K., Ito, H. and Omura, S., "Gas-Particle Heat Transfer in a Packed Fluidized Bed", J. Chem. Eng. Japan, 12, no.5 403-405, (1979)
61. McGaw, D.R., "Heat Transfer in Shallow Crossflow Fluidized Bed Heat Exchangers - II. Experimental", Int. J. Heat Mass Transfer, 19, 665-671, (1976)
62. Matheson, G., Herbst, W. and Holt, P., "Characteristics of Fluid Solid Systems", Ind. Eng. Chem., 41, 1099-1104, (1949)
63. Furukawa, J. and Omae, T., "Liquid-like Properties of Fluidized Systems", Ind. Eng. Chem., 50, no.5, 821-828, (1958)
64. Kramers, H., "The Viscosity of a Bed of Fluidized Solids", Chem. Eng. Sci., 1, 35-37, (1951)
65. McGuigan, S.J., "The Flow Behaviour of Shallow Fluidized Beds", PhD thesis, Univ. of Aston in Birmingham, (1974)
66. Verloop, J., De Nie, L.H. and Heertjes, P.M., "Residence Time of Solids in Gas-Fluidized Beds", Pow. Tech., 2, 32-42, (1968/9)
67. McGaw, D.R., "The Design of Shallow Fluidized Bed Heat Exchanger Equipment", Pow. Tech., 6, 159-165, (1972)
68. McGaw, D.R., "Heat Transfer in Shallow Crossflow Fluidized Bed Heat Exchangers - I. A Generalized Theory", Int. J. Heat Mass Transfer, 19, 657-663, (1976)
69. McGaw, D.R., "The Effect of Particle Residence Time Distribution on Heat Transfer in Fluidized Bed Heat Exchanger", Pow. Tech., 11, 33-36, (1975)
70. Ishida, M., Hatano, H. and Shirai, T., "The Flow of Solid Particles in an Aerated Inclined Channel", Pow. Tech., 27, 7-12, (1980)
71. Botterill, J.S.M. and Abdul-Halim, B.H., "The Open-Channel Flow of Fluidized Solids", Pow. Tech., 23, 67-78, (1979)

72. Shinohara, K. and Tanaka, T., "A New Device for Pneumatic Transport of Particles", J. Chem. Eng. Japan, 5, 279-285, (1972)
73. Shinohara, K. and Yasuda, A., "Heat transfer of Particles in Pneumatic Escalator", J. Chem. Eng. Japan, 11, 296-301, (1978)
74. Leung, L.S., "The Ups and Downs of Gas-Solid Flow - a Review", Proc. Int. Fluidization Conference, 25-68, Plenum, N.Y., (1980)
75. Yousfi, Y. and Gau, G., "Aerodynamique de L'ecoulement Vertical de Suspensions Concentrees Gaz-Solides - I. Regimes D'ecoulement et Stabilite Aerodynamique", Chem. Eng. Science, 29, 1939-1946, (1974)
76. Arastoopour, H. and Gidaspow, D., "Vertical Pneumatic Conveying Using Four Hydrodynamic Models", American Chem. Soc., 18, no.2, 123-130, (1979)
77. Konno, H., Saito, S. and Maeda, S., "Pneumatic Conveying of Solids through Horizontal Straight Pipes", Chem. Eng. (Japan), 31, 243-250, (1967)
78. Modi, M.V., Talwalker, A.T. and Punwani, D.V., "Pressure Drop Correlations for Designing Vertical Dilute-Phase Gas-Solids Lift Lines for Materials Used in Coal Conversion Processes", Proc. Int. Pow. and Bulk Solids Handling and Processing Conference, Pow. Advisory Centre, Chicago, (1978)
79. Scott, A.M., "Pneumatic Conveyor Design - Art or Science?", Proc. 4th Int. Pow. Tech. and Bulk Solids Conference, 10-17, Pow. Advisory Conference, Harrogate, (1977)
80. Leung, L.S. and Jones, P.J., "Coexistence of Fluidized Solids Flow and Packed Flow in Standpipes", pp.116-121 in Proc. Int. Fluidization Conference, Ed. Davidson, J.F., Cambridge Univ., (1978)
81. Eleftheriades, C.M. and Judd, M.R., "Design of Downcomers - Joining Gas-Fluidized Beds in Multistage Systems", Pow. Tech., 21, 217-225, (1978)

82. Knowlton, T.M. and Aquino M.R.Y., "A Comparison of Several Lift-Line Feeders", Proc. 2nd Congress of Chem. Eng., Montreal, (1981)
83. Dryden, I.G.C., "The Efficient Use of Energy", IPC Science and Technology, Guildford, (1975)
84. Applegate, G., "Heating a Factory for Nothing", Heating & Vent. Eng., 44, 21-24, (1970)
85. Mortimer, J., "Exchanging Heat to Save Fuel", The Engineer, 34-37, 2/9 August, (1973)
86. Dunn, P.D. and Reay, D.A., "Heat Pipes", Pergamon Oxford, (1978)
87. Reay, D.A., "Heat Recovery at Low Temperature", Energy Management in the Process Industries, Inst. Chem. Engineers, paper-K, (1982)
88. Reay, D.A., "Industrial Energy Conservation", Pergamon, Oxford, (1979)
89. Westwood, C.G., "Development in Alloy Fabrications to Reduce Fuel Consumption and Operating Costs in Heat Treatment Furnaces", Heat Treatment of Metals, no.2, 25-34, (1980)
90. Peyman, M. and Laguérie, C., "Heat Transfer between Solids and Gas in a Multistaged Fluidized Bed", pp.243-251 in Fluidization, Plenum, N.Y., (1980)
91. Toei, R. and Akao, T., "Multi-Stage Fluidised Bed Apparatus with Perforated Plates", Ins. Chem. Eng. Symp. Ser., no.30, 34-42, (1968)
92. Sanderson, P.R. and Howard, J.R., "Towards More Versatile Fluidised-Bed Heat Exchangers", Applied Energy, 3, 115-125, (1977)
93. Noordergraaf, I.W., Roes, A.W.M. and van Swaaij, W.P.M., "Axial Mixing and Mass Transfer in a Zig-Zag Contactor", pp.341-348 in Fluidization, Plenum, N.Y., (1980)
94. Chatterjee, A., "Spout-Fluid Bed Technique", Ind. Eng. Chem. Process Des. Develop., 9, no.2, (1970)